

University of Windsor

Scholarship at UWindor

Electronic Theses and Dissertations

Theses, Dissertations, and Major Papers

1993

Cryogenic recovery of tire rubber.

Antonio (Tony). Mancina
University of Windsor

Follow this and additional works at: <https://scholar.uwindsor.ca/etd>

Recommended Citation

Mancina, Antonio (Tony)., "Cryogenic recovery of tire rubber." (1993). *Electronic Theses and Dissertations*. 1591.

<https://scholar.uwindsor.ca/etd/1591>

This online database contains the full-text of PhD dissertations and Masters' theses of University of Windsor students from 1954 forward. These documents are made available for personal study and research purposes only, in accordance with the Canadian Copyright Act and the Creative Commons license—CC BY-NC-ND (Attribution, Non-Commercial, No Derivative Works). Under this license, works must always be attributed to the copyright holder (original author), cannot be used for any commercial purposes, and may not be altered. Any other use would require the permission of the copyright holder. Students may inquire about withdrawing their dissertation and/or thesis from this database. For additional inquiries, please contact the repository administrator via email (scholarship@uwindsor.ca) or by telephone at 519-253-3000ext. 3208.



National Library
of Canada

Acquisitions and
Bibliographic Services Branch

395 Wellington Street
Ottawa, Ontario
K1A 0N4

Bibliothèque nationale
du Canada

Direction des acquisitions et
des services bibliographiques

395, rue Wellington
Ottawa (Ontario)
K1A 0N4

Your file: Votre référence

Our file: Notre référence

NOTICE

The quality of this microform is heavily dependent upon the quality of the original thesis submitted for microfilming. Every effort has been made to ensure the highest quality of reproduction possible.

If pages are missing, contact the university which granted the degree.

Some pages may have indistinct print especially if the original pages were typed with a poor typewriter ribbon or if the university sent us an inferior photocopy.

Reproduction in full or in part of this microform is governed by the Canadian Copyright Act, R.S.C. 1970, c. C-30, and subsequent amendments.

AVIS

La qualité de cette microforme dépend grandement de la qualité de la thèse soumise au microfilmage. Nous avons tout fait pour assurer une qualité supérieure de reproduction.

S'il manque des pages, veuillez communiquer avec l'université qui a conféré le grade.

La qualité d'impression de certaines pages peut laisser à désirer, surtout si les pages originales ont été dactylographiées à l'aide d'un ruban usé ou si l'université nous a fait parvenir une photocopie de qualité inférieure.

La reproduction, même partielle, de cette microforme est soumise à la Loi canadienne sur le droit d'auteur, SRC 1970, c. C-30, et ses amendements subséquents.

CRYOGENIC RECOVERY OF TIRE RUBBER

BY

TONY MANCINA

**A THESIS SUBMITTED TO THE FACULTY OF GRADUATE STUDIES AND
RESEARCH THROUGH THE DEPARTMENT OF CIVIL & ENVIRONMENTAL
ENGINEERING IN PARTIAL FULFILMENT OF THE REQUIREMENTS
FOR THE DEGREE OF MASTER OF APPLIED SCIENCE
AT THE UNIVERSITY OF WINDSOR**

**Windsor, Ontario, Canada
1993**



National Library
of Canada

Acquisitions and
Bibliographic Services Branch

395 Wellington Street
Ottawa, Ontario
K1A 0N4

Bibliothèque nationale
du Canada

Direction des acquisitions et
des services bibliographiques

395, rue Wellington
Ottawa (Ontario)
K1A 0N4

Your file *Votre référence*

Our file *Notre référence*

The author has granted an irrevocable non-exclusive licence allowing the National Library of Canada to reproduce, loan, distribute or sell copies of his/her thesis by any means and in any form or format, making this thesis available to interested persons.

L'auteur a accordé une licence irrévocable et non exclusive permettant à la Bibliothèque nationale du Canada de reproduire, prêter, distribuer ou vendre des copies de sa thèse de quelque manière et sous quelque forme que ce soit pour mettre des exemplaires de cette thèse à la disposition des personnes intéressées.

The author retains ownership of the copyright in his/her thesis. Neither the thesis nor substantial extracts from it may be printed or otherwise reproduced without his/her permission.

L'auteur conserve la propriété du droit d'auteur qui protège sa thèse. Ni la thèse ni des extraits substantiels de celle-ci ne doivent être imprimés ou autrement reproduits sans son autorisation.

ISBN 0-315-93291-0

Name ANTONIO S. MANCINA

Dissertation Abstracts International is arranged by broad, general subject categories. Please select the one subject which most nearly describes the content of your dissertation. Enter the corresponding four-digit code in the spaces provided.

AUTOMOTIVE / CHEMICAL
SUBJECT TERM

0540 U·M·I
SUBJECT CODE
0542

Subject Categories

THE HUMANITIES AND SOCIAL SCIENCES

COMMUNICATIONS AND THE ARTS
Architecture 0729
Art History 0377
Cinema 0900
Dance 0378
Fine Arts 0357
Information Science 0723
Journalism 0391
Library Science 0399
Mass Communications 0708
Music 0413
Speech Communication 0459
Theater 0465

EDUCATION
General 0515
Administration 0514
Adult and Continuing 0516
Agricultural 0517
Art 0273
Bilingual and Multicultural 0282
Business 0688
Community College 0275
Curriculum and Instruction 0727
Early Childhood 0518
Elementary 0524
Finance 0277
Guidance and Counseling 0519
Health 0680
Higher 0745
History of 0520
Home Economics 0278
Industrial 0521
Language and Literature 0817
Mathematics 0280
Music 0522
Philosophy of 0998
Physical 0523

Psychology 0525
Reading 0535
Religious 0527
Sciences 0714
Secondary 0533
Social Sciences 0534
Sociology of 0340
Special 0529
Teacher Training 0530
Technology 0710
Tests and Measurements 0288
Vocational 0747

LANGUAGE, LITERATURE AND LINGUISTICS
Language
General 0679
Ancient 0269
Linguistics 0290
Modern 0291

Literature
General 0401
Classical 0294
Comparative 0295
Medieval 0297
Modern 0298
African 0316
American 0591
Asian 0305
Canadian (English) 0352
Canadian (French) 0353
English 0593
Germanic 0311
Latin American 0312
Middle Eastern 0315
Romance 0313
Slavic and East European 0314

PHILOSOPHY, RELIGION AND THEOLOGY
Philosophy 0422
Religion
General 0318
Biblical Studies 0321
Clergy 0319
History of 0320
Philosophy of 0322
Theology 0469

SOCIAL SCIENCES
American Studies 0323
Anthropology
Archaeology 0324
Cultural 0326
Physical 0327
Business Administration
General 0310
Accounting 0272
Banking 0770
Management 0454
Marketing 0338
Canadian Studies 0385
Economics
General 0501
Agricultural 0503
Commerce-Business 0505
Finance 0508
History 0509
Labor 0510
Theory 0511
Folklore 0358
Geography 0366
Gerontology 0331
History
General 0578

Ancient 0579
Medieval 0581
Modern 0582
Black 0328
African 0331
Asia, Australia and Oceania 0332
Canadian 0334
European 0335
Latin American 0336
Middle Eastern 0333
United States 0337
History of Science 0385
Law 0398
Political Science
General 0615
International Law and Relations 0616
Public Administration 0617
Recreation 0814
Social Work 0452
Sociology
General 0626
Criminology and Penology 0627
Demography 0631
Ethnic and Racial Studies 0631
Individual and Family Studies 0628
Industrial and Labor Relations 0629
Public and Social Welfare 0630
Social Structure and Development 0700
Theory and Methods 0344
Transportation 0709
Urban and Regional Planning 0999
Women's Studies 0453

THE SCIENCES AND ENGINEERING

BIOLOGICAL SCIENCES
Agriculture
General 0473
Agronomy 0285
Animal Culture and Nutrition 0475
Food Science and Technology 0359
Forestry and Wildlife 0478
Plant Culture 0479
Plant Pathology 0480
Plant Physiology 0817
Range Management 0777
Wood Technology 0746

Biology
General 0306
Anatomy 0287
Biostatistics 0308
Botany 0309
Cell 0329
Ecology 0329
Entomology 0353
Genetics 0369
Limnology 0793
Microbiology 0410
Molecular 0307
Neuroscience 0317
Oceanography 0416
Physiology 0433
Radiation 0821
Veterinary Science 0778
Zoology 0472

Biophysics
General 0786
Medical 0760

EARTH SCIENCES
Biogeochemistry 0425
Geochemistry 0996

Geodesy 0370
Geology 0372
Geophysics 0373
Hydrology 0388
Mineralogy 0411
Paleobotany 0345
Paleontology 0426
Palaeontology 0418
Palaeozoology 0985
Physiology 0427
Physical Geography 0368
Physical Oceanography 0415

HEALTH AND ENVIRONMENTAL SCIENCES
Environmental Sciences 0768
Health Sciences
General 0566
Audiology 0300
Chemotherapy 0992
Dentistry 0567
Education 0350
Hospital Management 0769
Human Development 0758
Immunology 0982
Medicine and Surgery 0564
Mental Health 0347
Nursing 0569
Nutrition 0570
Obstetrics and Gynecology 0380
Occupational Health and Safety 0354
Ophthalmology 0381
Pathology 0571
Pharmacology 0419
Pharmacy 0572
Physical Therapy 0382
Public Health 0573
Radiology 0574
Recreation 0575

Speech Pathology 0460
Toxicology 0383
Home Economics 0386

PHYSICAL SCIENCES
Pure Sciences
Chemistry
General 0485
Agricultural 0749
Analytical 0486
Biochemistry 0487
Inorganic 0488
Nuclear 0738
Organic 0490
Pharmaceutical 0491
Physical 0494
Polymer 0495
Radiation 0754
Mathematics 0405
Physics
General 0605
Acoustics 0986
Astronomy and Astrophysics 0606
Atmospheric Science 0608
Atomic 0748
Electronics and Electricity 0607
Elementary Particles and High Energy 0798
Fluid and Plasma 0759
Molecular 0609
Nuclear 0610
Optics 0752
Radiation 0756
Solid State 0611
Statistics 0463

Applied Sciences
Applied Mechanics 0346
Computer Science 0984

Engineering
General 0537
Aerospace 0538
Agricultural 0539
Automotive 0540
Biomedical 0541
Chemical 0542
Civil 0543
Electronics and Electrical 0544
Heat and Thermodynamics 0548
Hydraulic 0545
Industrial 0546
Marine 0547
Materials Science 0794
Mechanical 0548
Metallurgy 0743
Mining 0551
Nuclear 0552
Packaging 0549
Petroleum 0765
Sanitary and Municipal 0554
System Science 0790
Geotechnology 0428
Operations Research 0796
Plastics Technology 0795
Textile Technology 0994

PSYCHOLOGY
General 0621
Behavioral 0384
Clinical 0622
Developmental 0620
Experimental 0623
Industrial 0624
Personality 0625
Physiological 0989
Psychobiology 0349
Psychometrics 0632
Social 0451



AC20999

© Antonio S. Mancina 1993

Dedicated, with love, to my family.

ABSTRACT

A comprehensive investigation of the cryogenic recovery of tire rubber was conducted with laboratory, pilot plant and industrial equipment.

A critical literature review indicated that a fundamental understanding was required of:

- A tire's matrix
- Disposal techniques for scrap tires
- Recycling methods for tires which include reclamation and comminution by ambient, cryogenic or wet solution methods.
- Cryogenics as a science
- Cryogenic processing techniques and equipment for the comminution of tires
- The uses for recycled tire rubber.

Experiments were conducted with specimens of tire rubber to determine:

- Cooling curves for scrap tire rubber dipped in liquid nitrogen.
- Cooling curves for scrap tire rubber cooled by nitrogen vapour.
- Cooling curves for virgin tire rubber dipped in liquid nitrogen.
- Cooling curves for different size cubes of tire rubber cooled simultaneously by nitrogen vapour.
- Cooling curves for tire rubber cooled and then recooled to investigate material degradation.

Electron microphotographs of scrap and virgin tire treads were compared in terms of physical characteristics. The used tire rubber specimen appeared to have a granular structure.

Air trapped in the interstices hindered the heat transfer process. On the other hand, the virgin tire specimen appeared to be homogeneous. This structure enabled the virgin material to cool at a higher rate than the used material.

Electron photomicrographs of ambiently and cryogenically ground rubber crumbs were also compared. Different sizes of crumb rubber were evaluated. The ambiently ground rubber displayed more surface area than the cryogenically ground material. This increase was created by the torn edges of the ambiently ground rubber. The faceted surfaces of the cryogenically processed rubber provide smoother surfaces of lower area.

Experimental and theoretical data were used to design a small fine-grind system which was proposed for the processing of $\frac{1}{8}$ inch pellets of tire rubber to a fine size less than 30 mesh. The details of this design have been provided.

When frozen tire chips are passed through a hammermill, an entanglement of steel and nylon fibre results. This entanglement creates a serious problem when mechanical separation of the steel and fibre fluff into separate streams is undertaken. When entangled, the fluff and steel are virtually worthless, but when separated both have economic value. Separation of this entanglement by various means was thoroughly investigated. The details of the testing conducted on the fluff and steel entanglement, and the development of a separation device that utilizes the principle of inertial

impaction have been discussed comprehensively. Theoretical and experimental data were applied to the modifications of the industrial-size plant in Cambridge, Ontario. The improvements to the industrial system made it more efficient than the original designs. These developments are explained in detail.

A number of recommendations have been made for continuation of this basic investigation.

ACKNOWLEDGEMENTS

I wish to take this opportunity to express my sincere gratitude to my advisors, Dr. A.W. Gnyp and Dr. A.T. Alpas for their invaluable guidance, constructive criticisms and encouragement during the course of this project.

I am also grateful to Mr. G. Ryan and Mr. G. Kuhun for their technical assistance.

I would also like to thank Recovery Technologies Inc. for their assistance and cooperation during the course of this project.

A special appreciation goes to the Ministry of Colleges and Universities for the University Research Incentive Fund grant, without their financial support this investigation could not have been done.

TABLE OF CONTENTS

	Page
ABSTRACT	v
ACKNOWLEDGEMENTS	viii
TABLE OF CONTENTS	ix
LIST OF FIGURES	xii
LIST OF TABLES	xvii
I. INTRODUCTION	1
II. BACKGROUND	3
2.1 History of Recycling	3
2.2 Cryogenic Recycling of Solid Wastes	4
2.3 The Tire	6
2.4 Specific Disposal Methods	9
2.5 Reprocessed Rubber	13
2.5.1 Reclaim Rubber	14
2.5.2 Ground Rubber	14
2.5.2.1 Ambient Grinding	15
2.5.2.2 Cryogenic Comminution	17
2.5.2.3 Wet or Solution Grinding	17
2.6 Cryogenically Recycled Materials	19
2.7 Cryogenic Operations And Processes	20
2.7.1 Presizing	25
2.7.2 Freezing Systems	25
2.7.2.1 Immersion Batch Freezing	25
2.7.2.1 Liquid Cryogen Freezing Systems	25
2.7.3 Size Reduction Of Materials	26
2.7.4 Product Separation	27
2.8 Potential Applications For Cryogenic Tire Crumb	28
III. DETERMINING A WORST CASE MODEL	29
3.1 Conduction	31
3.1.1 Fourier's Law	31
3.1.2 Thermal Properties Of Matter	34
3.1.3 Thermal Diffusivity	34
3.2 Determining A Worst Case Model	35
IV. THEORETICAL COOLING CURVES	38
4.1 Lumped Capacitance Method	39
4.2 Spatial Effects	41
4.2.1 Graphical Representations	42
4.2.2 Multidimensional Systems	47
4.2.3 Heat Transfer In Multidimensional Systems	49

	Page
4.2.4 Multidimensional Problems	49
4.3 Theoretical Investigation	53
4.4 Summary Of Theoretical Investigation	58
V. COOLING EXPERIMENTS	60
5.1 Experimental Equipment	60
5.2 Procedures	61
5.3 Specimen Preparation	61
5.4 Methods	65
VI. EXPERIMENTAL RESULTS & DISCUSSION	71
VII. MICROGRIND COOLING TUNNEL DESIGN	86
7.1 Design Considerations	87
7.1.1 Mixing	87
7.1.2 Conveying	87
7.2 Donated Cryotunnel	88
7.3 Proposed Tunnel Design	91
VIII. FIBRE AND STEEL SEPARATION	95
8.1 Separation Tests	96
8.1.1 Drop Test	96
8.1.2 Combing Test	97
8.1.3 Shaker Test (Inertial Impaction Test)	97
8.2 Fibre Separation Recommendations	101
IX. AMBIENTLY AND CRYOGENICALLY GROUND RUBBER	105
X. APPLICATION OF BASIC PRINCIPLES ON AN INDUSTRIAL SCALE	108
XI. CONCLUSIONS & RECOMMENDATIONS	113
REFERENCES	116
APPENDIX I Dipping One Inch Cube Of Scrap Tire Rubber Into Liquid Nitrogen (Theoretical)	118
APPENDIX II Gas Phase Cooling Over Liquid Nitrogen Of A One Inch Cube Of Tire Rubber (Theoretical)	125
APPENDIX III Spraying A One Inch Cube Of Tire Rubber With Liquid Nitrogen (Theoretical)	132
APPENDIX IV Nitrogen Consumption For Dipping Rubber Into Liquid Nitrogen	139

	Page
APPENDIX V Nitrogen Consumption For Gas Phase Cooling Of Rubber	142
APPENDIX VI Nitrogen Consumption For Spraying Of Rubber	145
APPENDIX VII Experiment One Results: One Inch Cube Of Tire Rubber Dipped Into Liquid Nitrogen	148
APPENDIX VIII Experiment Two Results: One Inch Cube Of Tire Rubber Cooled By Liquid Nitrogen Vapour	159
APPENDIX IX Experiment Three Results: Different Sizes Of Tire Rubber Specimens Cooled Simultaneously By Liquid Nitrogen Vapour	170
APPENDIX X Experiment Four Results: One Inch Cube Of Virgin Tire Rubber Dipped In Liquid Nitrogen	176
APPENDIX XI Experiment Five Results: One Inch Cube Of Tire Rubber Resubmerged In Liquid Nitrogen	187
APPENDIX XII Photomicroscopes Of Ambiently & Cryogenically Ground Tire Rubber Of Different Material Sizes	193
VITA AUCTORIS	200

LIST OF FIGURES

Figure	Page
2.1: The World Snake; a symbol of self-renewal.	3
2.2: The Rubber Matrix Of A Typical Tire	7
2.3: U.S. Landfills In Operation	11
2.4: Average U.S. Landfill Costs	11
2.5: U.S. Recycled Rubber Market, 1990.	14
2.6: Basic Ambient Tire Grinding Process	16
2.7: Basic Cryo Grinding System	16
2.8: Basic Wet Grinding System	18
2.9: Materials Classification	19
2.10: Yield Stress And Fracture	21
2.11: A Schematic Of A Basic Recovery System For Recovering Tire Components	24
2.12: Cross-sectional View Of A Typical Liquid Nitrogen Freezing Tunnel	26
3.1: A Cross-section Of A Typical Tire	30
3.2: One Dimensional Heat Transfer By Conduction	32
3.3: Heat Flux Vectors In A 3-dimensional Coordinate System	33
3.4: Range Of Thermal Conductivity For Various States Of Matter At Normal Temperatures And Pressure	34
3.5: A Pre-sized Piece Of Tire Containing Rubber, Nylon & Steel	37
4.1: A Piece Of Rubber Immersed In A Quenching Liquid	39
4.2: Midplane Temperature For An Infinite Plate	43

Figure	Page
4.3: Midplane Temperature For An Infinite Plate (Blow-up)	44
4.4: Temperature As A Function Of Center Temperature In An Infinite Plate	45
4.5: Dimensionless Heat Loss Of An Infinite Plate	45
4.6: Infinite Rectangular Bar	47
4.7: Product Solution For Rectangular Parallelepiped System	48
4.8: Dependence Of Centre Temperature On Cooling Time For Three Cooling Modes. ($\frac{1}{2}$ " Cube)	54
4.9: Dependence Of Centre Temperature On Cooling Time For Three Cooling Modes. (1" Cube)	55
4.10: Dependence Of Centre Temperature On Cooling Time For Three Cooling Modes. (2" Cube)	56
4.11: Nitrogen Consumption For Three Modes	57
5.1: Thermocouple In Contact With Fibre Or Steel, Giving An Inconsistent Reading	62
5.2: Illustrations Of Specimen Preparation	64
5.3: Layout Of Experiment In Which A One Inch Cube Of Rubber Was Submerged Into Liquid Nitrogen	66
5.4: Layout Of Experiment In Which A One Inch Cube Of Rubber Was Suspended Over Liquid Nitrogen	68
5.5: Layout Of Experiment In Which Different Sizes Of Rubber Cubes Were Simultaneously Cooled By Liquid Nitrogen Vapour	69
6.1: One Inch Cube Of Tire Rubber Dipped Into Liquid Nitrogen (Experimental Average)	72
6.2: One Inch Cube Of Tire Rubber Cooled With Liquid Nitrogen Vapour (Experimental Average)	74

Figure	Page
6.3: Theoretical Results Of A One Inch Cube Of Tire Rubber Cooled With Vapour And Liquid Nitrogen	75
6.4: The Structure Of Tire Rubber On A Microscopic Level	77
6.5: $\frac{1}{4}$ ", $\frac{1}{2}$ ", $\frac{3}{4}$ ", 1 $\frac{1}{4}$ " Cubes Cooled Simultaneously Cooled In Colder Nitrogen Vapours	78
6.6: $\frac{1}{4}$ ", $\frac{1}{2}$ ", 1" Cubes Cooled Simultaneously In Warmer Nitrogen Vapours	80
6.7: One Inch Cube Of Virgin Tire Rubber Dipped Into Liquid Nitrogen (Experimental Average)	82
6.8: One Inch Cube Of Rubber Recooled In Liquid Nitrogen	83
7.1: Schematic Of The Cryotunnel Donated By RTI	89
7.2: Proposed Conveying System Utilizing Helicoid Flights	94
8.1: Two Hand Held Combs Which Were Used In Each Of The Combing Tests	98
8.2: Illustration Of How The Combing Tests Were Conducted	99
8.3: Shaker Comb Used In The Inertial Impaction Tests	100
8.4: An Illustration Of A Mechanized Shaker	102
8.5: Separation Method Utilizing Impacting Fingers On A Spinning Roller	104
9.1: Photomicrograph of Ambiently Ground Rubber	105
9.2: Microscopy Of Cryogenically Ground Rubber	106
10.1: Schematic Of The Pilot Plant In Cambridge	109
I.1 to $\frac{1}{2}$ ", 1", 2" Cubes Of Tire Dipped In LIN (Theory)	120
I.3	

Figure	Page
II.1 to ¼", 1", 2" Cubes Cooled By LIN Vapours (Theory) II.3	127
III.1 to ¼", 1", 2" Cubes Cooled By LIN Spray (Theory) III.3	134
VII.1 to One Inch Cube Dipped Into LIN Test 1-10 VII.10	149
VIII.1 to One Cube Cooled By LIN Vapours Test 1-10 VIII.10	160
IX.1: ¼", ½", ¾", 1¼" Cubes Cooled Simultaneously By Colder LIN Vapours Test 1	171
IX.2: ¼", ½", ¾", 1¼" Cubes Cooled Simultaneously By Colder LIN Vapours Test 2	172
IX.3: ¼", ½", ¾", 1¼" Cubes Cooled Simultaneously By Colder LIN Vapours Test 3	173
IX.4: ¼", ½", 1" Cubes Cooled Simultaneously By Warmer LIN Vapours Test 4	174
IX.5: ¼", ½", 1" Cubes Cooled Simultaneously By Warmer LIN Vapours Test 5	175
X.1 to 1" Cube Of Virgin Rubber Dipped In LIN Test 1-10 X.10	177
XI.1 to One Inch Cube Recooled With LIN Test 1-5 XI.5	188
XII.1: Photomicrograph Of Ambiently Ground Tire Rubber (10 Mesh)	194
XII.2: Photomicrograph Of Ambiently Ground Tire Rubber (20 Mesh)	195
XII.3: Photomicrograph Of Ambiently Ground Tire Rubber (30 Mesh)	196
XII.4: Photomicrograph Of Cryogenically Ground Tire Rubber (10-20 Mesh)	197

Figure	Page
XII.5: Photomicrograph Of Cryogenically Ground Tire Rubber (20-30 Mesh)	198
XII.6: Photomicrograph Of Cryogenically Ground Tire Rubber (30-40 Mesh)	199

LIST OF TABLES

Table	Page
2.1: The Composition Of A Typical Tire In Weight Percentages	8
2.2: Scrap Tire Solutions	10
2.3: Products Of Pyrolysis	12
2.4: Classification Of Metals	22
2.5: Classification Of Polymers	23
3.1: Composition Of A Typical Automobile Tire	29
7.1: Data Obtained From Tests Conducted On Donated Cryotunnel	90
8.1: Composition Of A Typical Automobile Tire	96
I.1 to ½", 1", 2" Cubes Of Rubber Dipped In LIN (Theory) I.3	119
II.1 to ½", 1", 2" Cubes Cooled By LIN Vapours (Theory) II.3	126
III.1 to ½", 1", 2" Cubes Cooled By LIN Spray (Theory) III.3	133

I. INTRODUCTION

In the mid 1800s, Charles Goodyear developed a technique for vulcanizing rubber. He blended natural rubber with sulphur and heated it on his wood stove, where the rubber cured into a water-impermeable sheet. That development led to the design of the present day tire.

There is approximately one tire disposed annually for every person in North America. Only a small fraction of these discarded tires is actually recycled or reused in any form. As a result, there are billions of discarded tires in North America sitting in landfills, stockpiled or illegally dumped somewhere. In the United States, federal and state laws make it difficult to dispose of scrap tires. Consequently, these laws seem to be creating a monster that won't go away. Tires are not biologically degradable. When they are buried in a landfill they do not stay buried. The breathing action of the tires causes them to resurface when passed over with compactors. Once uncovered they serve as a breeding ground for mosquitos and other pests.

The use of cryogenics for recycling specific solid waste materials appears to be a relatively new solution to an age old problem. Some materials exhibit glass-like properties when subjected to cryogenic conditions. Once frozen, the material can be shattered into a powder for convenient recycling.

This thesis discusses basic cryogenic principles with a

focus on experimental and theoretical analyses of tire rubber characteristics that are important to the development of a newly proposed mini-mill cryotunnel. This knowledge was also applied to the design of an industrial-size plant in Cambridge, Ontario.

The matrix of a typical automobile tire can present significant problems when efficient cryogenic recovery of the components is required. The tire rubber, steel and nylon fibre have different properties which create problems when separation into three separate streams is necessary. When they pass through a hammermill, the steel and fibre become so entangled that the desired separation between the two is minimal. As a result the entangled fibres and steel become virtually worthless. This thesis addresses this problem and presents possible solutions. The shapes of ambiently ground rubber and cryogenically ground rubber crumbs were examined and compared.

II. BACKGROUND

The purpose of this chapter is to give the reader some background knowledge of recycling and the different methods of recycling. A fairly comprehensive effort will be made to help the reader understand the cryogenic recycling of scrap tires.

2.1 History of Recycling

The World Snake which is an illustration of a crowned dragon that eats its own tail is depicted in Figure 2.1. It is an ancient alchemical symbol of self-renewal and regeneration dating back to 3000 B.C. [Eleazar]. Man has been well aware of the value of metals to society. The physical properties of metals allowed them to be shaped into tools and utensils. When damaged the metal objects could not be repaired but could be reclaimed by remelting. The early regeneration of metals and other materials has come to be known as recycling, which is the transformation of waste materials into usable products.



Figure 2.1: The World Snake; a symbol of self-renewal.

2.2 Cryogenic Recycling of Solid Wastes

Cryogenics is a branch of physics that relates to the production and effects of very low temperatures. Cryogenic temperatures can be achieved with liquid refrigerants, such as liquid oxygen, liquid carbon dioxide, and liquid nitrogen (LIN). LIN is the most commonly used refrigerant in cryogenic recycling because of its availability and relatively low cost [Allen & Biddulph].

The use of cryogenics for recycling certain solid waste materials appears to be a relatively new solution to an age old problem. Cryogenic conditions permit some materials to exhibit glass like properties, that are not evident under ambient conditions. Once frozen they can be shattered into a powder and thus recycled.

The concept of freezing to enhance recycling of solid wastes was initiated in the late 1960s and early 1970s by the College of Engineering at the University of Wisconsin. In an effort to aid the auto salvage dealers in solving the problem of derelict and abandoned automobiles, the problem of scrap tires surfaced [Braton]. Cryogenic recovery of scrap at that time proved to be economically expensive.

In North America, there is approximately one tire disposed annually for every man, woman, and child. Only a small fraction of these discarded tires is actually recycled or reused in any form. Consequently, there are literally billions of discarded tires in North America sitting in

landfills, stockpiled or illegally dumped somewhere. Each disposed tire occupies 3 ft' of space, on the average, and with landfills available at a premium price, it becomes quite costly to dispose of them. Furthermore, tires are not biologically degradable. When they are buried in a landfill they do not stay buried. The breathing action of the tires eventually causes them to resurface when subjected to the activities of compactors [Ctvrtnicek, Search & Blodgett]. When they surface they serve as a breeding ground for mosquitos and pests. It is for these environmental reasons that local municipalities have banned landfilling of scrap tires. In the United States, federal and state laws, making it difficult to dispose of scrap tires, seem to be creating a monster that won't go away [Irwin].

Tires consist of valuable materials and should not be abandoned. Each tire represents the consumption of approximately 8 gallons of oil. Five gallons are used in manufacturing and 3 gallons are used as energy in the curing process.

The rubber from recycled tires can be used in the manufacturing of a number of products. The rubber from just one used tire could prolong the life of a driveway by several hundred percent.

An average auto tire consists of 12 pounds of rubber, 6 pounds of fibre, and 1 pound of steel. These materials have

value if they can be recycled into their own separate streams. It is no wonder that tires are often referred to as *black gold* [Braton].

2.3 The Tire

In the mid 1800s, Charles Goodyear developed a technique for vulcanizing rubber. He blended natural rubber with sulphur and placed it on his wood stove, where the rubber cured into a water impermeable sheet. That development led to the design of the present day tire [Sverdrup & Wendrow].

The rubber matrix of a typical tire is illustrated in Figure 2.2. The rubber matrix consists of:

- Tread
- Black Sidewall
- White Sidewall
- Shoulder Wedge
- Plycoat or Carcass
- Inner Liner
- Apex/Chafer

Table 2.1 provides the composition of a typical tire in weight percentages. The rubber make-up of a tire is basically oils and plasticizers consisting of different types of rubber (e.g. natural rubber, styrene-butadiene). These materials alone cannot give the tire its required strength and durability. To achieve the necessary characteristics in a tire, fillers are added [Klingensmith]. Typical fillers are:

- Carbon Blacks (20-30%)
- Silicas and Silicates (0-5%)
- Clays and Talcs (0-5%)

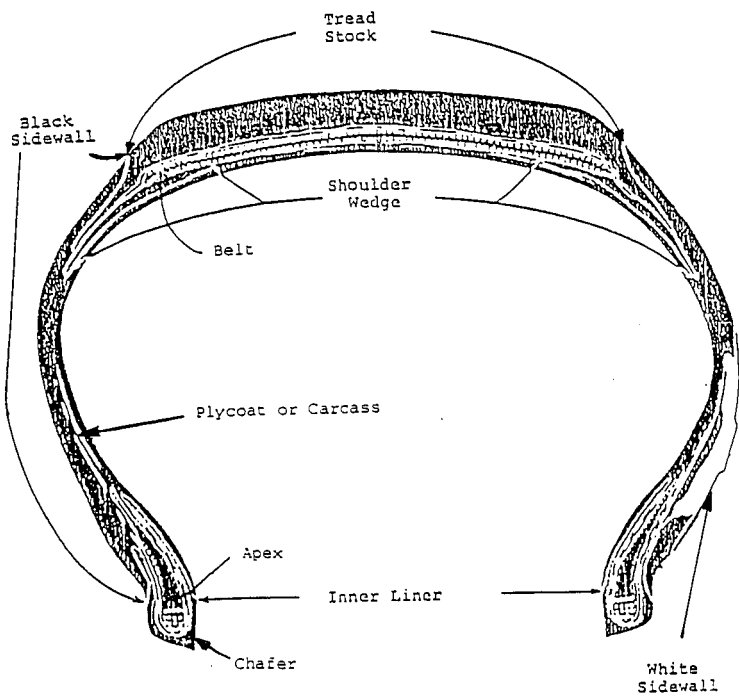


Figure 2.2: The Rubber Matrix Of A Typical Tire

Source: Rubber Recycling Update, 1993.

TABLE 2.1: THE COMPOSITION OF A TYPICAL TIRE
IN WEIGHT PERCENTAGES.

	PASSENGER TIRE (%)	TRUCK TIRE (%)
TREAD		
CAP	29.0	20.0
BASE OR UNDERTREAD	6.0	14.0
CARCASS	8.5	18.0
LINER	8.5	8.0
BLACK SIDEWALL	11.0	9.0
BEAD INSULATION	1.0	1.0
CHAFER/APEX	8.0	1.0
BELT	7.0	1.5
TOTAL	79.0	72.5
REINFORCING COMPONENTS	21.0	27.5
	100	100

AVERAGE TIRE WEIGHT

20 POUNDS

100 POUNDS

- Calcium Carbonates (0-3%)
- Fumed Metal Oxides (0-5%)
 - Zinc Oxides
 - Titanium Dioxide
 - Aluminum Oxide

2.4 Specific Disposal Methods

With a growing environmental awareness and stricter legislation, the development of more efficient methods for disposing of scrap tires has become necessary. Table 2.2 obtained from the USEPA summarizes solutions using several methods along with targets and future trends in the U.S.

Dumping has now become an expensive operation, and is normally discouraged by local authorities because such sites are fire risks as well as unsightly. Landfill sites are becoming more scarce as Figure 2.3 illustrates and the cost of landfilling only increases as Figure 2.4 shows. Although these figures are representative of conditions in the U.S., the direction of the trends still apply to Canada.

A wide range of other disposal techniques are being investigated. These techniques include:

- building artificial tire reefs,
- installations of dock fenders,
- implementation of road crash barriers,
- use as river bed filling.

Unfortunately, these approaches provide only a minor solution to the whole disposal problem [Fletcher & Wilson].

Incineration is an old idea which has been reborn in recent years. Incineration of tires without heat recovery

TABLE 2.2: SCRAP TIRE SOLUTIONS

SOLUTION	1990 (%)	2000 (%)	FUTURE PROJECTED
RETREAD	11.7	13	13
BURNING FOR ENERGY	6.8	30	30
ASPHALT/CRUMB	0.5	15	30
NON-TIRE RECYCLED RUBBER	2	7	15
TIRE RELATED RECYCLED RUBBER	1	5	8
OTHER USES INCLUDING PYROLYSIS	1	2	4
LANDFILL	76.8	28	0

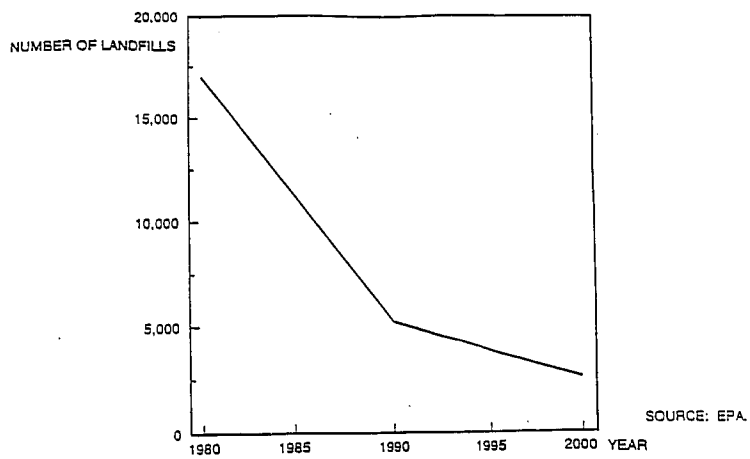


Figure 2.3: U.S. Landfills In Operation

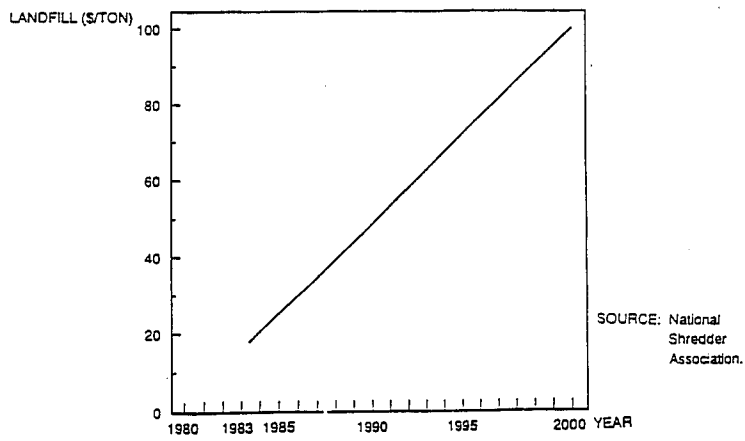


Figure 2.4: Average U.S. Landfill Costs

is disadvantageously placed in an energy-conscious environment, as none of the potential energy content of the tire may be recovered. However, the incorporation of a waste-heat recovery system is attractive. Environmental consequences of such systems force compliance requirements through clean air legislation. It is the cost of compliance which almost always outweighs the benefits of incineration. Also with a growing environmentally conscious society, incineration is anything but friendly to the environment even with state of the art air pollution control systems.

Pyrolysis is a breakdown of the basic molecular structure of the tire material by the action of heat. Heating takes place under anaerobic conditions referred to as destructive distillation or more commonly pyrolysis [Fletcher & Wilson]. Pyrolysis products include char, gas and liquid organics. Table 2.3 shows the products of pyrolysis along with their respective percentages.

Table 2.3: Products Of Pyrolysis

Products	% By Weight
Liquid Organics (oil)	50
Char (80-90% carbon black)	38
Gas	12

Source: Foster Wheeler Power Products, 1980

The practice of pyrolysis for profit on a large production scale is unusual because of the unreliability and high cost

of operation of a typical plant [Nakajima & Matsuyuki].

2.5 Reprocessed Rubber

Unvulcanized and thermoplastic elastomers present no special reclaiming problems since they can be simply chopped, milled and blended with new materials for recycling directly back into the same types of products from which they came.

Vulcanization of an elastomer serves to chemically cross-link the long polymer chains to restrict their movement. This process changes the characteristics of a polymer from a millable plastic material to a fairly rigid thermoset that in most cases cannot be replasticized by simple milling [Smith et al.].

The production of reprocessed rubber requires the processing of rubber products, like tires, to generate rubber fillers or ingredients that can be reincorporated in virgin rubber compounds. There are two basic methods for reprocessing rubbers. They involve:

- severing of cross-links by chemical or steam digestion to produce reclaim
- grinding rubber compounds by some form of mechanical method.

Figure 2.5 shows the distribution of the recycled rubber market in the U.S., with ground rubber taking the majority of the market.

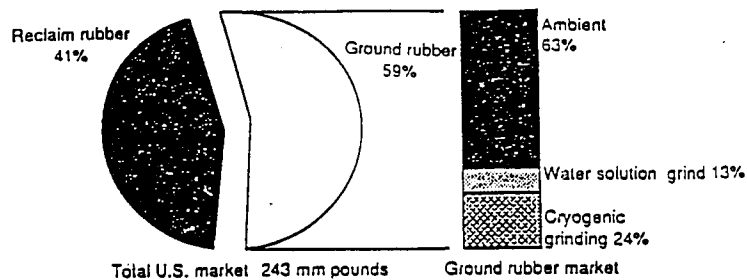


Figure 2.5: U.S. Recycled Rubber Market, 1990.

2.5.1 Reclaim Rubber

Reclaiming rubber by chemical digestion has been practised since the mid 1800s. The chemical digestion method remains in use today. It involves the use of chemical reagents, such as sodium hydroxide which acts as a devulcanizing agent.

One of the shortcomings of rubber reclaim is that it lowers the green strength and tensile strength of the compounds in which it is used. Reclaim was extensively used in tire components for many years, but with the advent of the radial tire and its need for specific properties, the use of reclaim in tires has been reduced significantly [Smith et al.].

2.5.2 Ground Rubber

Scrap rubber can be recycled by size-reduction, to produce *crumb* which can be used in a wide variety of applications or can be further processed by devulcanization

to produce reclaim. Devulcanization is more easily achieved with a fine feed and the reclaim can be used for new products. Comminution can also be a first step in pyrolysis and incineration where the increased surface area, increases the rate of process reaction.

There are three basic techniques for recycling scrap tires. These three techniques are:

- Ambient Grinding
- Cryogenic Comminution
- Wet or Solution Grinding

2.5.2.1 Ambient Grinding

Ambient grinding uses effective types of mechanical grinding equipment usually cracker mills or granulators. Particle reduction is accomplished by a shearing or tearing action [Baker]. Figure 2.6 depicts a flow diagram of a typical ambient grinding system. The rubber is ground to a particle size ranging from 10 to 30 mesh. A significant amount of heat is generated in this process. It can be sufficient to cause thermal degradation of the material. This degradation can sometimes lead to the formation of explosive gas mixtures. The elevated temperatures generated by the process also increases the risk of dust explosions. In conventional ambient systems, heat is removed by using large volumes of cool air [Daborn & Derry].

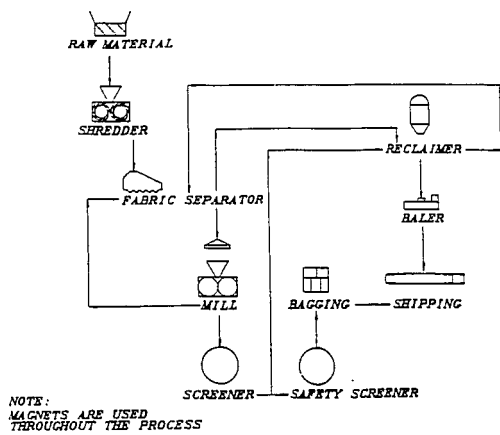


Figure 2.6: Basic Ambient Tire Grinding Process

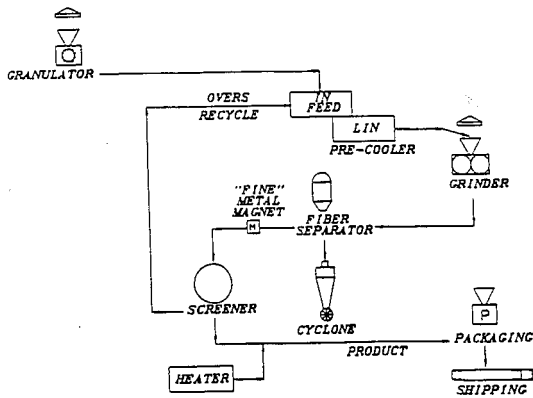


Figure 2.7: Basic Cryo Grinding System

2.5.2.2 Cryogenic Comminution

Cryogenic size reduction refers to a technique which uses the brittle behaviour of some materials at reduced temperatures (usually by liquid nitrogen (LIN) submersion) to aid in the shattering of the material to a reduced size. Figure 2.7 provides a schematic of a basic cryogenic grinding system. Cryogenics facilitate the crushing or grinding of material at a reduced power consumption relative to that at ambient temperatures. The market requirements for ground rubber are heading towards a finer grade of ground material. Cryogenics permit the size reduction of materials to much finer particles than can be achieved with ambient systems. The technique of cryogenic comminution also minimizes a build-up of heat in materials that might degrade. Economic viability of any scrap treatment technique is important when considering a cryogenic comminution process. The benefits gained must offset the costs (largely refrigerant) which would not be incurred with conventional ambient systems.

2.5.2.3 Wet or Solution Grinding

Wet or solution grinding is an ambient grinding process that reduces the particle size of rubber by grinding in a liquid medium. The process involves putting a coarse ground rubber crumb of 10 to 20 mesh into a liquid medium, usually water, and grinding the crumb between two closely spaced grinding wheels. Particle size is controlled by the time

spent in the grinding process. Particle sizes of less than 80 mesh can be expected from this system. The wet grind process requires a very effective drying system which is not required for ambient or cryogenic systems. The production capacity of a wet grind system is very limited compared to the ambient and cryogenic systems. Figure 2.8 provides a flowchart of a basic wet grinding system.

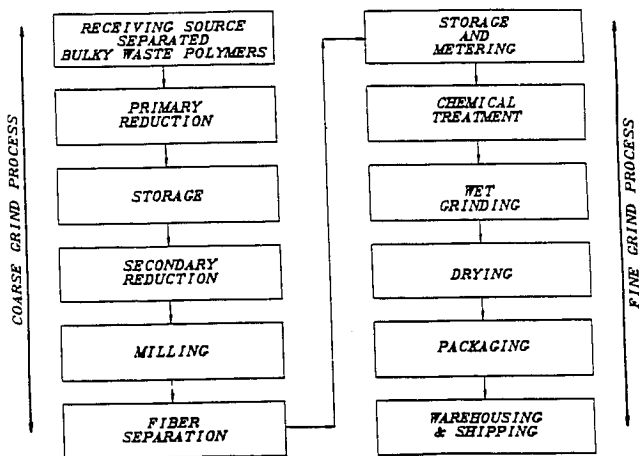


Figure 2.8: Basic Wet Grinding System

2.6 Cryogenically Recycled Materials

Determining whether a material can be affected by cryogenic temperatures and to what degree is critical, when trying to recycle solid waste cryogenically.

All recyclable materials can be classified into three categories [Michalski]. These classes include metals, ceramics, and polymers as illustrated in Figure 2.9.

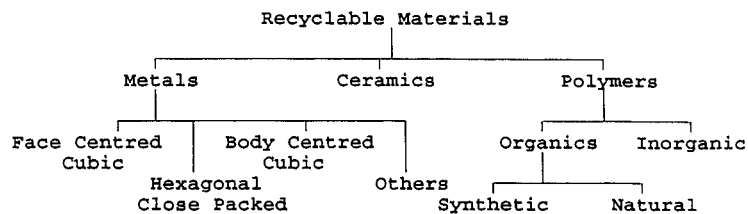


Figure 2.9: Materials Classification

Source: Michalski, P.H., A Classification of Materials Which Can Be Cryogenically Recycled, 1976.

The fundamental principle of the cryogenic process is the embrittlement of the material by simple cooling. The embrittled material will then fracture easily, to facilitate simple physical separation of the components. A material must be fractured in a brittle state to be classified as cryogenically recyclable. When a material exhibits no plastic deformations while being fractured, it is said to be brittle.

Some materials such as glass are brittle at room

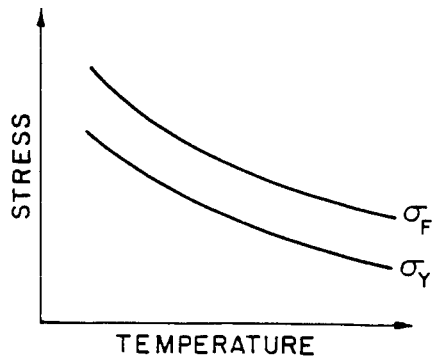
temperatures. Others such as tire rubber must be cooled well below ambient temperatures before they can become brittle. Materials such as aluminum are ductile at both ambient and at cryogenic temperatures.

To better understand brittle fracture and the factors affecting brittle fracture, it is helpful to first understand the yield (σ_y) and fracture (σ_f) stress behaviour of materials. Figure 2.10(a) provides an example of a material which would fracture in a ductile manner, yielding before fracture (unaffected by temperatures). Therefore, this material would not be classified as cryogenically recyclable. Figure 2.10(b) illustrates the yield (σ_y) and fracture (σ_f) stress behaviour of a material which is ductile at room temperature but brittle at some lower temperature. This type of material is said to go through a ductile-to-brittle transition at the brittle temperature T_b . Below T_b , the material would fracture in a brittle manner, fracturing before yielding. This type of material would be classified as cryogenically recyclable. Tables 2.4 and 2.5 provide listed classifications of metals and polymers which were tested by P.H. Michalski.

2.7 Cryogenic Operations And Processes

Once the cryogenically brittle characteristics of a material have been identified, the next step would be to process this material on a practical and cost effective basis using specific operations. Rubber which is ductile at

A) DUCTILE MATERIAL



B) MATERIAL WHICH GOES THROUGH A DUCTILE TO BRITTLE TRANSITION

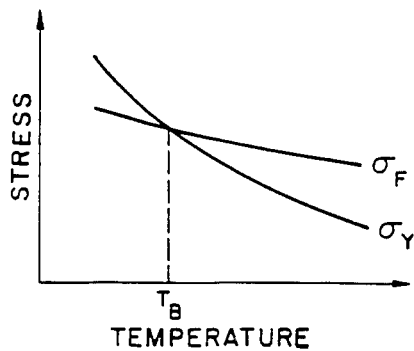


Figure 2.10: Yield Stress And Fracture of A) a ductile material and B) a material which goes through a ductile-to brittle transition.
Source: Michalski, P.H., A Classification Of Materials Which Can Be Cryogenically Recycled, M.S. thesis, University of Wisconsin-Madison, 1976.

TABLE 2.4: CLASSIFICATION OF METALS

Materials	Source	Brittle at 20°C	Brittle at -196°C	Ductile at -196°C
Iron				
Steel				
CR 1018	RRSN		X	
SAE 1020	Falk		X	
HR 1020	RRSN		X	
SAE 1045	Falk			X h
CR 1045	RRSN		X	
HR 1045	RRSN			X
Mild steel water pipe	—		X	
SAE 6155 (chrome vanadium)	Falk			X h
Stainless steel				
17-4 PA	RRSN			X
203 EZ	RRSN			X
303	RRSN			X
304	RRSN			X
316	RRSN			X
410	RRSN		X	
Stainless steel 416	RRSN			X
Cast iron				
Ductile	G&L*		X h	
Ductile (fully annealed)	Chromfed.* Mal.*	X h		
Ductile (80-55-06)	Chromfed. Mal.		X h	
Grey	Mil. Mat.*	X h		
Grey	Falk		X h	
Malleable	Mil. Mal.		X h	
Cast steel				
As cast #1	Falk			X h
As cast #1 (quenched and tempered)	Falk			X h
As cast #2	Falk			X h
Cast ASTM-A148	Falk			X h
Pelton P3	Pelton*		X h	
Pelton P4	Pelton		X h	
Pelton P10	Pelton			X h
Cast 4140	SIGNICAST		X	
Cast 8620	SIGNICAST		X	
Cast stainless				
SS 316	SIGNICAST			X
SS 25-5PH	SIGNICAST			X
Lead base babbit	Falk	X h		
Tin base babbit	Falk		X h	

* Industry supplying materials for the test.

Courtesy of Michalski, P. H., A Classification of Materials Which Can Be Cryogenically Recycled, M. S. thesis, University of Wisconsin—Madison, 1976, 42.

TABLE 2.5: CLASSIFICATION OF POLYMERS

Materials	Source	Brittle at 20°C	Brittle at -196°C	Ductile at -196°C
Acrylonitrile butadien styrene (ABS)	FLMB*		X	
Acrylonitrile butadien styrene (ABS)	WSTRN PLSTCS*		X	
Alkyd molded parts	PL*	X		
Cellulose acetate butyrate	WSTRN PLSTCS		X	
Fiberglass rod	RRSON*	X		
Melamine/phenolic	PL	X		
Melamine/phenolic	Red Rock*	X		
Nylon	FLMB			X
66 Nylon	Bemis*			X
66 Nylon	WSTRN PLSTCS			X
Nylon filled with molybdenum disulfate	WSTRN PLSTCS			X
66 nylon plus modifier	G.E.*	X		
Phenolic	G.E.	X		
Phenolic	P.L.	X		
Phenolic	P.L.	X		
Phenolic	Red Rock	X		
Phenolic	Red Rock	X		
Phenolic	LAPCOR*	X		
Polyacetal	G.E.	X		
Polyacetal	WSTRN PLSTCS	X		
Polyacetal celcon	FLMB	X		
Polybutylene terephthalate	LWS*	X		
Polycarbonate	G.E.			X
Polycarbonate	Dstt*			X
Polycarbonate	FLMB			X
Polycarbonate	WSTRN PLSTCS			X
Polycarbonate	LWS			X
Polyester plus glass Fibers	G.E.	X		
Polyethylene — low density	FLMB			X
Polyethylene — low density	WSTRN PLSTCS			X
Polyethylene — low density	LWS			X
Polyethylene — low density	LWS			X
Polyethylene — low density	WSTRN PLSTCS			X
Polyethylene — high density	FLMB			X
Polyethylene — high density	Burton*			X
Polyisoprene (natural rubber)	G.E.	X		
Polymethylmethacrylate (PMMA)	G.E.	X		
Polymethylmethacrylate (PMMA)	Dstt	X		
Polypropylene	FLMB			X
Polypropylene	LWS	X		
Polypropylene	WSTRN PLSTCS	X		
Polypropylene — impact grade	WSTRN PLSTCS			X
Polypropylene — co-polymer	LWS			X
Polypropylene — oxide	LWS			X
Polystyrene	FLIXIB	X		
Polystyrene	WSTRN PLSTCS	X		
Polystyrene	LWS	X		
Polystyrene — medium impact grade	WSTRN PLSTCS	X		

room temperature will fracture when its temperature is reduced to -62°C (-80°F) [Braton]. Cryogenic processing liberates the components in a tire (namely rubber, fibre and steel) into clean streams having monetary value. The main criterion for cryogenic processing is that one or more of the components in an item must have an attainable cold cracking temperature. In a tire that component would be the rubber, since the steel and fibre retain their ductile characteristics at cryogenic temperatures. Figure 2.11 provides a schematic flowchart of the basic operations for recovering the components (rubber, steel and fibre) from a tire.

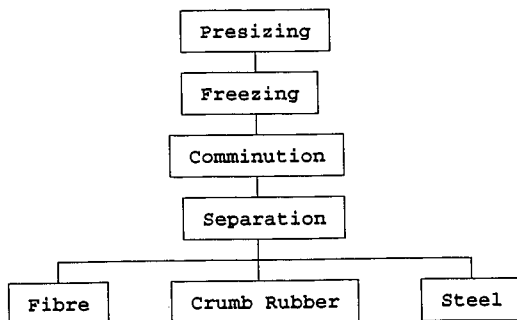


Figure 2.11: A Schematic Of A Basic Recovery System For Recovering Tire Components.

2.7.1 Presizing

The scrap tire is reduced in size to pieces that are easier to process and handle. The size of the stock entering the freezing system, generally determines the required time of freezing needed to ensure that the temperature of the material is reduced to its embrittlement temperature.

2.7.2 Freezing Systems

In cryogenic processing of scrap tires, it is critical that the scrap tire chips are reduced to their cold cracking temperature (-62°C) just prior to being comminuted. This is done by subjecting the material to a cryogenic environment for a sufficient period of time. The cooling media can be liquid, gaseous, or liquid-gaseous.

2.7.2.1 Immersion Batch Freezing

In this freezing method the material is simply submerged in the liquid refrigerant for a sufficient period of time, to reduce the material to its embrittlement temperature. Caution must be taken when using this method, since violent boiling of the liquid occurs when the material is submerged into the cryogen.

2.7.2.1 Liquid Cryogen Freezing Systems

The most efficient use of a cryogen would be to utilize the liquid and the vaporized liquid systems. When the liquid is sprayed on to the material, it vaporizes and it is this vapour that is used to precool the material. A

tubular chamber would be suited for this method of cooling. Near the discharge end of the tunnel the product is sprayed with the liquid cryogen. The vapourized cryogen is directed down the tunnel toward the feed end. Heat is removed from the product as this vapour progresses over the incoming raw material in a counterflow pattern [Biddulph]. Figure 2.12 illustrates a typical liquid nitrogen freezing tunnel system. The tunnel is sectioned into two regions. The discharge end is the cooler section. The larger area near the feed end is the precooler. An exhaust fan is utilized to pull the vapour towards the inlet and provide precooling.

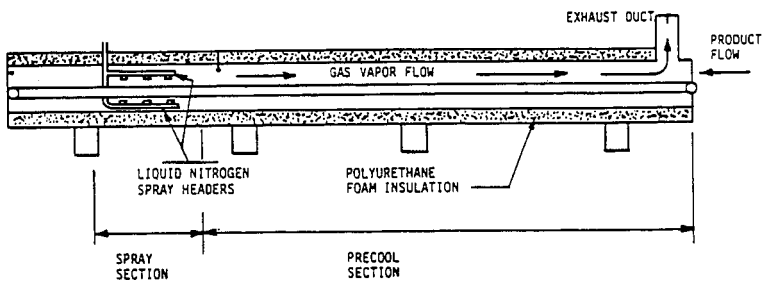


Figure 2.12: Cross-sectional View Of A Typical Liquid Nitrogen Freezing Tunnel.

2.7.3 Size Reduction Of Materials

Following the freezing operation, a material must be comminuted by some method. There are four mechanical methods for reducing the size of materials. These methods are:

- Attrition

- Shearing
- Compression
- Impaction

Attrition is the physical destruction of one material by another which is harder than the first. The sharpening of a tool by a grinding wheel is an example of attrition.

Shearing is accomplished by passing material between two adjacent blades as they move past each other. The cutting action of scissors is an example of shearing.

In Compression, objects are fragmentized by applying a compressive force to the object at rest.

In Impaction, brittle objects can be fragmented by subjecting them to a force. If a pane of glass is struck with a hammer, it will shatter into many pieces. Hammermills are machines which operate on this principle. They have been used for decades to pulverize materials.

2.7.4 Product Separation

After scrap materials have been pulverized by some method of size reduction, the resulting product must be processed further to separate the ground tire into separate rubber, fibre and steel streams. This is accomplished by using methods such as magnetic attraction, oscillating or rotating screens, gravity systems, or fluidized bed techniques.

2.8 Potential Applications For Cryogenic Tire Crumb

The key to commercialization of cryogenic processing for scrap tires, as with most recycling operations, lies in finding suitable applications for the output of the process. The most obvious uses for the products are those which utilize the properties built into the original tires [McMillan]. Some present and potential applications include:

Rubber Crumb

- Commercial carpet underlay
- Industrial flooring
- Playgrounds
- Floor tiles
- Subsoil drainage
- Irrigation pipes
- Cable Insulation
- Car underseal
- Weather proof coatings
- Cattle runs & stables
- Friction linings (brakes)
- Asphalt
- Mouldings (shoe soles, car mats)
- Domestic surfacing (patios, paths)
- Sports surfaces (running tracks, tennis courts)

Fibre

- Building boards
- Felt
- Insulation
- Concrete filler

Steel

- Scrap recycling

III. DETERMINING A WORST CASE MODEL

In any design the worst case conditions must always be considered in determining an adequate working model. Figure 3.1 illustrates a cross-section of a typical used tire which consists of rubber, nylon, and steel. From Table 3.1 it is possible to determine the characteristics of an average piece of pre-sized rubber tire, but how accurately will it represent the actual composition of a typical pre-sized piece of tire? After all, most pieces will not be like the average piece, because some may not contain any nylon or steel. This variation in composition is critical because all components of the piece will affect its cooling rate. A model designed for the average will fail for those pieces that are below average.

This chapter will provide some properties of materials that will facilitate the development of a worst case model.

Table 3.1: Composition of a typical automobile tire.

Component	Weight (lbs.)*	% Weight
Rubber	12	63
Nylon	6	32
Steel	1	5
	Σ 19	Σ 100

* For an average tire

Source: Cryogenic Recycling Of Solid Wastes; N.R. Braton)

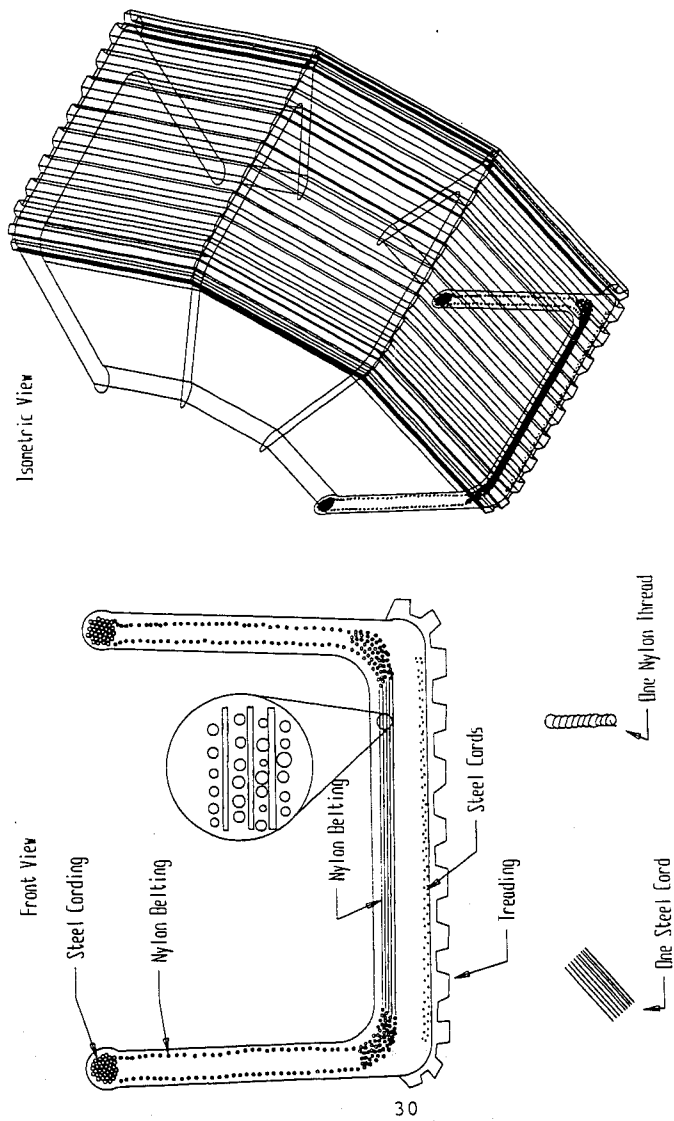


Figure 3.1: A Cross-section Of A Typical Tire.

3.1 Conduction

Conduction may be viewed as the transfer of energy from the more energetic to the less energetic particles of a substance due to interactions between the molecules [Incropera & Dewitt]. Higher temperatures are associated with higher molecular energies, through constant collisions with their neighbours, a transfer of energy from the more energetic to the less energetic molecules must occur.

In the presence of a temperature gradient, energy transfer by conduction must occur in the direction of decreasing temperature [Holman].

The net transfer of energy by random molecular motion can be described as a *diffusion* of energy [Incropera & Dewitt].

An example of conduction heat transfer occurs when an object at room temperature is suddenly immersed in an ice cold liquid bath. There will be significant heat loss from the object to the ice bath. This loss is principally due to conduction heat transfer through the walls of the object to the liquid.

3.1.1 Fourier's Law

The heat transfer process is quantified in terms of rate equations. These equations may be used to compute the amount of energy being transferred per unit time.

For heat conduction, the rate equation is known as *Fourier's Law*. For a one dimensional wall shown in Figure

3.2 having a temperature distribution $T(x)$, the rate equation is expressed as, [Incropera & Dewitt]

$$q''_x = -k \, dT/dx$$

where,

q''_x = heat flux (W/m^2), is the heat transfer rate in the x direction per unit area perpendicular to the direction of transfer,

dT/dx = temperature gradient in the x direction,

k = proportionality constant, is a transport property known as the thermal conductivity ($W/m \cdot K$) and is a characteristic of the wall material.

The minus sign simply indicates that heat is transferred in the direction of decreasing temperature.

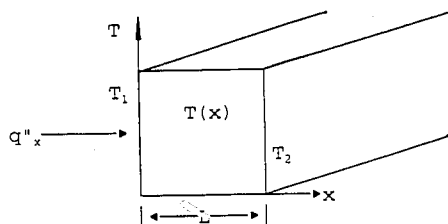


Figure 3.2: One Dimensional Heat Transfer By Conduction.

Since q''_x is the heat flux, the heat transfer rate may be expressed using q''_x , according to: [Holman]

$$Q_x = A \cdot q''_x = -k \cdot A \cdot dT/dx$$

where

Q_x = Heat transfer rate (W),

A = Area (m^2) perpendicular to direction of heat transfer,

q''_x = Heat flux (W/m^2).

Figure 3.2 illustrates the direction of heat flow q''_x in a one dimensional coordinate system when the temperature gradient dT/dx is negative.

Recognizing that the heat flux is a vector quantity, Figure 3.3 provides a general statement of the conduction rate equation according to Fourier's law in the form, [Incropera & Dewitt]

$$q'' = -k\nabla T = -k [i(dT/dx) + j(dT/dy) + k(dT/dz)]$$

where

∇ = is the three dimensional del operator,

$T(x,y,z)$ = is the scalar temperature field.

A more general and simplified form of the heat conduction rate can be written in terms of:

$$q''_x = -k \frac{\delta T}{\delta x} \quad q''_y = -k \frac{\delta T}{\delta y} \quad q''_z = -k \frac{\delta T}{\delta z}$$

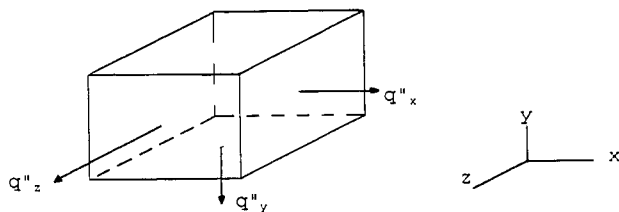


Figure 3.3: Heat Flux Vectors In A 3-dimensional Coordinate System.

Each of these expressions relate the heat flux across a surface to the temperature gradient in a direction perpendicular to the surface.

3.1.2 Thermal Properties Of Matter

Fourier's law requires values of thermal conductivity. This property is referred to as a transport property, and provides an indication of the rate at which energy is transferred by diffusion. It depends on the physical structure of matter (atomic and molecular), which is related to the state of the matter. Figure 3.4 illustrates the range of thermal conductivities for various states of matter.

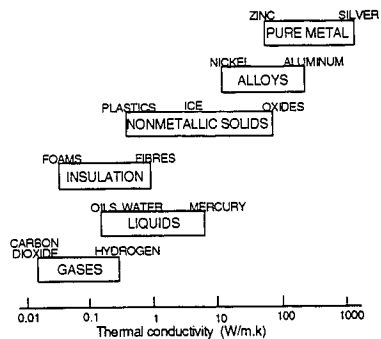


Figure 3.4: Range Of Thermal Conductivity For Various States Of Matter At Normal Temperatures And Pressure.

3.1.3 Thermal Diffusivity

In an analysis of heat transfer involving tire rubber, it is necessary to incorporate several properties of the tire rubber. These properties are generally referred to as thermophysical properties and include two distinct categories, transport and thermodynamic properties.

Transport properties include the thermal

conductivity(k) while thermodynamic properties include density(ρ) and specific heat(C_p).

The product ρC_p (J/m^3K) is commonly called the volumetric heat capacity, and measures the ability of a material to store thermal energy [Incropera & Dewitt].

In heat transfer analysis, the ratio of the thermal conductivity to the volumetric heat capacity is an important property termed the thermal diffusivity(α) where:

$$\alpha = k/(\rho C_p) \quad (m^2/s)$$

This quantity defines the ability of a material to conduct thermal energy relative to its ability to store thermal energy [Incropera & Dewitt]. Materials having high α values will respond quickly to changes in their thermal environment, while materials having low α values will respond more sluggishly, taking longer to reach a new equilibrium condition [Incropera & Dewitt]. In practice, tire rubber requires a long residence time to reach its embrittlement temperature because of its inability to conduct energy which is due to its low thermal diffusivity ($6.2 \cdot 10^{-8} \text{ m}^2/\text{s}$).

3.2 Determining A Worst Case Model

To determine which materials in a tire control the rate of cooling, the thermal diffusivities of all three materials must be compared using the following data:

	Steel	Nylon	Rubber	
k	43 ^a	0.24 ^b	0.15 ^b	(W/m'C)
Cp	473 ^a	1674 ^c	2010 ^b	(J/kg'C)
ρ	7801 ^a	1140 ^c	1200 ^a	(kg/m ³)

^a Heat Transfer, Holman

^b Elastomers, Synthetic Vol. 5

^c Engineering Properties & Application Of Plastics, Kinney

Thermal Diffusivity Calculations

$$\alpha_{\text{rubber}} = k/\rho C_p = 0.15/(1200 \cdot 2010) = \underline{6.22 \cdot 10^{-8}} \text{ m}^2/\text{s}$$

$$\alpha_{\text{nylon}} = k/\rho C_p = 0.24/(1140 \cdot 1674) = \underline{1.26 \cdot 10^{-7}} \text{ m}^2/\text{s}$$

$$\alpha_{\text{steel}} = k/\rho C_p = 43/(7801 \cdot 473) = \underline{1.17 \cdot 10^{-5}} \text{ m}^2/\text{s}$$

3.3 Discussion

The thermal diffusivity of rubber is clearly the lowest, with the value for nylon being twice that of rubber. Steel has a still higher thermal diffusivity. These data indicate that rubber will respond more sluggishly to a temperature difference than nylon or steel. In other words nylon actually cools at a faster rate than rubber. The make-up of any pre-sized piece of tire which contains nylon and/or steel is illustrated in Figure 3.5. The nylon and/or steel run straight through the rubber. This arrangement helps the cooling process. The nylon and/or steel act as conductors with respect to the rubber.

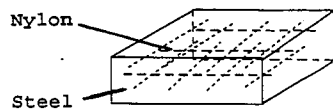


Figure 3.5: A pre-sized piece of tire containing rubber, nylon & steel.

Therefore, the worst case condition to reach a given cryogenic temperature would be that of a solid piece of rubber rather than of a composite piece.

IV. THEORETICAL COOLING CURVES

If a solid body is suddenly subjected to a change in its environment, some time must elapse before an equilibrium temperature is established in the body. This equilibrium condition is defined as steady state.

Transient heating and cooling occur during an interim period before equilibrium is established. Analysis must be designed to account for the change in energy of the body with time. The boundary conditions must be adjusted to match the physical conditions that prevail during the unsteady-state heat-transfer operation [Holman]. For example, when the surface temperature of a system is altered, the temperature at each point in the system will also begin to change. The changes will continue until a steady-state temperature distribution is reached.

Unsteady-state heat-transfer analysis is of practical interest because of the large number of heating and cooling operations that must be examined in industrial applications.

Some cases for which solutions have been obtained by previous investigations are discussed in detail later. Because such solutions are often difficult to obtain, the simplest approach is preferred whenever possible. The lumped capacitance method is one approach which may be used when temperature gradients within the solid are small [Incropera & Dewitt].

4.1 Lumped Capacitance Method

Simple transient conduction occurs when a solid experiences a sudden change in its thermal environment. Consider a piece of rubber, initially at a uniform temperature T_i , that is quenched by immersion in a liquid of lower temperature $T_{oo} < T_i$, as shown in Figure 4.1.

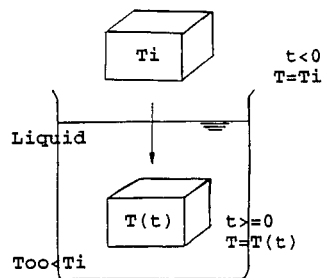


Figure 4.1 : A Piece Of Rubber Immersed In A Quenching Liquid.

If quenching begins at time $t=0$, the temperature of the solid will decrease for some time $t>0$, until it eventually reaches T_{oo} . This reduction in temperature is due to convective heat transfer at the solid-liquid interface [Incropera & Dewitt]. The lumped capacitance method is valid when temperature gradients within the solid are negligible.

The convective heat loss from the body is equivalent to a decrease in the internal energy of the body, as shown in

Figure 4.1; according to

$$Q_{\text{conv}} = hA(T - T_{\infty}) = -C \rho V \frac{dT}{dt}$$

where

A is the surface area for convection,

V is the volume of the body.

If the initial condition is written as

$$T = T_i \quad @ \quad t = 0$$

the solution is, [Holman]

$$\frac{T - T_{\infty}}{T_i - T_{\infty}} = \exp\left(-\frac{hA}{\rho CV}t\right)$$

The quantity $C\rho V/hA$ is called the time constant of the system because it has the dimensions of time.

$$t = \frac{C\rho V}{hA}$$

Lumped Capacity Analysis Applicability

An analysis may be expected to yield reasonable estimates when the following condition is met [Holman]

$$Bi = \text{Biot Number} = \frac{h(V/A)}{k} < 0.1$$

where

k is the thermal conductivity of the solid, (W/m°C)
 V is the volume, (m³)
 A is the surface area, (m²)
 h is the heat transfer coefficient of the environment, (W/m²°C).

The following example demonstrates the applicability of the lumped capacity method.

Example [Holman]

A steel ball [$C_p=0.46$ KJ/Kg°C, $k=35$ W/m°C] 5.0 cm in diameter, and initially at a uniform temperature of 450°C is suddenly placed in a controlled environment in which the temperature is maintained at 100°C. The convective heat transfer coefficient is 10 W/m²°C. Calculate the time required for the ball to attain a temperature of 150°C.

Solution

Check Bi;

$$Bi = \frac{h(V/A)}{k} = \frac{10[(4/3)\pi(0.025)^3]}{4\pi(0.025)^2(35)} = 0.0023 < 0.1$$

Therefore, the Lumped Capacity Method may apply.

For,

$T=150^\circ\text{C}$	$\rho=7800$ kg/m ³
$T_{\infty}=100^\circ\text{C}$	$h=10$ W/m ² °C
$T_0=450^\circ\text{C}$	$C=460$ J/kg°C

$$\frac{hA}{\rho CV} = \frac{(10)4\pi(0.025)^2}{7800(460)(4\pi/3)(0.025)^3} = 3.344 \times 10^{-4} \text{ sec}^{-1}$$

$$\frac{T-T_{\infty}}{T_0-T_{\infty}} = \exp^{-[hA/\rho CV]t}$$

$$\frac{150-100}{450-100} = \exp^{-3.344 \times 10^{-4}t}$$

$$t = 5819 \text{ sec} = 1.62 \text{ hr.}$$

4.2 Spatial Effects

Situations frequently arise for which the lumped capacitance method is inappropriate and alternative methods must be used. Regardless of the particular method, we must

now appreciate that the thermal gradients within the medium are no longer negligible [Incropera & Dewitt].

Exact, analytical solutions to transient conduction problems have been obtained for many simplified geometries and boundary conditions. Several mathematical techniques, including the method of separation of variables, may be used. However this series may be approximated by a single term and the results may be represented in a convenient graphical form.

4.2.1 Graphical Representations

Graphical representations of the approximate relations for the transient temperature distributions and energy transfers were first presented by Heisler and Grober et al. [Incropera & Dewitt]. The graphs have been widely used for nearly four decades. In addition to offering computational convenience, they illustrate the functional dependence of the transient, dimensionless temperature distributions on the Biot and Fourier numbers.

The results for the plane wall presented in Figures 4.2, 4.3, 4.4 and 4.5 may be used to obtain the midplane temperature of the wall, $T(0,t)=T_0(t)$, at any time during the transient process. If T_0 is known for particular values of Fo and Bi , Figure 4.4 may be used to determine the corresponding temperature at any location off the midplane.

Figure 4.4 must be used in conjunction with Figure 4.2 and/or Figure 4.3. For example, to determine the surface

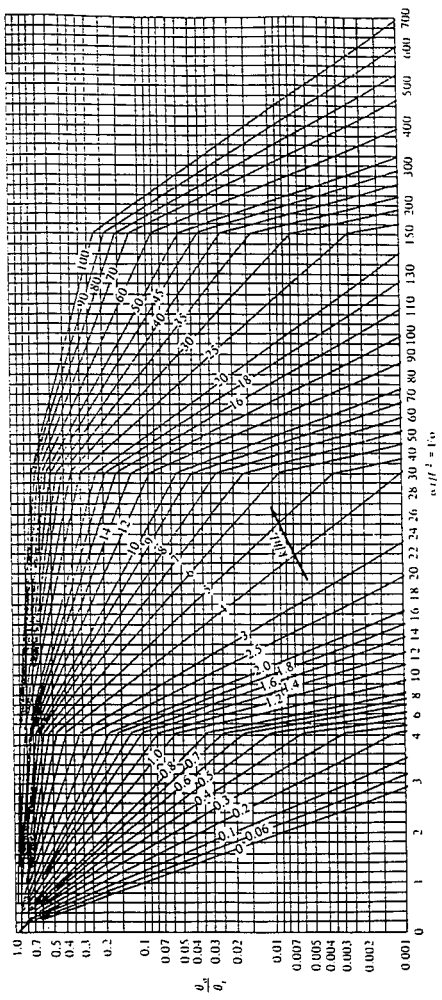


Figure 4.2: Midplane Temperature For An Infinite Plate.

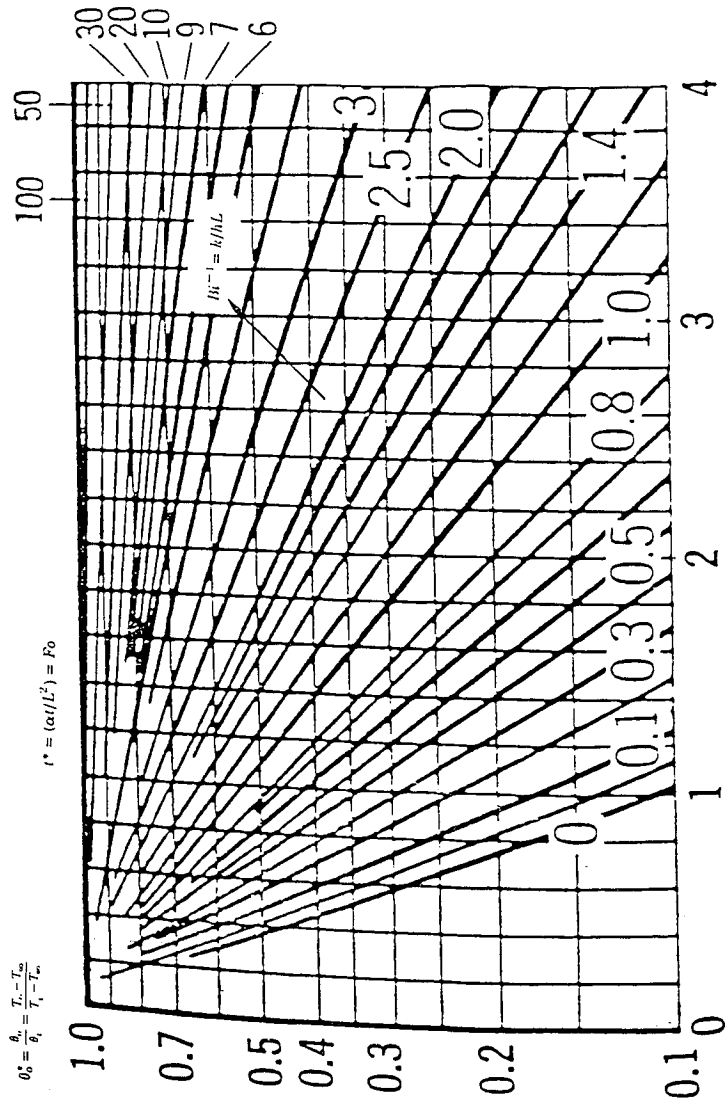


Figure 4.3: Midplane Temperature For An Infinite Plate (Blow-up).

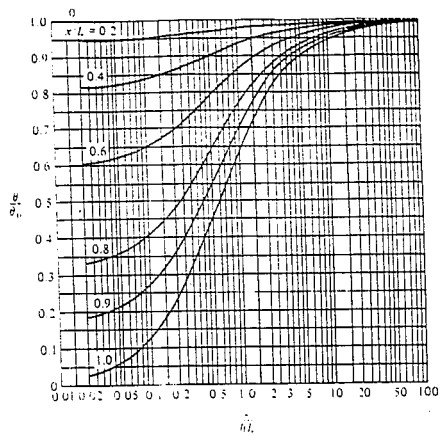


Figure 4.4: Temperature As A Function Of Center Temperature In An Infinite Plate.

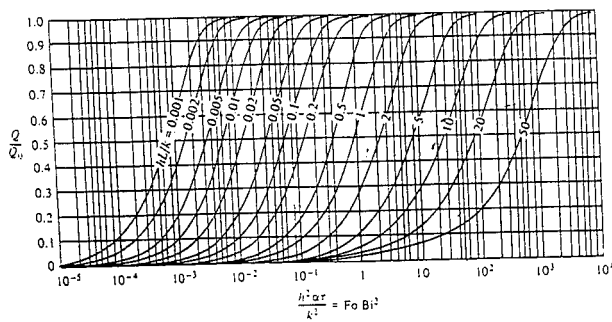


Figure 4.5: Dimensionless Heat Loss Of An Infinite Plate.

temperature at some time t , Figure 4.2 and/or Figure 4.3 would first be used too determine T_o at t . Figure 4.4 would then be used to determine the surface temperature from a knowledge of T_o .

Graphical results for the energy transferred from a plane wall over the time interval t are presented in Figure 4.5. The dimensionless energy transfer Q/Q_o is expressed exclusively in terms of the Fourier(F_o) and Biot(Bi) numbers. Q_o represents the initial internal energy content of the body with reference to the environment temperature according to

$$Q_o = \rho * C * V * (T_i - T_{oo}) = \rho * C * V * \theta_i$$

where,

T_i = initial temperature
 T_{oo} = environment temperature

In these figures, Q is the actual heat lost by the body during time t required to reduce the body temperature to $T(t)$.

The applicability of the Heisler Charts is restricted to values of the Fourier number greater than 0.2 for absolute accuracy.

The time required for the centre of a piece of rubber to reach embrittlement temperature is of greatest interest. The Fourier number for this determination is well within the parameters for accuracy. As a result the graphical methods will be appropriate for this investigation [Holman].

4.2.2 Multidimensional Systems

The Heisler charts may be used to obtain the temperature distribution in an infinite plate of thickness $2L$. When a wall whose height and depth dimensions are not large compared to the thickness, additional space coordinates are necessary to specify the temperature. Consequently the charts are no longer applicable. As a result we are forced to seek another method of solution. Fortunately, it is possible to combine the solutions for the one dimensional systems in a very straightforward way to obtain solutions for the multidimensional problems.

It can be shown that the dimensionless temperature distribution may be expressed as a product of the solutions for two plates thickness $2L_1$ and $2L_2$, (as in the case of a bar). Figure 4.6 shows an infinite rectangular bar with dimensions $2L_1 \times 2L_2$.

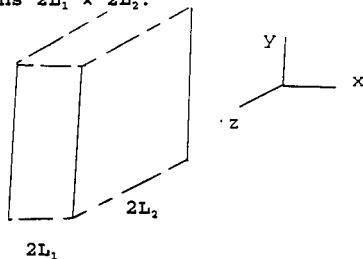


Figure 4.6 : Infinite Rectangular Bar.

According to this approach it is possible to write

$$\frac{T-T_{\infty}}{T_i-T_{\infty}}_{\text{bar}} = \frac{T-T_{\infty}}{T_i-T_{\infty}}_{2L_1 \text{ plate}} * \frac{T-T_{\infty}}{T_i-T_{\infty}}_{2L_2 \text{ plate}}$$

where

T_i is the initial temperature of the bar and

T_{oo} is the environment temperature.

The product solutions are assumed to be

$$T_1 = T_1(x,t) \quad T_2 = T_2(z,t)$$

Therefore, the dimensionless temperature distribution for the infinite rectangular bar may be expressed as a product of the solutions for two plate problems of thickness $2L_1$ and $2L_2$ [Holman].

$$T(x,z,t) = T_1(x,t) * T_2(z,t)$$

Similarly, the solution for a three-dimensional block may be expressed as a product of three infinite plate solutions for plates having the thicknesses as shown in Figure 4.7.

Figure 4.7 shows product solution for temperatures in a multidimensional rectangular parallelepiped system.

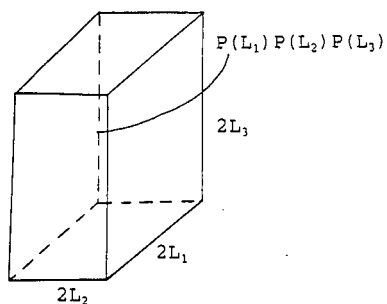


Figure 4.7 : Product Solution For Rectangular Parallelepiped System.

4.2.3 Heat Transfer In Multidimensional Systems

It is possible to superimpose the heat-loss solutions for one-dimensional bodies, to obtain the heat loss for a multidimensional body. For a multidimensional body formed by intersection of three one-dimensional systems, the loss is given by [Holman]

$$(Q/Q_0)_{tot} = (Q/Q_0)_1 + (Q/Q_0)_2 [1 - (Q/Q_0)_1] + (Q/Q_0)_3 [1 - (Q/Q_0)_1] [1 - (Q/Q_0)_2]$$

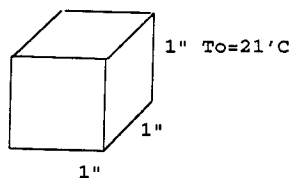
4.2.4 Multidimensional Problems

The following calculation is a straightforward, step-by-step manipulation of a typical three dimensional problem.

A 1" cube of rubber is immersed into liquid nitrogen. The liquid nitrogen is at a temperature of -180°C and the initial temperature of the cube is 21°C . Find,

- centre temperature after 300 sec,
- heat-loss,
- time required to cool the centre to -80°C .

$T_{\infty} = -180^{\circ}\text{C}$



$$\rho' = 1200 \text{ kg/m}^3 \quad C_p' = 2010 \text{ J/kg} \cdot \text{C}$$

$$k' = 0.15 \text{ W/m} \cdot \text{C} \quad \alpha' = 6.2 \cdot 10^{-8} \text{ m}^2/\text{s}$$

$h' = 100 \text{ W/m}^2 \cdot \text{K}$ (dipping into liquid nitrogen)

$h' = 20 \text{ W/m}^2 \cdot \text{K}$ (gas phase cooling over liquid nitrogen)

$h' = 400 \text{ W/m}^2 \cdot \text{K}$ (splashing liquid nitrogen)

'A Heat Transfer Textbook, Lienhard
Cryogenic Embrittlement Of Steel, Biddulph

Solution

a) Centre temperature after 300 seconds

Check Bi for Lumped capacity analysis.

$$\text{Volume } V = (0.0254)^3 = 1.64 \cdot 10^{-5} \text{ m}^3 \quad \text{Area } A = 6(0.0254)^2 = 3.87 \cdot 10^{-3} \text{ m}^2$$

$$\text{Bi} = \frac{h(V/A)}{k} = \frac{100(1.64 \cdot 10^{-5} / 3.87 \cdot 10^{-3})}{0.15} = 2.83 > 0.1$$

Therefore, Lumped Capacity Analysis is inappropriate.

Use Multidimensional Systems.

For a rubber block (1" cube), using the solution from

Figure 4.7,

$$\frac{k}{hL} = \frac{0.15}{100(0.0127)} = 0.118 \quad \text{Fo} = \frac{\alpha \cdot t}{L^2} = \frac{6.2 \cdot 10^{-8}(300)}{(0.0127)^2} = 0.0115$$

From Figures 4.3 and 4.4

$$\frac{\theta_c}{\theta_i} = 0.95 \quad \frac{\theta_c}{\theta_o} = 1 \quad \text{where } (x/L) = 0/0.0127 = 0 \\ x = 0 \text{ @ centre}$$

$$(\theta/\theta_i)_{\text{plate}} = (0.95)(1) = 0.95$$

$$\text{Therefore, Sol'n} = (\theta/\theta_i)_{\text{cube}} = P(x_1)P(x_2)P(x_3) \\ = 0.95(0.95)0.95 \\ = 0.857$$

Therefore,

$$\begin{aligned} T_c &= T_{oo} + 0.857(T_o - T_{oo}) \\ &= -180 + 0.857(21 - (-180)) \\ &= -7.743 \text{ } ^\circ\text{C} \\ &= 265.3 \text{ } ^\circ\text{K} \end{aligned}$$

b) Heat loss for cube

Start with the heat-loss ratio for an infinite plate for which

$$L = 0.0127 \text{ m}$$

Using properties of rubber;

$$\frac{hL}{k} = \frac{100(0.0127)}{0.15} = 8.47$$

$$\begin{aligned} FoBi^2 &= \frac{h^2 \alpha t}{k^2} = \frac{100^2(6.2 \times 10^{-8})(300)}{(0.15)^2} \\ &= 8.27 \end{aligned}$$

From Figure 4.5

$$(Q/Q_o) = 0.15 \quad \text{since dimensions in all directions are equal (cube),}$$

therefore,

$$(Q/Q_o) = (Q/Q_o)_1 = (Q/Q_o)_2 = (Q/Q_o)_3$$

$$\begin{aligned} (Q/Q_o)_{\text{tot}} &= (Q/Q_o)_1 + (Q/Q_o)_2 [1 - (Q/Q_o)_1] + (Q/Q_o)_3 [1 - (Q/Q_o)_1] [1 - (Q/Q_o)_2] \\ &= 0.15 + 0.15(1 - 0.15) + 0.15(1 - 0.15)(1 - 0.15) \\ &= 0.386 \end{aligned}$$

$$\begin{aligned} Q_o &= \rho C V (T_o - T_{oo}) = \rho C V \theta_i \\ &= 1200(2010)(1.64 \times 10^{-5})(21 - (-180)) \\ &= 7950.9 \text{ J} \end{aligned}$$

Therefore the actual heat loss in 300 seconds time is,

$$\begin{aligned} Q &= 7950.9(0.386) \\ &= 3069.1 \text{ J} \end{aligned}$$

c) Time required to cool the centre to -80°C.

$$\begin{aligned} T_c &= T_{\infty} + (\theta/\theta_1)_{\text{cube}}(T_0 - T_{\infty}) \\ -80 &= -180 + (\theta/\theta_1)_{\text{cube}}(21 - (-180)) \\ (\theta/\theta_1)_{\text{cube}} &= 0.498 \end{aligned}$$

$$(\theta/\theta_1)_{\text{cube}} = P(x_1)P(x_2)P(x_3)$$

$$\begin{aligned} P(x_1) &= P(x_2) = P(x_3) \\ P(x) &= (0.498)^{(1/3)} \\ &= 0.793 \end{aligned}$$

$$(\theta/\theta_1)_{\text{plate}} = 0.793$$

where $x/L=0$ @ the centre, from Figure 4.4,

$$\theta/\theta_0 = 1$$

$$\theta/\theta_1 = \theta_0/\theta_1 * \theta/\theta_0$$

$$\theta/\theta_1 = 0.793$$

Therefore from Figure 4.2 and/or 4.3,

$$Fo = \frac{\alpha * t}{L^2} = 0.24 \quad \text{---> } k/(hL) = 0.15/(100(0.0127)) = 0.118$$

$$\begin{aligned} t &= \frac{L^2(0.24)}{\alpha} = \frac{(0.0127)^2(0.24)}{6.2 * 10^{-8}} \\ &= 624.3 \text{ sec} \\ &= 10.4 \text{ min} \end{aligned}$$

4.3 Theoretical Investigation

A series of theoretical calculations were carried out for rubber blocks of different sizes. These blocks were cubes of the following sizes 1/2", 1" and 2". Three different modes of cooling were investigated:

- Dipping into liquid nitrogen,
- Gas phase cooling in liquid nitrogen, and
- Splashing or spraying of liquid nitrogen.

All three sized blocks were assumed to be cooled according to the three modes. The objective of the investigation was to determine the relationship between time and centre temperature for the cubes. Appendices I, II, and III provide the results in the form of tables and graphs, which were derived from all three sizes of cubes and all three cooling modes. Figures 4.8, 4.9, and 4.10 illustrate the results for the 1/2", 1", and 2" sizes respectively.

Appendices IV, V and VI illustrate the calculations for nitrogen consumption for each mode (grams of nitrogen/grams of rubber). Figure 4.11 provides a plot of nitrogen consumption in grams per gram of rubber versus centre temperature of a 1" cube of rubber for all three cooling modes.

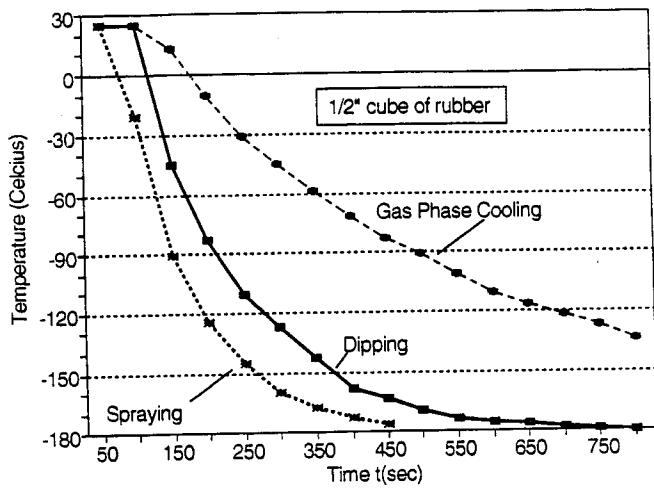


Figure 4.8: Dependence of centre temperature on cooling time for three cooling modes.

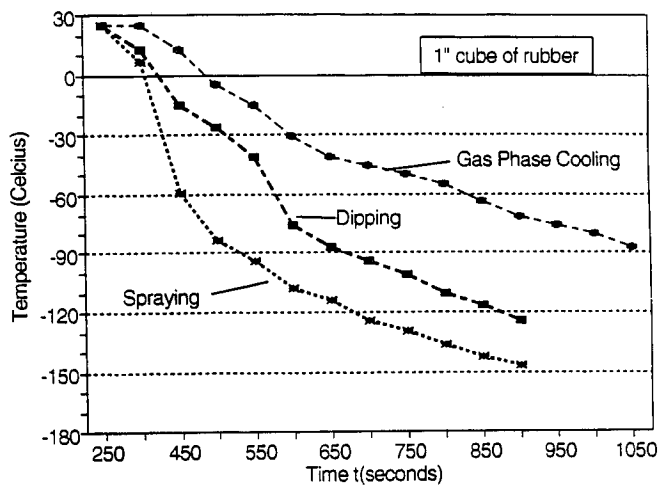


Figure 4.9: Dependence of centre temperature on cooling time for three cooling modes.

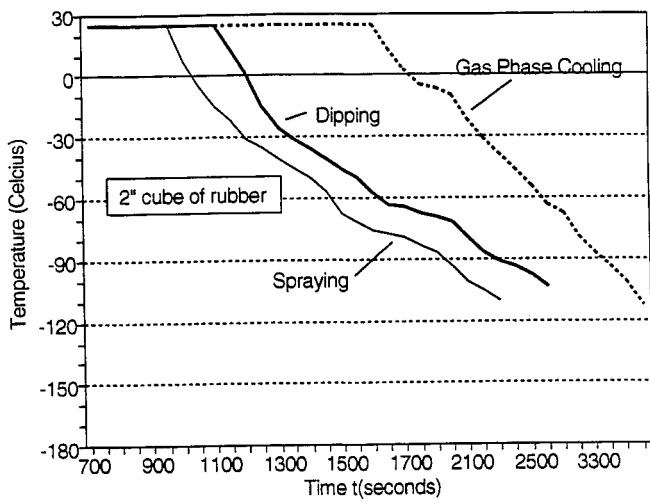


Figure 4.10: Dependence of centre temperature on cooling time for three modes.

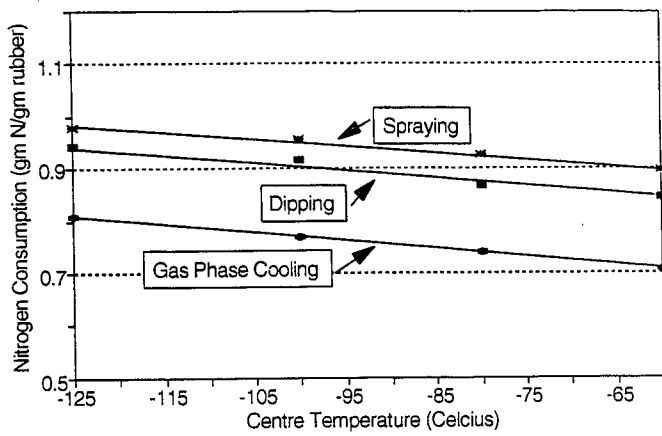


Figure 4.11: Nitrogen Consumption For Three Modes Of Cooling.

4.4 Summary Of Theoretical Investigation

The general trends in all the temperature versus time plots were similar. In each one there was an interval before any change in temperature at the centre was predicted. The only differences were in the rates of cooling and the times at which the centre temperatures began to show change.

The sizes of the cubes also played a significant role in determining the patterns of the time versus centre temperature relationships. The smallest cube (1/2") required the least amount of time to attain its embrittlement temperature (-62 °C). The 2" cube required the most time. This order occurred for all three cooling modes. The temperature of interest within the rubber is at the centre which is the warmest point. The centre must be brought down to the embrittlement temperature to facilitate complete fracturing of the cube.

It is apparent that the best results were obtained when cooling was achieved by splashing or spraying liquid nitrogen over the cubes. This is to be expected since the motion of the liquid across the surface promotes heat transfer as a result of forced convection and avoids blanketing of the heat transfer surface by vapour.

The thermal diffusivity of rubber is low, consequently the material provides an important resistance to heat transfer. Whether this resistance is dominant or not

depends on the value of the heat transfer coefficient at the surface. If the unsteady-state rate of heat transfer is essentially completely controlled by the thermal properties of rubber then the temperature gradient in the material adjusts itself to assume the greatest value possible [Biddulph].

Nitrogen usage was determined for a 1" cube of rubber and an embrittlement temperature of -62°C [Braton]. The heat-loss per gram of rubber was calculated for all three modes.

Gas phase cooling over liquid nitrogen was determined to be the mode of least nitrogen consumption, followed by dipping and then splashing. It is evident that the required residence times decreased noticeably, starting with gas phase cooling to dipping and finally splashing, at the expense of the usage of liquid nitrogen. This trend is to be expected because it represents the usual trade off between running costs and capital costs [Biddulph].

Experimental testing was be conducted to confirm the results that were calculated during this theoretical investigation.

V. COOLING EXPERIMENTS

One of the objectives of the experimental program was to determine the time required for different sized cubes of tire rubber to be cooled to the embrittlement temperature of -62°C . These experiments were conducted under two specific cooling conditions;

1. Total submergence of tire rubber tread specimens in liquid nitrogen.
2. Suspension of tire rubber tread specimens over liquid nitrogen, to provide cooling by nitrogen vapour.

Other objectives were to:

- Determine some correlation between specimen size and required freezing time.
- Determine the validity of the theoretical calculations of cooling times done previously.
- Demonstrate whether cooling would facilitate the fracture of rubber specimens.

5.1 Experimental Equipment

The equipment used in the experiments consisted of:

- a microcomputer
- a data acquisition system (MEGADAC TCS 3000) by Optum; calibrated by Optum.
- T-type thermocouples (copper constantan) by Omega
- a double insulated Dewar flask for liquid nitrogen containment.
- a blade heater connected to a rheostat
- all necessary protective equipment

5.2 Procedures

Five different experiments were conducted using:

1. A 1" cube of used tire rubber dipped into liquid nitrogen;
2. A 1" cube of used tire rubber suspended over liquid nitrogen;
3. Several cubes of used tire rubber ranging in sizes from $\frac{1}{4}$ " to $1\frac{1}{4}$ " that were cooled simultaneously over liquid nitrogen;
4. A 1" cube of virgin tire rubber dipped into liquid nitrogen;
5. A 1" cube of used tire rubber that was cooled twice.

Composite samples were not used because there would have been difficulty in obtaining consistent and representative cooling curves. The fibre and steel running through the rubber would have acted as conductors. As a result the thermocouples which had been positioned into the centre of the cubes would yield inconsistent data. An illustration of this problem is provided in Figure 5.1. Consequently, only solid rubber tread specimens were chosen, since they would model the worst case theoretical situation discussed in Chapter 3.

5.3 Specimen Preparation

In selecting samples which could best represent the typical behaviour of tire rubber, materials were selected randomly. All samples regardless of their size, were shaped and cut as accurately as possible with razor sharp cutting

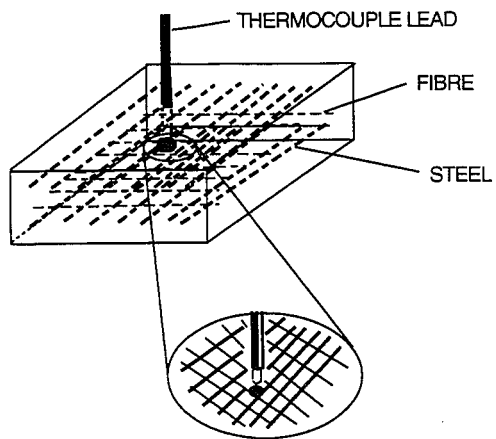


FIGURE 5.1: THERMOCOUPLE IN CONTACT WITH FIBRE OR STEEL GIVING AN INCONSISTENT READING.

blades into cubes. Thermocouples were then placed into the centre of each cube, since the temperature at the centre would be most critical. Different attempts were made to place thermocouples into the centres of the rubber cubes without the use of any lubricants. Any influence by the lubricants on the cooling rates had to be avoided. The best method of insertion was achieved by drilling, with a very small drill bit, into the rubber cube centre. The thermocouple wire was then forced into the cube with pliers (taking care not to damage the thermocouple tip). Absolutely no space was permitted between the wire and cube to eliminate direct contact between the centre of the cube and the liquid or vapourized nitrogen. A slight exception was made to the specimens that were dipped into liquid nitrogen. A precaution was made to avoid contact between the thermocouple lead and the liquid nitrogen. A neck that was large enough to sufficiently shield the lead from the liquid nitrogen, but small enough to negate any influence on the cooling curves, was incorporated into the cube shape. Figure 5.2 provides sketches of the specimens used in the experiments.

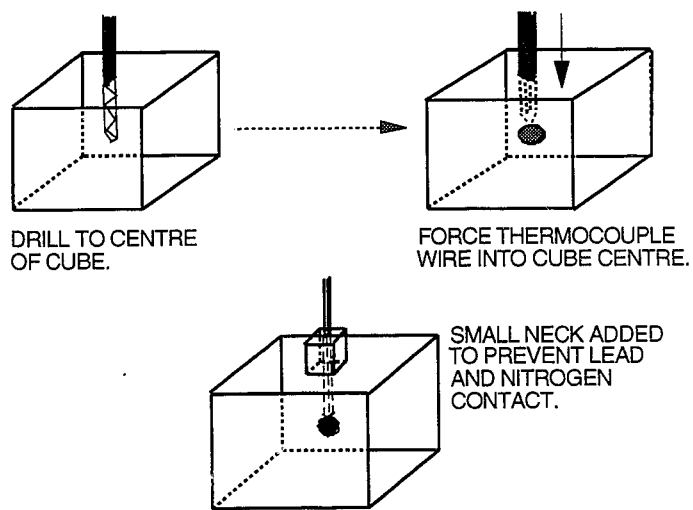


FIGURE 5.2: ILLUSTRATIONS OF SPECIMEN PREPARATION.

5.4 Methods

Limiting factors led to the selection of specimens that were no larger than 1¼" in size. The limitations were imposed by:

- The size of the tire rubber specimens that could be made from the supply of tires;
- The neck of the freezing vessel which could not accommodate cubes larger than 1¼".

As mentioned earlier, five different freezing experiments were conducted.

Experiment One: One Inch Cube Of Used Tire Rubber Dipped Into Liquid Nitrogen.

A one inch cube of used tire rubber with the thermocouple in place was submerged into liquid nitrogen, carefully avoiding contact between the lead and the liquid nitrogen. Another thermocouple was positioned in the liquid nitrogen to measure its temperature. At the moment the cube was submerged, the data acquisition system began data collection. Once the centre of the cube reached a temperature well below -62°C the experiment was concluded. Several replicate tests were conducted. The results of these tests will be discussed later. A schematic of this experiment is illustrated in Figure 5.3.

Experiment Two: One Inch Cube Of Used Tire Rubber Cooled By Liquid Nitrogen Vapour.

A one inch cube of used tire rubber with a thermocouple in the centre was suspended over liquid nitrogen. Another thermocouple was suspended near the rubber cube to monitor the vapour temperature. It was critical to control the

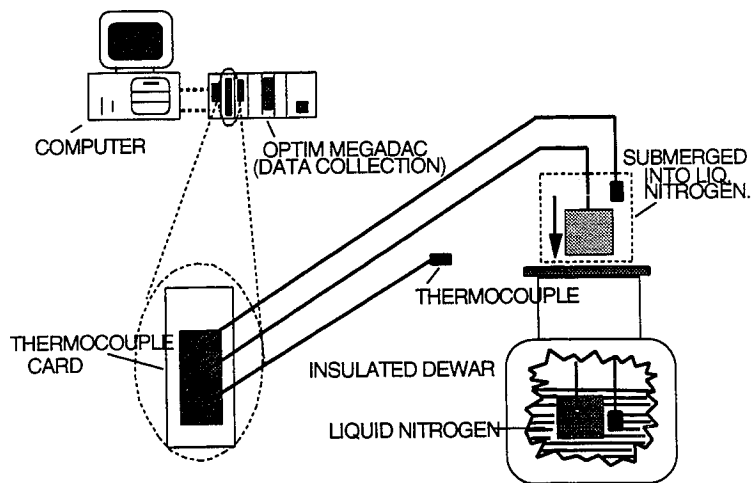


FIGURE 5.3: LAYOUT OF EXPERIMENT IN WHICH A ONE INCH CUBE OF RUBBER WAS SUBMERGED INTO LIQUID NITROGEN.

vapour temperature. It was important to simulate the actual vapour temperature that would occur in the cooling tunnel of the pilot plant. The vapour temperature was controlled with a blade heater. Without any external involvement, the vapour temperature was too warm. The vapour temperature was maintained between -90°C and -110°C . As in the previous experiment, the moment the cube was in place over the liquid nitrogen, the data acquisition system began collecting data until the cube centre was well below -62°C . The results will be discussed later in detail. Figure 5.4 illustrates the experimental layout of this test.

**Experiment Three: Different Sizes Of Rubber
Specimens Cooled Simultaneously
By Liquid Nitrogen Vapour.**

In this experiment, some correlation between the size of the cube and the time required to embrittle the cube was investigated. The basic cooling method was similar to that of experiment two with the exception that different sizes of cubes were suspended over the liquid nitrogen. The sizes of the cubes ranged from $\frac{1}{4}$ " to $1\frac{1}{4}$ ". A schematic of the experimental layout is depicted in Figure 5.5. The samples had to be sufficiently separated, to prevent any interference from one another. All of the specimens were suspended at exactly the same level above the liquid nitrogen. This was done to ensure that all the cubes were subjected to exactly the same vapour temperature.

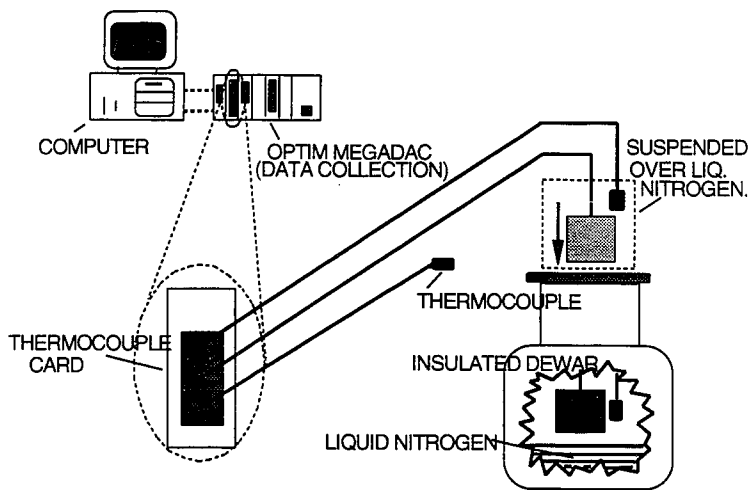


FIGURE 5.4: LAYOUT OF EXPERIMENT IN WHICH A ONE INCH CUBE OF RUBBER WAS SUSPENDED OVER LIQUID NITROGEN.

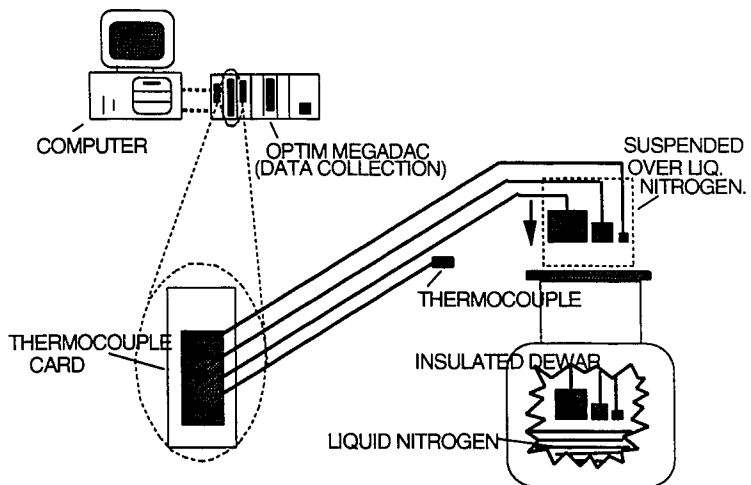


FIGURE 5.5: LAYOUT OF EXPERIMENT IN WHICH DIFFERENT SIZES OF RUBBER CUBES WERE SIMULTANEOUSLY COOLED BY LIQUID NITROGEN VAPOUR.

Experiment Four: One Inch Cube Of Virgin Tire Rubber Submerged In Liquid Nitrogen.

The method for this experiment was similar to that of experiment one with the exception that virgin rubber was used instead of worn scrap material. Virgin rubber was tested to see whether scrap rubber or unused virgin scrap would require more time for embrittlement.

Experiment Five: One Inch Cube Of Tire Rubber Resubmerged In Liquid Nitrogen.

The method of cooling in this experiment was the same as the method of cooling in experiment one. However, once the cube had been cooled well below the embrittlement temperature, it was removed and sufficient time was provided for the specimen to warm to the ambient temperature. Once at ambient temperature the cube was resubmerged in liquid nitrogen and data were rerecorded. The purpose of this experiment was to determine whether the cooling process itself would fracture the cube structure without any external force being applied to the cube.

VI. EXPERIMENTAL RESULTS & DISCUSSION

The initial strategy for the experiments adopted the principle of simulating the pilot plant cooling process under laboratory constraints. The objective was to determine how helpful theoretical calculations were in the design of a cryogenic cooling system.

A cryotunnel consists of two regions, a precooling section and a freezing section. The precooling section utilizes the vapourized nitrogen to precondition the tire chips to a lower temperature. Once past the precooler, the tire chips are then cooled to embrittlement conditions by a liquid nitrogen spray.

It seemed essential to reproduce these two conditions in the experiments. By doing this it was possible to determine the time required to embrittle the tire chips with the efficient use of liquid nitrogen. It is the liquid nitrogen consumption that is the greatest economic expenditure in operating a cryogenic system. Consequently, the liquid nitrogen consumption must be minimized.

In experiments 1 and 2, several tests were conducted with one inch cubes of used tire rubber to determine the time required to sufficiently freeze the tire rubber. The results of experiment 1 and 2 are provided in Appendices VII and VIII. Figure 6.1 shows the average experimental results of experiment 1 (indicating a required residence time of 185 seconds for cooling in liquid nitrogen). The average

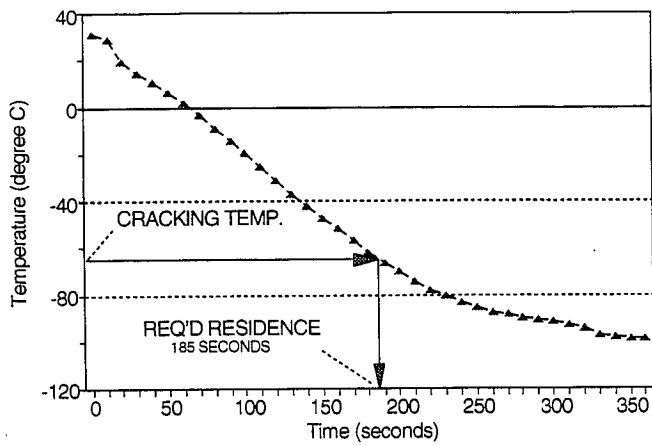


FIGURE 6.1: ONE INCH CUBE OF TIRE RUBBER DIPPED INTO LIQUID NITROGEN (EXPERIMENTAL AVG.)

experimental results of experiment 2 are illustrated in Figure 6.2. When cooling, one inch cubes of used tire rubber with nitrogen vapour, an average residence time of 420 seconds was required.

From a comparison of the experimental cooling curves in Figures 6.1 and 6.2 with the theoretical cooling curves depicted in Figure 6.3, obvious discrepancies are readily evident. Although the basic shapes and trends of the curves are similar, the experimental cooling curves are much faster than the theoretically calculated curves. Some differences can be rationalized by two major parameters specified in the theoretical calculations:

- The temperature of the surrounding environment,
- The convective heat transfer coefficients.

The theoretical surrounding temperature (-181°C) is slightly warmer than the experimental dipping temperature (-196°C), but cooler than the experimental vapour temperature (-120°C). However, this difference can account for only a 10% variance in the cooling rates. The values of the heat transfer coefficients used in the theoretical calculations, were ceiling values from the available literature. Therefore the discrepancies cannot be entirely due to the two parameters.

The immediate responses of the experimental curves to temperature changes were inconsistent with the theoretical predictions. This difference suggests that cracks or

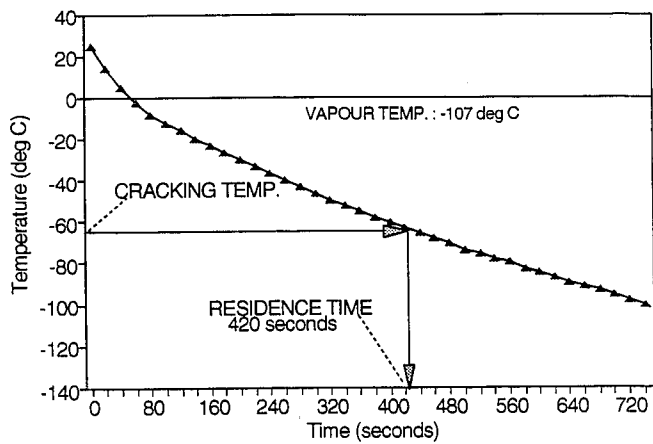


FIGURE 6.2: ONE INCH CUBE OF TIRE RUBBER COOLED WITH LIQUID NITROGEN VAPOUR (EXPERIMENTAL AVG.)

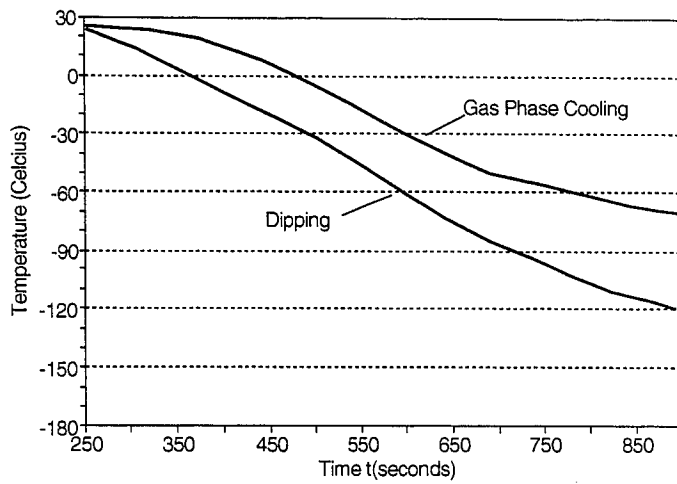


FIGURE 6.3: THEORETICAL RESULTS OF A ONE INCH CUBE OF TIRE RUBBER COOLED WITH VAPOUR AND LIQUID NITROGEN.

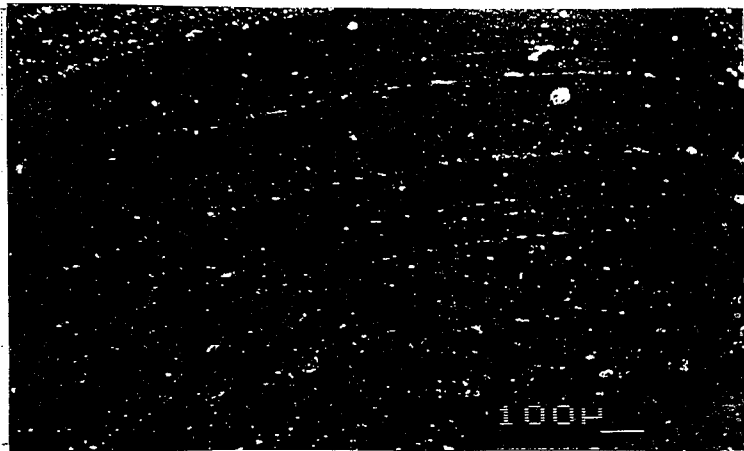
pathways may exist in the rubber. These cracks or pathways can permit the cold nitrogen to penetrate to the centre of the cubes much more rapidly than simple conduction can remove heat.

To investigate the possibility of cracks or pathways existing in the rubber, Dr. Alpas of the Department of Mechanical Engineering, magnified a sample of used tire rubber tread and virgin tire rubber tread to view the structure on a microscopic basis. The sample was taken perpendicularly to the radius of the tread. Enlargements of the electron microscopy results are provided in Figure 6.4. No distinct cracks are evident in 6.4(a) or (b) but the granular structure in 6.4(a) reveals a three dimensional network of interstices that would be filled with air. This condition hinders the heat conduction process in the used rubber. The homogeneous structure of the new tire rubber facilitates heat transfer through the material. Consequently, new tire specimens cool at a faster rate than used rubber specimens.

The theoretical calculations assumed the tire rubber specimens to be pure rubber without any of the fillers normally included in the make-up of a tire. Since these fillers are comprised of metals, such as zinc oxide, they conduct heat much more readily than rubber. As a result the theoretical cooling curves depict lower cooling rates than found experimentally with new and used rubber.



USED TIRE RUBBER TREAD



VIRGIN TIRE RUBBER TREAD

Figure 6.4: The Structure Of Tire Rubber On A Microscopic Level.

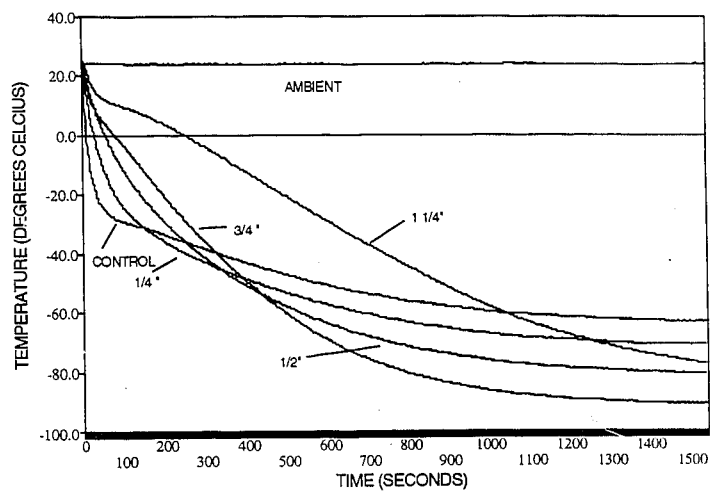


FIGURE 6.5: 1/4", 1/2", 3/4", 1 1/4" CUBES COOLED SIMULTANEOUSLY IN COLDER NITROGEN VAPOURS.

There is a possibility of the cryogenic temperatures degrading the structural integrity of the material. This possibility was investigated by recooling the specimens. The results are discussed in detail later in this chapter.

In experiment 3, a possible correlation between the size of the cube and the time required to embrittle the cube was investigated. Figure 6.5 shows typical cooling curves for four different sized cubes cooled simultaneously by nitrogen vapours at temperatures below -90°C . The $\frac{1}{4}$ " and $1\frac{1}{4}$ " curves approximated the trends of the theoretical curves. However, the curves for the control (thermocouple alone), $\frac{1}{4}$ " and $\frac{1}{2}$ " cubes showed normal trends while temperatures were above -20°C . At lower temperatures they began to traverse the curves of the larger cubes and eventually levelled off at temperatures much warmer than the nitrogen vapour temperature (-90°C). This behaviour is inconsistent with the normal expectations, which would show the smaller cubes cooling at faster rates. Discussions with Bob Davis of Praxair (Union Carbide) suggested the possibility of vapour barriers being developed around the smaller cubes and control thermocouple. Due to the intensely cold vapour, only natural convection is occurring and not forced convection which would continuously remove any vapour barrier being formed. The vapour barrier, although cool, is relatively warm compared to the nitrogen vapour and in reality acts as an insulating blanket around

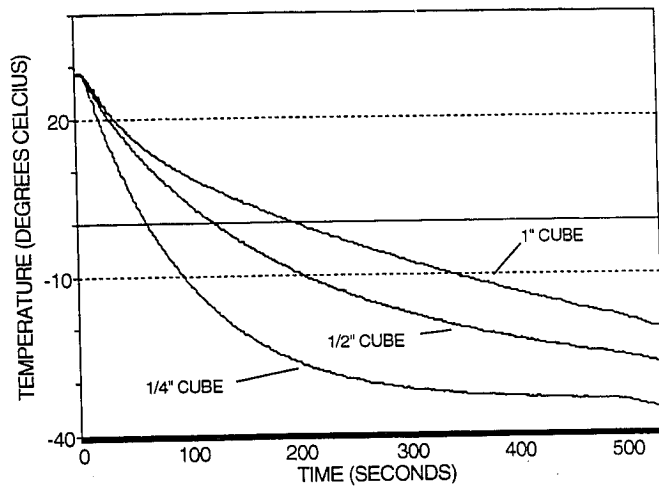


FIGURE 6.6: 1/4", 1/2", 1" CUBES COOLED SIMULTANEOUSLY IN WARMER NITROGEN VAPOURS.

the smaller cubes and control thermocouple. Figure 6.6 shows cooling curves for $\frac{1}{4}$ ", $\frac{1}{2}$ " and 1" cubes cooled by warmer nitrogen vapours at -40°C . All three curves behaved normally at the lower cooling temperatures. If vapour barriers were generated they would be formed at temperatures approximating the nitrogen vapour temperature and thus would not behave as insulating blankets. Other tests supporting this suspicion are provided in Appendix IX. In the actual plant process, forced and not natural convection occurs due to the constant movement of the material in the tunnel. As a result the possibility of vapour barriers being formed around smaller cubes is minimized or even eliminated.

Virgin rubber was tested in experiment 4 to see whether scrap rubber or unused virgin material would require more time for embrittlement. Appendix X provides the test results from experiment 4. Figure 6.7 shows the experimental average data for one inch cubes of virgin tire rubber dipped in liquid nitrogen. According to Figure 6.7, a residence time of only 95 seconds was required where as for the dipping of used scrap rubber embrittlement required 185 seconds. These residence times would indicate that the virgin rubber cooled at a faster rate than the used scrap rubber. This statement cannot be considered to be conclusive. Although the virgin rubber was Goodyear and the used rubber was also Goodyear, the probability of them having the same rubber composition is unlikely. For the

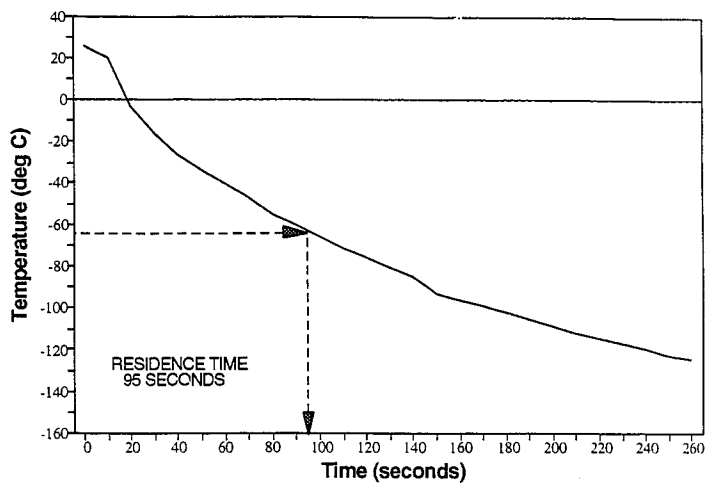


FIGURE 6.7: ONE INCH CUBE OF VIRGIN TIRE RUBBER DIPPED INTO LIQUID NITROGEN (EXPERIMENTAL AVG.)

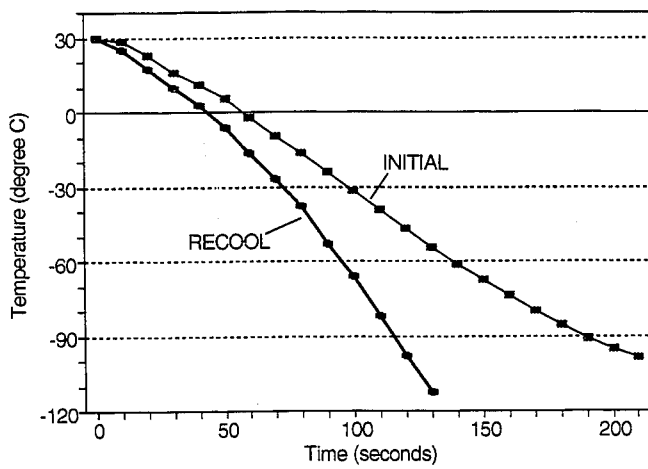


FIGURE 6.8: ONE INCH CUBE OF RUBBER RECOOLED IN LIQUID NITROGEN.

results to be conclusive, specimens of virgin and used rubber of the same composition must be tested.

Experiment 5 was conducted to determine whether the intense cooling process itself would facilitate the breakdown of the rubber structure without any external force being applied to the cube. One inch cubes were cooled and then re-cooled. Figure 6.8 shows a typical result of this experiment. The cooling curves demonstrate that the re-cooling process occurred at a faster rate than the initial cooling. These results suggest that the intense cooling process has some spontaneous effect on the degradation of the structural integrity of the rubber. Appendix XI provides additional data from experiment 5.

The basic principles of heat transfer apply to the cooling process, but the theoretical and experimental values are distinctly different. Consequently, only the experimental results should be used as a basis for all design considerations. The experimental results can best represent the conditions associated with the industrial process.

When designing a cooling tunnel, a combination of the vapour cooling curves along with the dipping in liquid nitrogen cooling curves must be considered. For example, the time required to precool the material to an arbitrary temperature of approximately -40°C must be established, then the time required to cool with liquid nitrogen from -40°C to

-62°C must also be determined. Together these times can be used to determine the required residence time for a cryogenic cooling tunnel design.

An important design consideration is the material size. In actual practise the chips are not cube shaped but rather irregular. The actual chips are approximately 2" squares with a thickness ranging from a ½" to 1". The condition of the material entering the cooling tunnel is significant. Most of the tire chips are composites which require less residence time. On occasion the chips are muddy, wet and sometimes covered with ice. Such conditions, increases the nitrogen load required to embrittle the chips.

VII. MICROGRIND COOLING TUNNEL DESIGN

Cryogenic processing of scrap tires is based on the principle that the rubber in the tire will exhibit brittle characteristics when the temperature is reduced to -62°C . Once the tire material has been sufficiently frozen to its embrittlement temperature, it can be fragmentized by a hammermill. This is done by subjecting the material to a cryogenic environment for a sufficient period of time with liquid nitrogen as the cooling medium.

The most efficient use of the liquid nitrogen would be to utilize the liquid and the vapourized liquid in the system. When the liquid is sprayed on to the material, it vapourizes and it is this vapour that is used to precool the tire material. A tubular chamber is suited for this cooling method. The cooling chamber is sectioned into two regions. The discharge end is the cooler section and the larger area near the feed end is the precooler. The precooled tire chips are sprayed with liquid nitrogen near the discharge end of the tunnel. The vapourized nitrogen is pulled by a fan toward the feed end of the tunnel to enable the vapour to precool the tire chips. Heat is removed from the material in a counterflow pattern.

A mini-mill cryotunnel was donated to the University of Windsor by Recovery Technologies Inc (RTI). After, this cryotunnel was evaluated on the basis of performance according to its original design, a new one was proposed.

7.1 Design Considerations

The most essential requirements for a cryogenic tire chip cooling system are:

- Provision of sufficient mixing of the rubber pieces, to increase the heat transfer rate.
- Ability to convey the rubber crumb uniformly through the cooling tunnel to the hammermill.

The mixing and conveying characteristics determine the consumption of liquid cryogen per unit of material cooled. As was mentioned in previous chapters, it is the cryogen which is the largest economic expenditure in a cryogenic system. Consequently, it is critical that nitrogen consumption be efficient and at a minimum.

7.1.1 Mixing

Efficient mixing is critical when cooling tire rubber to its embrittlement temperature. Sufficient mixing ensures that all of the tire crumb will come in contact with the cooling medium, and not buried in other material. Mixing also enhances forced convection of heat from the tire material. Heat from the material is removed much more quickly with forced convection because the cooling medium actually carries the heat away.

7.1.2 Conveying

The conveying system controls the movement of the material from the feed end to the discharge end. More importantly, it controls the time that the material resides

in the tunnel (residence time). Too high or too low residence times make the system inefficient. An effective conveying system will also maintain a constant level of material in the tunnel in a steady-state operation. If a buildup of material occurs in the tunnel, the cooling rate will be reduced since material congestion would also effect proper mixing.

7.2 Donated Cryotunnel

The purpose of a mini-mill cryotunnel is to reprocess oversized clean rubber crumbs, which are approximately $\frac{1}{2}$ " in size. The oversized crumb rubber is diverted from the cryogenic whole tire processing system because the larger system did not properly reduce the tire chips. The cryotunnel donated by RTI was tested on the basis of:

1. Residence Time
2. Mixing Capability
3. Conveying Capability

Figure 7.1 provides a schematic representation of the basic configuration of the donated cryotunnel. Basically, it consists of an insulated tubular vessel with 3 fins running through the length of the tunnel. These fins are responsible for the mixing of the material. Table 7.1 summarizes the results of the tests conducted on the donated tunnel with tire crumb which was operated at different rotational speeds (starting at 1 rpm to a maximum of 4 rpm) and different angles of decline (from 3.25 degrees

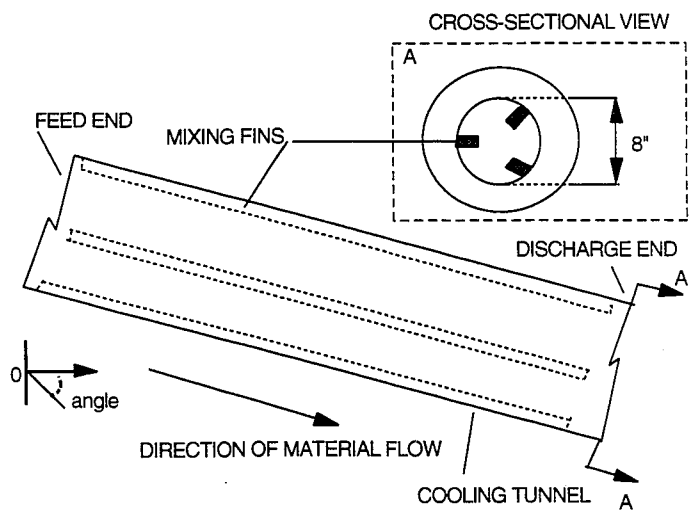


FIGURE 7.1: SCHEMATIC OF THE CRYOTUNNEL DONATED BY RTI.

TABLE 7.1: DATA OBTAINED FROM TESTS CONDUCTED ON DONATED CRYOTUNNEL

ROTATION (RPM)	ANGLE (DEGREES)	MATERIAL DEPTH (INCHES)	THROUGHPUT		RESIDENCE TIME (MIN.)
			(LBS/HR)	(KG/HR)	
1	-7.00	4	64	29.0	62.22
1	-5.25	4	58	26.3	66.66
1	-3.25	4	42	19.1	94.81
2	-7.00	4	125	56.7	31.86
2	-5.25	4	120	54.4	33.18
2	-3.25	4	84	38.1	47.40
3	-7.00	4	180	81.7	22.12
3	-5.25	4	165	74.9	24.13
3	-3.25	4	117	53.1	34.03
4	-7.00	4	256	116.2	15.55
4	-5.25	4	230	104.4	17.31
4	-3.25	4	172	78.0	23.15

BULK DENSITY OF MATERIAL = 1222.22 lbs/m³

EFFECTIVE LENGTH OF TUNNEL
 L = 11 ft = 3.35 m
 TUNNEL DIAMETER
 D = 8 inches = 0.2 m

CROSS SECTIONAL AREA
 A = 50.24 inches²
 = 0.0324 m²

TUNNEL VOLUME
 V_T = L * A = 6631.68 inches³
 = 0.1085 m³
 MATERIAL (STOCK) VOLUME
 V_S = (4/8) * V_T = 3315.84 inches³
 = 0.0543 m³

to a maximum of 7 degrees). Residence times as well as throughputs were determined for a constant material depth, maintained at a level of four inches.

The conveying capability of the tunnel depends entirely on gravity whose effect was determined by the angle of decline.

The results in Table 7.1 show that the maximum output of 256 lbs/hr was achieved with a residence time of just over 15 minutes. This residence time is much too long. On the basis of the cooling curve data discussed earlier, the required residence time should be less than 1 minute for material less than $\frac{3}{8}$ " in size. A side profile of the tunnel showed a buildup of material at the feed end. Obviously, a better conveying system would increase output, reduce residence time, and maintain a consistent level of material in the tunnel.

Material mixing by the fins was not continuous because an insufficient number of fins was provided in the original design.

7.3 Proposed Tunnel Design

In any proposed design, improvements must be made to the screw feeder. The screw feeder is responsible for introducing the tire crumbs into the tunnel for processing. Also the rotational capability of the tunnel should be increased. The existing mechanism was limited to 4 rpm.

Modifications were made to the existing tunnel design

to improve its performance. A helicoid (ribbon) flighting system was implemented along with the existing mixing fins. The flighting system was used to improve the conveying capability without any downward slope in the direction of material flow. This design permits the suspension of the nitrogen-spray probe in the middle of the tunnel. As a result, the probe can spray the material without any obstruction. A screw conveyor would obstruct the spraying of the material under the screw. By eliminating the slope of the tunnel it is possible to prevent the discharged nitrogen from exiting with the cooled tire material into the hammermill. This design also enables the cryogen to completely cool the tire crumb along the length of the tunnel.

Testing of this design proved that the helicoid conveying system was very effective in moving the material consistently without any visually recognizable material buildup in the tunnel. The helicoid system also assisted in the mixing of the tire crumbs. However, the original mixing fins hindered the conveying system slightly, because a portion of the crumbs was picked up and dropped behind the section of flight that was carrying this material. Essentially this action causes the material to move forward, then fall back and then move forward again. This pattern appeared to be consistent throughout the testing. Although the throughput was significantly increased, the residence

time was still too high. These results indicated that a faster conveying system was necessary.

Because the flighting mixed the material as well as conveyed it, the mixing fins could be eliminated from the new design. Instead, a series of three helicoid flights was installed in a shifted position. This orientation is illustrated in Figure 7.2. The new arrangement helps to mix and convey the material more effectively. This new design has yet to be tested. Although this design would be the logical step in tunnel improvement some other factors had to be considered. It became evident that the flights should be sectioned into shorter segments to avoid tunnel twisting due to the expansion and contraction caused by the severe temperature fluctuations in the tunnel environment.

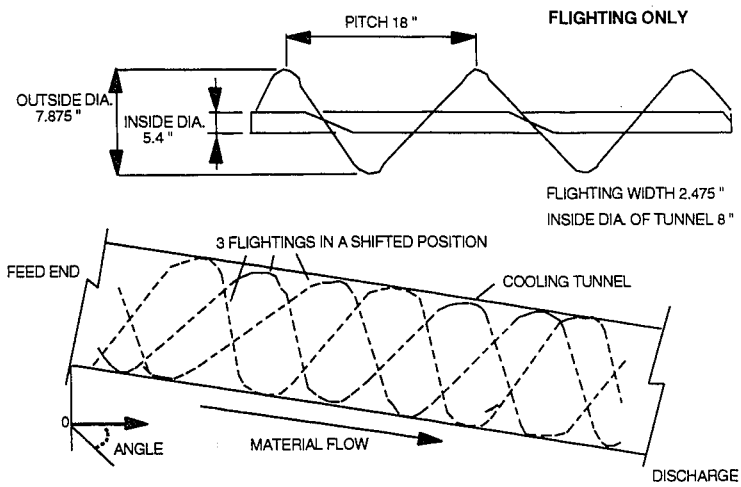


FIGURE 7.2: PROPOSED CONVEYING SYSTEM UTILIZING HELICOÏD FLIGHTINGS.

VIII. FIBRE AND STEEL SEPARATION

The matrix of a typical automobile tire can present problems when efficient cryogenic recovery of the components is required. A typical tire composition is shown in Table 8.1. The tire rubber, steel and nylon fibre have different properties and present a problem when separation into three distinctive streams is necessary. At cryogenic temperatures only the rubber is brittle and can be shattered like glass for separation from the steel and fibre. The steel and fibre remain ductile at cryogenic temperatures. When they pass through a hammermill they become so entangled that any separation between the two is minimal. As a result the entangled fibre and steel become virtually worthless. Table 8.1 shows that a typical tire contains only 63% rubber. The remainder is comprised of fibre and steel at 32% and 5% respectively. When the fibre and steel cannot be separated approximately 30 to 35% of the stream is scrap. There are markets for all three of these materials, assuming they are relatively clean and separated from each other. The following chapter will explain in detail experiments conducted on the separation of the steel and fibre fluff with recommendations for future work.

Table 8.1: Composition of a typical automobile tire.

Component	Weight (lbs.)	% Weight
Rubber	12	63
Nylon	6	32
Steel	1	5
Total	19	100

8.1 Separation Tests

Three different experiments were conducted to investigate the steel and fibre entanglement. Typical experiments involved a:

- Drop test,
- Combing test,
- Shaker test (inertial impactation)

8.1.1 Drop Test

The drop test was a simple study. An entangled mass of steel and fibre was dropped from specific distances from the ground. Once the material had free-fallen to the ground, it was examined to see if any separation had occurred as a result of the impact between the ground and entangled mass.

The testing distances above the ground were:

- 2 feet,
- 3 feet,
- 5 feet,
- 10 feet

None of these attempts were successful in separating the steel and fibre. In fact, it appeared the fibre and steel

were entwined more tightly as a result of the drop test. The poor results indicated that mechanical separation of the entanglement was required.

8.1.2 Combing Test

Figure 8.1 shows two hand held combs which were manufactured for this test. An appropriate size of entangled steel and fibre sample was placed on a flat working area. Figure 8.2 illustrates how the fluff was combed apart. The two combs were moved across the working area, to pull the entanglement apart. Several samples were combed and examined. Significant amounts of very fine rubber were also separated from the fluff. The size of the rubber that was collected appeared to be finer than 20 mesh. Even though combing results appeared to be successful, practical application of this principle may be too complicated and labour intensive for commercial purposes.

8.1.3 Shaker Test (Inertial Impaction Test)

Preliminary testing was conducted on mixed steel and fibre samples by simply hitting the material with a moving solid object. There was some separation between the steel and fibre. The inertia of the moving object achieved some separation of the steel and fibre. To reproduce this effect on an industrial basis, the combs from the combing experiments were used in an inverted position with the tips of the fingers of the combs pointing upward. Figure 8.3 illustrates this arrangement. The combs were moved back and

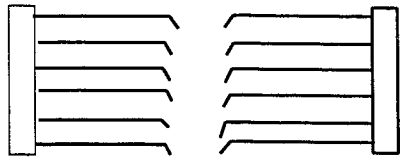


FIGURE 8.1: TWO HAND HELD COMBS WHICH WERE USED IN EACH OF THE COMBING TESTS.

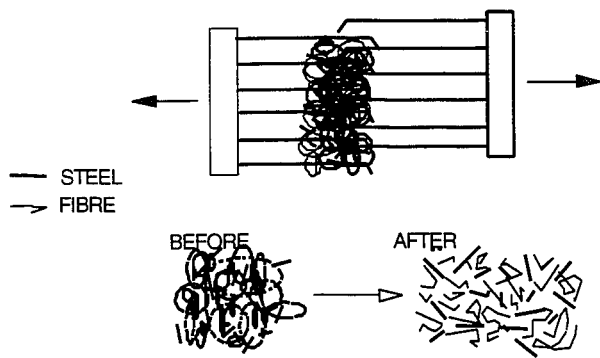


FIGURE 8.2: ILLUSTRATION OF HOW THE COMBING TESTS WERE CONDUCTED.

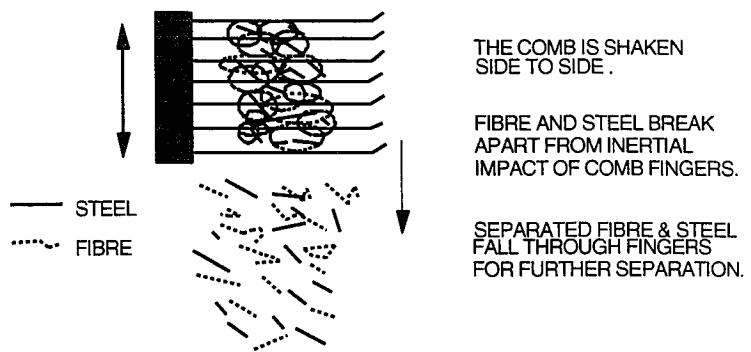


FIGURE 8.3: SHAKER COMB USED IN THE
 INERTIAL IMPACTION TEST.

forth along the bases of their longitudinal axes. This movement allowed the fingers of the comb to hit the steel and fibre fluff. This approach appeared to be very promising because the entangled material was completely separated with very little time and effort.

8.2 Fibre Separation Recommendations

The shaker tests were the most successful of the three experiments that were conducted. The entire fluff was completely separated with the least amount of energy. This concept was developed further into a working, motor operated, machine which incorporated the experimental combs.

A sketch of the motorized apparatus is provided in Figure 8.4. The back and forth sliding action of the combs was achieved by attaching the combs to a hollow tube with a smaller tube inside of it. This arrangement allowed the comb to move smoothly back and forth once the outer tube was connected to a cam. The combs moved back and forth through a distance of $\frac{1}{2}$ " when the fingers were an inch apart and $\frac{1}{4}$ " when the combs were $\frac{1}{2}$ " apart. The motor rotated at about 700 rpm.

If this method of fibre separation is to be used industrially, there should be different levels of combs with the fingers on the top level being an inch apart and the fingers of the bottom combs being approximately $\frac{1}{4}$ " apart. By incrementally decreasing the distances of the fingers, the time for fluff residence on the fingers can be reduced

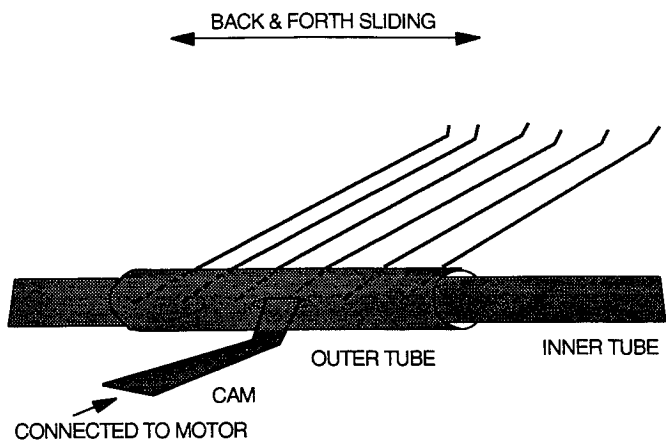


FIGURE 8.4: AN ILLUSTRATION OF A MECHANIZED SHAKER.

to a minimum. The entire surface of the combs should be utilized to prevent congestion on the fingers. This can be done by oscillating the feed on the fingers. Once the fluff has been separated by the combs, the steel and fibre should be moved from beneath the combs quickly to prevent re-entanglement. This can be done by a fast moving conveyor belt or a vibrational conveyor which will move the material away from the combs to a process which will further remove all the components from the stream.

The shaker method represents only one possible technique which utilizes the principle of inertial impaction. Another separation method was proposed by Bruno Grant of Recovery Technologies Inc.. A sketch of his idea is provided in Figure 8.5. In this method, the steel and fibre fluff is fed through pinching rollers onto another rapidly spinning roller with short fingers affixed to it. These fingers strike the fluff causing it to break apart.

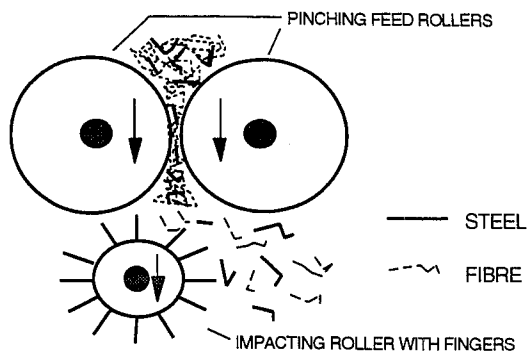


FIGURE 8.5: SEPARATION METHOD UTILIZING IMPACTING FINGERS ON A SPINNING ROLLER.

IX. AMBIENTLY AND CRYOGENICALLY GROUND RUBBER

This chapter will examine the shape of ambiently ground rubber and cryogenically ground rubber. It will indicate which type of material has the greater surface area and it will discuss the significance of such a difference.

The photomicrograph in Figure 9.1 clearly shows the torn edges of ambiently ground rubber particles. These torn edges provide an increased surface area that is not available with the faceted particles of cryogenically fractured rubber. The greater surface area permits more surface energy per unit volume, which provides more chemical driving force for sintering at high temperatures. However, the rubber material has not cleanly separated from the fibre and steel in a tire. As a result, there is not only a decrease in the percentage of rubber recovery, but also a



Figure 9.1: Photomicrograph of Ambiently Ground Rubber.

consequent loss in the value of the steel which is contaminated with clinging rubber.

The cleaved surfaces and fibre indentations in the cryogenically ground rubber shown in Figure 9.2 suggest that less energy will be required to size reduce and separate the three components of a tire than required for the ambient particles. The clean breaks in cryogenically fractured rubber facilitate the separation of the components in a tire into three distinct streams without any rubber attached to the steel or fibre. As a result, the value of the steel is increased and the recovery of rubber is maximized.



Figure 9.2: Microscopy Of Cryogenically Ground Rubber.

The percentage of rubber recovery is a very important factor. It not only indicates the process efficiency but also shows the level of potential revenue loss in the waste stream in the form of fibre with rubber clinging to it. Lost rubber also increases the cost for disposal of fibre in a landfill.

Additional photomicrographs comparing different sizes of ambient and cryogenically ground tire rubber are provided in Appendix XII.

X. APPLICATION OF BASIC PRINCIPLES ON AN INDUSTRIAL SCALE

When designing any large scale cryogenic system, it is absolutely critical that all the knowledge obtained from pilot-plant size systems and experiments conducted on a laboratory scale be integrated on the industrial level. In some instances, visual observation of the operation of industrial-size equipment is sufficient to define problems whose elimination or minimization will lead to improvements to the system. Ideally, experimentation with the industrial-size system presents more conclusive evidence of the required improvement to the system. However, this approach becomes quite costly when the experimental conditions are difficult to control. Consequently laboratory and pilot-plant size tests were conducted before basic principles and ideas were applied to the large scale process.

This chapter discusses what was accomplished during this investigation when modifications were made to the industrial-size process in Cambridge, Ontario. A schematic representation of the plant in Cambridge is provided in Figure 10.1.

Two years ago, the size of the material entering the cryogenic cooling tunnel from the shredder was very inconsistent. The sizes ranged from 4 inch to 10 inch slabs and quite often even larger pieces would enter the cryotunnel. The inability of the existing shredder to

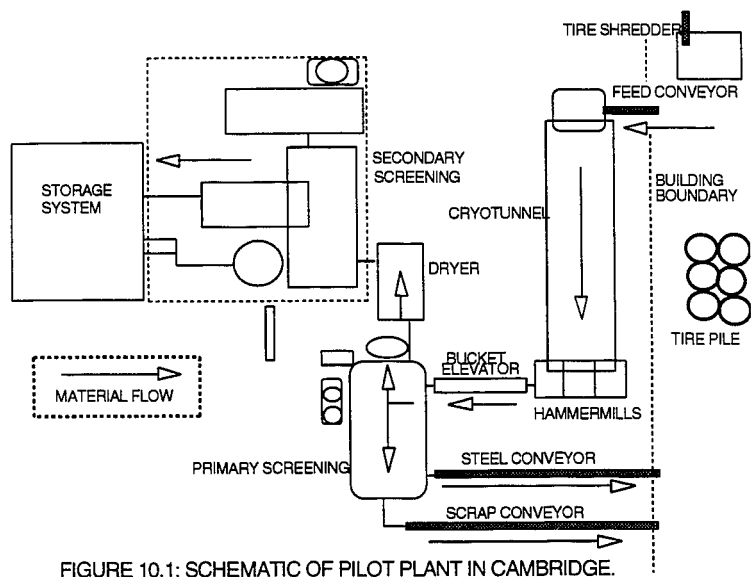


FIGURE 10.1: SCHEMATIC OF PILOT PLANT IN CAMBRIDGE.

provide small uniformly sized pieces created a strain on the hammermill which reduces the material to ground rubber, steel and fibre. More importantly, it reduced the cryotunnel's ability to mix and convey the tire pieces effectively. As a result, the residence times of the larger pieces of material were less than those of the smaller pieces. The larger pieces were virtually unaffected by the mixing system installed in the tunnel at that time. Consequently the larger material passed straight through the tunnel without the spinning experienced by the smaller pieces which were cooled much more effectively.

On the basis of the cooling curve data, the sizes of the tire pieces were reduced to 2 inch square chips, by a new shredder. This size reduction enabled the material to be handled much more easily, and it reduced the cooling time of the material in the tunnel without reducing the throughput of the system.

The residence time of the material in the cooling tunnel at the original plant in Ayr, Ontario was much too long. It was greatly reduced in the new generation design which is currently operating in Cambridge. The residence time was reduced by implementing a new conveying system design which incorporated the basic principles of the conveying system that was effective for the mini-mill cryotunnel that was discussed in an earlier chapter.

The operating angle of the industrial-size tunnel was

also reduced to essentially zero from its initial operating angle of 2 degrees uphill. This modification was implemented after measured readings indicated that the exhaust temperature of the tunnel was too warm. This condition suggested that a blockage at the feed end of the tunnel restricted the exhaust fan's ability to pull the nitrogen vapours to the feed-end where precooling of the material was required. The throughput was also significantly reduced as a result of this blockage condition. Apparently the material that was not being moved effectively by the conveying system was dropping back because of gravity and plugging the feeder through which the exhaust fan was pulling cold vapours. As soon as the angle of the tunnel was reduced to zero, the throughput was significantly increased and the feed-end blockage was eliminated.

Many of these modifications were incorporated in the new generation design of the industrial scale plants. Recovery Technologies Inc. has sold systems which are operating in Italy, Switzerland, and Mexico.

Extensive testing was conducted on a laboratory scale to address the problem of separating the steel and nylon fibre fluff entanglement occurring after the frozen tire chips passed through the hammermill. This problem was discussed in detail in an earlier chapter. The small scale tests and prototype design which incorporate the principle

of inertial impaction of the entanglement (to separate the steel and fibres) gave promising results. The next step would be to implement these techniques into the system in Cambridge. However, space constraints have limited the implementation until overall system modifications are rationalized.

Field Trips

Throughout the course of this project, a number of field trips were taken. Several visits were made to the plant in Ayr and Cambridge Ontario to conduct tests on the systems or to participate in technical meetings. Tests were conducted:

- On the cryotunnel to establish residence times as well as mixing and conveying capabilities.
- On the primary screener to determine effective material classification.
- On the fluidized dryer for moisture removal.
- On automotive plastic from Magna Corporation.
- On noise levels associated with the system.

In addition, there was active participation at the Rubber Recycling and Technology Update in Milwaukee, Wisconsin at the University Of Wisconsin (March 31 to April 2, 1993) and the Powder & Bulk Solids Conference held at the Rosemont Convention Center in Chicago Illinois (May 4-6, 1993).

XI. CONCLUSIONS & RECOMMENDATIONS

The basic principles of heat transfer apply to the cooling of tire rubber, but the theoretical and experimental cooling data are distinctly different. Although they follow the same trends, the experimental cooling rates are higher. Consequently, only the experimental results should be used as a basis for all design considerations. The simple experimental tests most closely represent the conditions associated with the industrial process.

When designing a cryogenic cooling tunnel, a combination of the vapour cooling curve data along with the dipping in liquid nitrogen cooling curve data must be considered. The time required to precool the material with nitrogen vapours, to a temperature of approximately -40°C must be established, then the time required to cool with liquid nitrogen from -40°C to -62°C must also be determined. Together, these times can be used to determine the required residence time for a cryogenic cooling tunnel design.

An important design consideration is the material size. In practise, the chips are not cube shaped but rather irregular slabs. The actual chips are approximately 2 inch squares with thicknesses ranging from a $\frac{1}{2}$ inch to 1 inch. The condition of the material entering the cooling tunnel is significant. Most of the tire chips are composites which require less residence time than determined by tests with tire tread rubber. On occasion, the chips are muddy, wet

and sometimes covered with ice. Such conditions, increases the nitrogen load required to embrittle the chips.

The mixing and conveying characteristics of a cooling tunnel determine the consumption of liquid cryogen per unit of material cooled. As was mentioned in previous chapters, it is the cryogen which is the largest economic expenditure in a cryogenic system. Consequently, it is critical that nitrogen consumption be efficient and at a minimum.

Modifications were made to the existing tunnel design to improve its performance. A helicoid conveying system was very effective in moving the material consistently without any visually recognizable material buildup in the tunnel. The helicoid system also assisted in the mixing of the tire pellets in the mini cryotunnel. This design permits the suspension of the nitrogen-spray probe in the middle of the tunnel. As a result, the probe can spray the material without any obstruction. A screw conveyor would obstruct the spraying of the material under the screw. A series of three helicoid flights should be used in a shifted position. This orientation helps to mix and convey the material more effectively.

A Prototype model incorporating the principle of inertial impaction was developed as a result of extensive testing conducted on the separation of steel and fibre fluff entanglement. Implementation of the proposed design into the industrial-scale plant is recommended.

Although this investigation has covered a wide spectrum of areas, research involving the cryogenic recovery of automotive tires is far from being completed. Further work should be done to completely model the newly proposed design for the mini-mill cryotunnel which could be used to process other thermoset materials having characteristics similar to those of tire rubber.

The recycling of heat sensitive thermosets such as automotive components which would require fine grinding to a size less than 30 mesh needs to be investigated. Preliminary tests have been conducted on foam car seats. They proved that polyurethane foam can be reduced to a material size of less than 40 mesh. Once reduced, the powdered polyurethane can be incorporated back into car seats. Tests were also conducted on exterior auto trim parts which consisted of layers of different types of thermoplastics. Cryogenic conditions facilitated the separation of these layers of different plastics by weakening the bonds between the layer surfaces.

Although the recycling of thermosets is not a new idea, it is still relatively undeveloped. This area of recycling is fuelled by the development of new environmental laws that limit disposal of recyclable thermosets. This legislation is, essentially, progressively uncompromising and is designed to force complete recovery of such materials.

REFERENCES

1. Allen, D.H. & Biddulph, M.W., The Economic Evaluation Of Cryopulverizing, Conservation & Recycling, University of Nottingham, England, 1979.
2. Baker Rubber Inc., FHWA Presentation On CRM Modifier Material, Federal Highway Administration, 1993.
3. Biddulph, M.W., Cryogenic Embrittlement Of Rubber, Conservation & Recycling, Vol. 1, University of Cape Town, S.A., 1977.
4. Biddulph, M.W., Cryogenic Embrittlement Of Steel, Conservation & Recycling, Vol. 1, University of Cape Town, S.A., 1977.
5. Braton, N.R., Cryogenic Recycling And Processing, CRC Press, Boca Raton, Fl., 1980.
6. Ctvrtnicek, T.E., Search, W.J., Blodgett, C.R., Scrap Tires: A Useful Waste?, Monsanto Research Corporation, Energy And The Environment Conference, Ohio, 1975.
7. Davis, Robert B., Sr. Development Associate, Praxair Inc., Tarrytown, N.Y., Personal Communications, May 26, 1993.
8. Daborn, G.R., & Derry, R., Cryogenic Communiton In Scrap Recycling, Resources, Conservation & Recycling, UK., 1987.
9. Eleazar, Abraham (Abraham The Jew), Urlates Chymisches Werk, Leipzig, 1760, Reproduced In Psychology And Alchemy, Pantheon Books, N.Y., 1953.
10. Fletcher, R., & Wilson, H.T., The Role Of Pyrolysis In The Disposal Of Waste Tyres, Resource Recovery & Conservation, Foster Wheeler Power Products Ltd., London, England, 1980.
11. Holman, J.P., Heat Transfer, 6th Edition, McGraw Hill, Santa Anna, California, 1986.
12. Incropera, F.P., Dewitt, D.P., Fundamentals Of Heat And Mass Transfer, 3rd Edition, John Wiley & Sons, Purdue University, 1990.
13. Irwin, J.B., Cryogenic Production Of Crumb Rubber From Scrap Tires, Technical & Economic Evaluation, Scrap Tire Conference, Crystal City, VA., 1989.

14. Klingensmith, W.H., Rubber Recycling And Technology Update, University of Wisconsin-Milwaukee, WI., 1993.
15. McMillan, F., Cryogenic Tyre Granulation, Third National Chemical Engineering Conference, Victoria, Australia, August, 1975.
16. Michalski, P.H., A Classification Of Materials Which Can Be Cryogenically Recycled, M.S. Thesis, University Of Wisconsin-Madison, 1976.
17. Nakajima, Y., Matsuyuki, M., Utilization Of Waste Tires As Fuel For Cement Production, Conservation & Recycling, Nokon Cement Company, Bridgestone Tire Co., Japan, 1981.
18. Smith, F.G., Rubber Recycling And Technology Update, University of Wisconsin-Milwaukee, WI., 1993.
19. Sverdrup, E.F., Wendrow, B.R., Rubber Reclaiming, Encyclopedia Of Polymer Science & Engineering, 1988.
20. U.S. Environmental Protection Agency, Burning Tires For Fuel & Tire Pyrolysis: Air Implications, Emission Standards Division, Research Triangle Park, N.C., 1991.

APPENDIX I

Dipping One Inch Cube Of Scrap Tire Rubber
Into Liquid Nitrogen (Theoretical).

TABLE 1.1 : Centre Temp. of a 1/2" cube
of rubber (dipped into liquid nitrogen)

t (sec)	Fo	X	Y	Z	Tc (°C)
50	0.077	1.00	1.0	1.000	25.0
100	0.154	1.00	1.0	1.000	25.0
150	0.231	0.87	1.0	0.659	-45.3
200	0.308	0.78	1.0	0.475	-63.2
250	0.385	0.70	1.0	0.343	-110.3
300	0.461	0.64	1.0	0.262	-127.0
350	0.538	0.57	1.0	0.185	-142.9
400	0.615	0.48	1.0	0.111	-158.2
450	0.692	0.44	1.0	0.085	-163.5
500	0.769	0.38	1.0	0.055	-169.7
550	0.846	0.33	1.0	0.036	-173.6
600	0.923	0.30	1.0	0.027	-175.4
650	1.000	0.27	1.0	0.020	-176.9
700	1.077	0.25	1.0	0.016	-177.8
750	1.154	0.21	1.0	0.009	-179.1
800	1.230	0.18	1.0	0.006	-179.8

Density = 1200 kg/m³
k = 0.15 W/m°C

C = 2010 J/Kg°C
alpha = 6.2E-8 m²/s

h = 100 W/m²/K

$$k/(hL) = 0.15/(100 \cdot 0.00635) = 0.236$$

$$Fo = \alpha t / (L^2)$$

$$= 6.2E-8 \cdot t / (0.00635^2) = 1.54E-3 t$$

X = From Fig. 4.2; blow-up Fig. 4,3

Y = @ centre line temperature, From Fig. 4.4, where x/L = 0

therefore Y = 1

Z = Sol'n = P(x1) * P(x2) * P(x3)

where : P(x) = X * Y, P(x) = P(x1) = P(x2) = P(x3) since cubed

Tc = Too + (To - Too) * Z

$$= -181 + (25 - (-181)) * Z$$

Figure I.1 : Centre temperature of a 1/2" cube rubber dipped into liquid nitrogen.

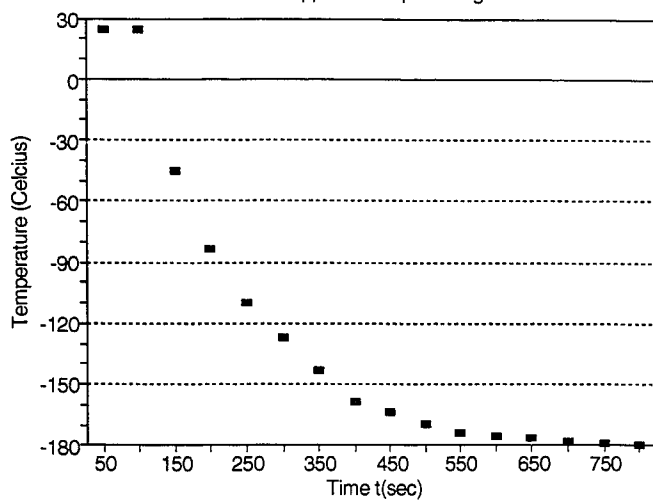


TABLE I.2 : Centre Temp. of a 1" cube
of rubber dipped into liquid nitrogen

t (sec)	Fo	X	Y	Z	Tc (°C)
250	0.096	1.00	1.00	1.000	25.0
300	0.115	0.98	1.00	0.941	12.9
450	0.173	0.93	1.00	0.804	-15.3
500	0.192	0.91	1.00	0.754	-25.8
550	0.211	0.88	1.00	0.681	-40.6
600	0.231	0.80	1.00	0.512	-75.5
650	0.250	0.77	1.00	0.457	-87.0
700	0.269	0.75	1.00	0.422	-94.1
750	0.288	0.73	1.00	0.389	-100.9
800	0.308	0.70	1.00	0.343	-110.3
850	0.327	0.68	1.00	0.314	-116.2
900	0.346	0.65	1.00	0.275	-124.4

Density = 1200 kg/m³
k = 0.15 W/m°C

C = 2010 J/Kg°C
alpha = 6.2E-8 m²/s

h = 100 W/m²K

$$k/(hL) = 0.15/(100 \cdot 0.0127) = 0.118$$

$$Fo = \alpha t / (L^2) = 6.2E-8 t / (0.0127^2) = 3.844E-4 t$$

X = From Fig. 4.2; blow-up Fig 4.3

Y = @ centre line temperature, From Fig. 4.4, where x/L = 0

therefore Y = 1

Z = Sol'n = P(x1)*P(x2)*P(x3)

where : P(x) = X*Y, P(x) = P(x1) = P(x2) = P(x3) since cubed

$$Tc = T_{\infty} + (T_0 - T_{\infty})Z = -181 + (25 - (-181))Z$$

Figure 1.2 : Centre temperature of a 1" cube rubber dipped into liquid nitrogen.

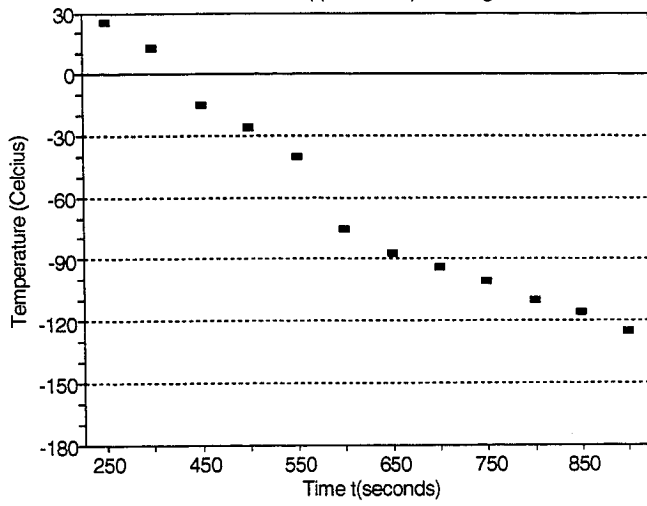


TABLE I.3: Centre Temp. of a 2" cube
of rubber dipped into liquid nitrogen

t (sec)	Fo	X	Y	Z	Tc (°C)
1000	0.096	1.00	1.00	1.000	25.0
1100	0.106	1.00	1.00	1.000	25.0
1150	0.111	0.98	1.00	0.941	12.9
1200	0.115	0.96	1.00	0.885	1.3
1250	0.120	0.93	1.00	0.804	-15.3
1300	0.125	0.91	1.00	0.754	-25.8
1350	0.130	0.90	1.00	0.729	-30.8
1450	0.139	0.88	1.00	0.681	-40.6
1550	0.149	0.86	1.00	0.636	-50.0
1650	0.159	0.83	1.00	0.572	-63.2
1850	0.178	0.82	1.00	0.551	-67.4
1950	0.187	0.81	1.00	0.531	-71.5
2200	0.211	0.77	1.00	0.457	-87.0
2350	0.226	0.75	1.00	0.422	-94.1
2500	0.240	0.74	1.00	0.405	-97.5
2700	0.259	0.72	1.00	0.373	-104.1

Density = 1200 kg/m³
k = 0.15 W/m°C

C = 2010 J/Kg°C
alpha = 6.2E-8 m²/s

h = 100 W/m²K

$$k/(hL) = 0.15/(100 \cdot 0.0254) = 0.059 \quad \text{Fo} = \alpha t / (L^2) = 6.2E-8 t / (0.0254^2) = 9.61E-5 t$$

X = From Fig. 4.2; blow-up Fig 4.3

Y = @ centre line temperature, From Fig. 4.4, where x/L = 0

therefore Y = 1

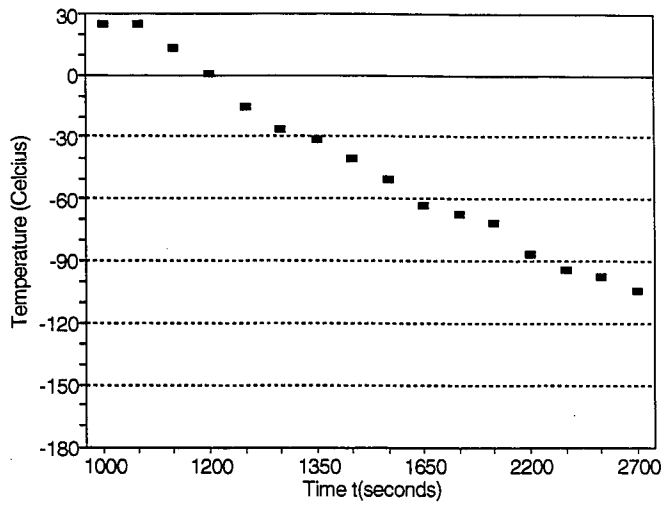
Z = Sol'n = P(x1)*P(x2)*P(x3)

where : P(x) = X*Y, P(x) = P(x1) = P(x2) = P(x3) since cubed

Tc = Too + (To - Too)*Z

= -181 + (25 - (-181))*Z

Figure 1.3 : Centre temperature of a 2" cube rubber dipped into liquid nitrogen.



APPENDIX II

Gas Phase Cooling Over Liquid Nitrogen
Of A One Inch Cube Of Tire
Rubber (Theoretical).

TABLE II.1 : Centre Temp. of a 1/2' cube
of rubber (gas phase cooling over liquid nitrogen)

t (sec)	Fo	X	Y	Z	Tc (°C)
50	0.077	1.00	1.0	1.000	25.0
100	0.154	1.00	1.0	1.000	25.0
150	0.231	0.98	1.0	0.941	12.9
200	0.308	0.94	1.0	0.831	-9.9
250	0.385	0.90	1.0	0.729	-30.8
300	0.461	0.87	1.0	0.659	-45.3
350	0.538	0.84	1.0	0.593	-58.9
400	0.615	0.81	1.0	0.531	-71.5
450	0.692	0.78	1.0	0.475	-83.2
500	0.769	0.76	1.0	0.439	-90.6
550	0.846	0.73	1.0	0.389	-100.9
600	0.923	0.70	1.0	0.343	-110.3
650	1.000	0.68	1.0	0.314	-116.2
700	1.077	0.66	1.0	0.287	-121.8
750	1.154	0.64	1.0	0.262	-127.0
800	1.230	0.61	1.0	0.227	-134.2

Density = 1200 kg/m³
k = 0.15 W/m°C

C = 2010 J/Kg°C
alpha = 6.2E-8 m²/s

h = 20 W/m²K

$$k/(hL) = 0.15/(20 \cdot 0.00635) = 1.81 \quad \text{Fo} = \alpha t / (L^2) = 6.2E-8 t / (0.00635^2) = 1.54E-3 t$$

X = From Fig. 4.2; blow-up Fig 4.3

Y = @ centre line temperature, From Fig. 4.4, where $x/L = 0$
therefore Y = 1

Z = Sol'n = P(x1) * P(x2) * P(x3)

where : P(x) = X * Y, P(x1) = P(x2) = P(x3) since cubed

$$T_c = T_{\infty} + (T_0 - T_{\infty}) Z = -181 + (25 - (-181)) Z$$

Figure II.1 : Centre temperature of a 1/2" cube rubber subjected to gas phase cooling.

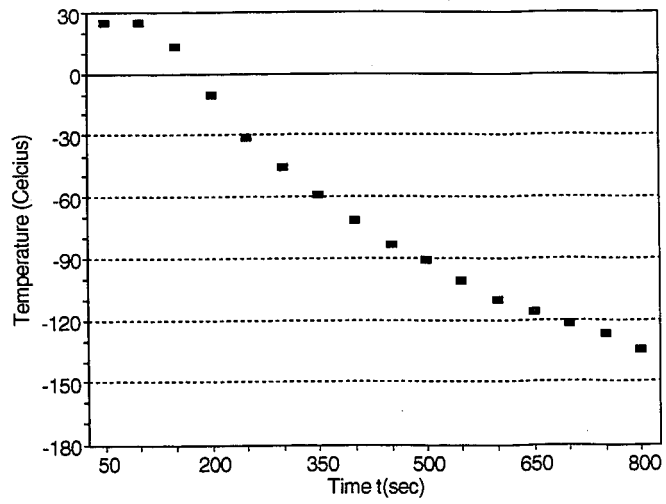


TABLE II.2: Centre Temp. of a 1" cube of rubber
(gas phase cooling over liquid nitrogen)

t (sec)	Fo	X	Y	Z	Tc (°C)
250	0.096	1.00	1.00	1.000	25.0
300	0.115	1.00	1.00	1.000	25.0
450	0.173	0.98	1.00	0.941	12.9
500	0.192	0.95	1.00	0.857	-4.4
550	0.211	0.93	1.00	0.804	-15.3
600	0.231	0.90	1.00	0.729	-30.8
650	0.250	0.88	1.00	0.681	-40.6
700	0.269	0.87	1.00	0.659	-45.3
750	0.288	0.86	1.00	0.636	-50.0
800	0.308	0.85	1.00	0.614	-54.5
850	0.327	0.83	1.00	0.572	-63.2
900	0.346	0.81	1.00	0.531	-71.5
950	0.365	0.8	1.00	0.512	-75.5
1000	0.384	0.79	1.00	0.493	-79.4
1050	0.404	0.77	1.00	0.457	-87.0

Density = 1200 kg/m³
k = 0.15 W/m°C

C = 2010 J/Kg°C
alpha = 6.2E-8 m²/s

h = 20 W/m²/K

$$k/(hL) = 0.15/(20 \cdot 0.0127) = 0.591$$

$$Fo = \alpha t / (L^2) = 6.2E-8 \cdot t / (0.0127^2) = 3.844E-4 t$$

X = From Fig. 4.2; blow-up Fig 4.3

Y = @ centre line temperature, From Fig. 4.4, where $x/L = 0$
therefore Y = 1

Z = Sol'n = P(x1) * P(x2) * P(x3)

where : P(x) = X * Y, P(x) = P(x1) = P(x2) = P(x3) since cubed

$$T_c = T_{\infty} + (T_0 - T_{\infty}) Z \\ = -181 + (25 - (-181)) Z$$

Figure II.2 : Centre temperature of a 1" cube rubber subjected to gas phase cooling.

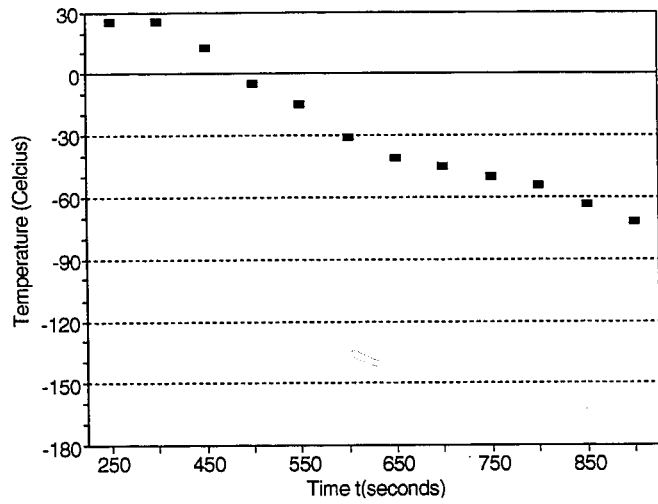


TABLE II.3: Centre Temp. of a 2" cube
of rubber (gas phase cooling over nitrogen)

t (sec)	Fo	X	Y	Z	Tc (°C)
1250	0.120	1.00	1.00	1.000	25.0
1300	0.125	1.00	1.00	1.000	25.0
1350	0.130	1.00	1.00	1.000	25.0
1450	0.139	1.00	1.00	1.000	25.0
1550	0.149	1.00	1.00	1.000	25.0
1650	0.159	0.98	1.00	0.941	12.9
1850	0.178	0.95	1.00	0.857	-4.4
1950	0.187	0.94	1.00	0.831	-9.9
2200	0.211	0.90	1.00	0.729	-30.8
2350	0.226	0.87	1.00	0.659	-45.3
2500	0.240	0.85	1.00	0.614	-54.5
2700	0.259	0.83	1.00	0.572	-63.2
2900	0.279	0.82	1.00	0.551	-67.4
3100	0.298	0.79	1.00	0.493	-79.4
3300	0.317	0.77	1.00	0.457	-87.0
3500	0.336	0.75	1.00	0.422	-94.1
3800	0.365	0.73	1.00	0.389	-100.9
4100	0.394	0.69	1.00	0.329	-113.3

Density = 1200 kg/m³
k = 0.15 W/m°C

C = 2010 J/Kg°C
alpha = 6.2E-8 m²/s

h = 20 W/m²°C

$$k/(hL) = 0.15/(20 \cdot 0.0254) = 0.295$$

$$Fo = \alpha t / L^2$$

$$= 6.2E-8 \cdot t / (0.0254^2) \\ = 9.61E-5 t$$

X = From Fig. 4.2; blow-up Fig 4.3

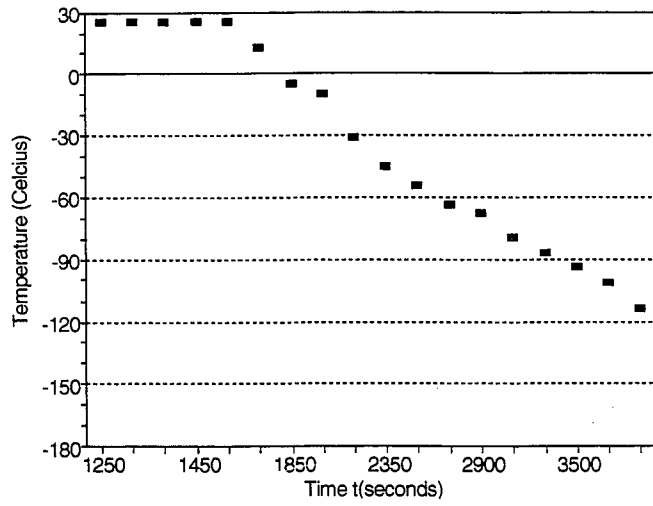
Y = @ centre line temperature, From Fig. 4.4, where $x/L = 0$
therefore Y = 1

Z = Sol'n = P(x1)*P(x2)*P(x3)

where : P(x) = X*Y, P(x) = P(x1) = P(x2) = P(x3) since cubed

Tc = Too + (To - Too)*Z
= -181 + (25 - (-181))*Z

Figure II.3 : Centre temperature of a 2" cube rubber subjected to gas phase cooling.



APPENDIX III

Spraying A One Inch Cube Of Tire Rubber
With Liquid Nitrogen (Theoretical).

TABLE III.1 : Centre Temp. of a 1/2' cube
of rubber (spraying of liquid nitrogen)

t(sec)	Fo	X	Y	Z	Tc(°C)
50	0.077	1.00	1.0	1.000	25.0
100	0.154	0.92	1.0	0.779	-20.6
150	0.231	0.76	1.0	0.439	-90.6
200	0.308	0.65	1.0	0.275	-124.4
250	0.385	0.56	1.0	0.176	-144.8
300	0.461	0.47	1.0	0.104	-159.6
350	0.538	0.40	1.0	0.064	-167.8
400	0.615	0.34	1.0	0.039	-172.9
450	0.692	0.28	1.0	0.021	-176.7

Density = 1200 kg/m³
k = 0.15 W/m°C

C = 2010 J/Kg°C
alpha = 6.2E-8 m²/s

h = 400 W/m²K

$$k/(hL) = 0.15/(400 \cdot 0.00635) = 0.06$$

$$Fo = \alpha t / (L^2) = 6.2E-8 t / (0.00635^2) = 1.54E-3 t$$

X = From Fig. 4.2; blow-up Fig 4.3

Y = @ centre line temperature, From Fig. 4.4, where x/L = 0
therefore Y = 1

Z = Sol'n = P(x1) * P(x2) * P(x3)

where : P(x) = X * Y, P(x) = P(x1) = P(x2) = P(x3) since cubed

Tc = Too - (To - Too) * Z
= -181 + (25 - (-181)) * Z

Figure III.1 : Centre temperature of a 1/2" cube rubber sprayed with liquid nitrogen.

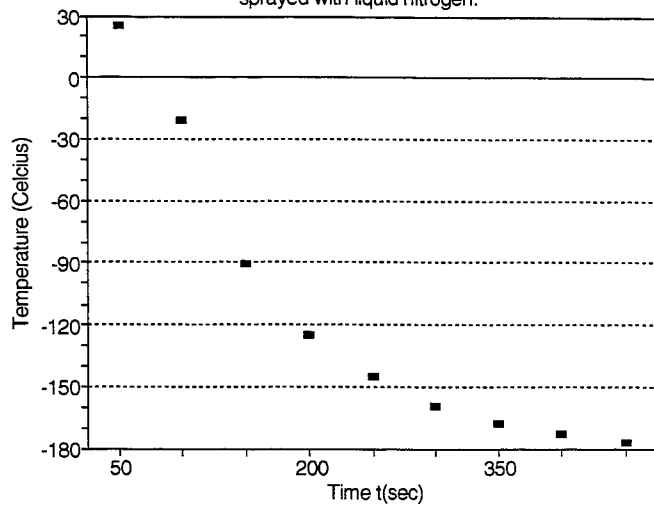


TABLE III.2 :Centre Temp. of a 1" cube
of rubber (spraying of liquid nitrogen)

t (sec)	Fo	X	Y	Z	Tc (°C)
250	0.096	1.00	1.00	1.000	25.0
300	0.115	0.97	1.00	0.913	7.0
450	0.173	0.84	1.00	0.593	-58.9
500	0.192	0.78	1.00	0.475	-83.2
550	0.211	0.75	1.00	0.422	-94.1
600	0.231	0.71	1.00	0.358	-107.3
650	0.250	0.69	1.00	0.329	-113.3
700	0.269	0.65	1.00	0.275	-124.4
750	0.288	0.63	1.00	0.250	-129.5
800	0.308	0.60	1.00	0.216	-136.5
850	0.327	0.57	1.00	0.185	-142.9
900	0.346	0.55	1.00	0.166	-146.7

Density = 1200 kg/m³
k = 0.15 W/m°C

C = 2010 J/Kg°C
alpha = 6.2E-8 m²/s

h = 400 W/m²K

$$k/(hL) = 0.15/(400 \cdot 0.0127) = 0.03$$

$$Fo = \alpha t / (L^2) = 6.2E-8 t / (0.0127^2) = 3.844E-4 t$$

X = From Fig. 4.2; blow-up Fig 4.3

Y = @ centre line temperature, From Fig. 4.4, where x/L = 0

therefore Y = 1

Z = Sol'n = P(x1)*P(x2)*P(x3)

where : P(x) = X*Y, P(x) = P(x1) = P(x2) = P(x3) since cubed

$$Tc = T_{\infty} + (T_0 - T_{\infty})Z = -181 + (25 - (-181))Z$$

Figure III.2 : Centre temperature of a 1" cube rubber sprayed with liquid nitrogen.

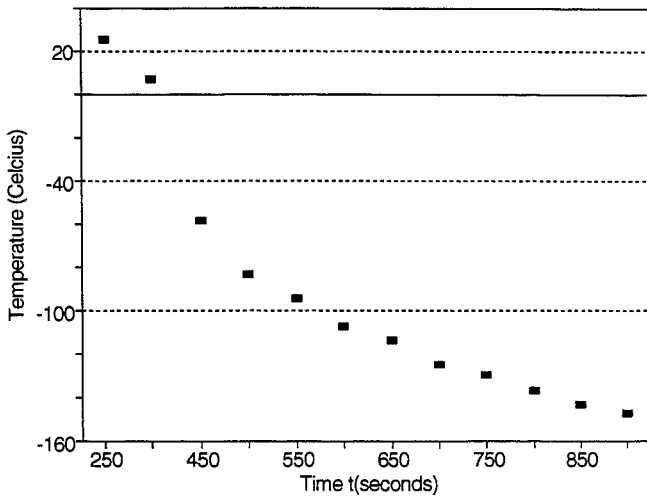


TABLE III.3: Centre Temp. of a 2" cube
of rubber (spraying liquid nitrogen)

t (sec)	Fo	X	Y	Z	Tc (°C)
700	0.067	1.00	1.00	1.000	25.0
750	0.072	1.00	1.00	1.000	25.0
800	0.077	1.00	1.00	1.000	25.0
850	0.082	1.00	1.00	1.000	25.0
900	0.086	1.00	1.00	1.000	25.0
950	0.091	1.00	1.00	1.000	25.0
1000	0.096	0.97	1.00	0.913	7.0
1050	0.101	0.95	1.00	0.857	-4.4
1100	0.106	0.93	1.00	0.804	-15.3
1200	0.115	0.90	1.00	0.729	-30.8
1300	0.125	0.88	1.00	0.681	-40.6
1400	0.135	0.86	1.00	0.636	-50.0
1500	0.144	0.82	1.00	0.551	-67.4
1600	0.154	0.80	1.00	0.512	-75.5
1700	0.163	0.79	1.00	0.493	-79.4
1900	0.183	0.77	1.00	0.457	-87.0
2100	0.202	0.73	1.00	0.389	-100.9
2300	0.221	0.70	1.00	0.343	-110.3

Density = 1200 kg/m³
k = 0.15 W/m°C

C = 2010 J/Kg°C
alpha = 6.2E-8 m²/s

h = 400 W/mK

$$k/(hL) = 0.15/(400 \cdot 0.0254) = 0.015$$

$$Fo = \alpha \cdot t / (L^2)$$

$$= 6.2E-8 \cdot t / (0.0254^2) \\ = 9.61E-5 t$$

X = From Fig. 4.2; blow-up Fig 4.3

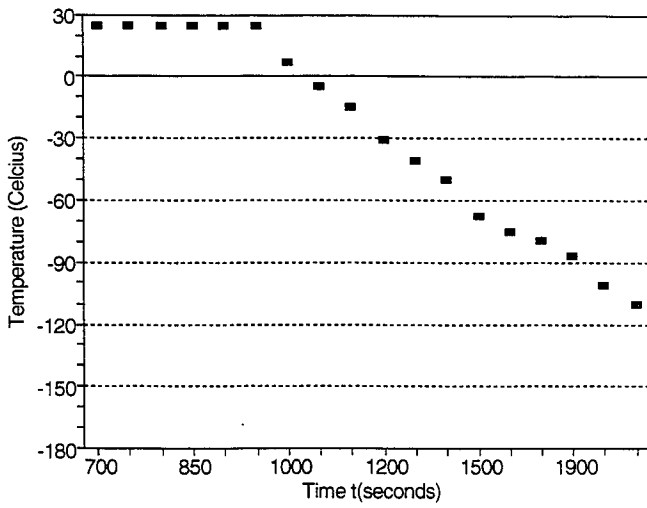
Y = @ centre line temperature, From Fig. 4.4, where x/L = 0
therefore Y = 1

Z = Sol'n = P(x1) * P(x2) * P(x3)

where : P(x) = X * Y, P(x) = P(x1) = P(x2) = P(x3) since cubed

Tc = Too + (To - Too) * Z
= -181 + (25 - (-181)) * Z

Figure III.3 : Centre temperature of a 2" cube rubber sprayed with liquid nitrogen.

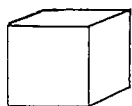


APPENDIX IV

**Nitrogen Consumption For Dipping Rubber
Into Liquid Nitrogen**

Dipping Into Liquid Nitrogen (Nitrogen Consumption)

Too=-181°C



To=25°C

Basis: 1" Cube

a) Time required for Tc=-100°C

$$T_c = T_{oo} + (\theta/\theta_i)_{\text{cube}}(T_o - T_{oo})$$

$$-100 = -181 + (\theta/\theta_i)_{\text{cube}}(25 + 181)$$

$$(\theta/\theta_i)_{\text{cube}} = 0.393$$

$$P(x) = P(x_1) = P(x_2) = P(x_3)$$

$$P(x) = (\theta/\theta_i)_{\text{cube}}^{(1/3)}$$

$$= (0.393)^{(1/3)}$$

$$P(x) = 0.732$$

$$(\theta/\theta_i)_{\text{plate}} = 0.732 = \theta_o/\theta_i * \theta/\theta_o \quad \text{where } \theta/\theta_o = 1 \text{ @ centre}$$

$$\text{Therefore, } \theta_o/\theta_i = 0.732$$

From Figure 4.3

$$\text{@ } \theta_o/\theta_i = 0.732 \quad \text{and } k/(hL) = 0.15 / (100(0.0127)) = 0.118$$

$$Fo = 0.3 = \frac{\alpha t}{L^2} = \frac{6.2 \times 10^{-8} t}{(0.0127)^2} \quad \text{-----> } t = 749 \text{ sec}$$

b) heat-loss to Tc=-100°C, and t=749 sec

-heat-loss ratio for infinite plate

L=0.0127 m, using properties of rubber;

$$hL/k = 100(0.0127)/0.15 = 8.47$$

$$FoBi^2 = \frac{h^2 \alpha t}{k^2} = \frac{100^2 (6.2 \times 10^{-8}) (749)}{0.15^2}$$

$$= 21.5$$

From Figure 4.5

$$Q/Q_o = 0.47$$

Since dimensions in all directions are equal (cubed),
therefore, $Q/Q_o = (Q/Q_o)_1 = (Q/Q_o)_2 = (Q/Q_o)_3$

$$(Q/Q_0)_{\text{tot}} = 0.47 + 0.47(1-0.47) + 0.47(1-0.47)(1-0.47) \\ = 0.851$$

$$Q_0 = \rho CV(T_0 - T_{\infty}) = 1200 \cdot 2010 \cdot 1.64 \cdot 10^{-5} [25 - (-181)] \\ = 8148.7 \text{ Joules}$$

The actual heat loss is:

$$Q = 8147.8(0.851) \\ = 6935.5 \text{ Joules}$$

c) Nitrogen Consumption

$$Q_{\text{rubber}} = Q_{\text{nitrogen}}$$

where, Q_{rubber} is heat-loss for a 1" cube

$$M = \rho \cdot V \\ = 1200(1.639 \cdot 10^{-5}) \\ = 19.7 \text{ grams}$$

Therefore, $Q_{\text{rubber}}/\text{gm}$ of rubber = $6936/19.7 = 352.1 \text{ J/gm}$

From (1),

$$L = 47.7 \text{ cal/gm} \quad C = 0.25 \text{ cal/gm}^\circ\text{C}$$

$$\text{Cal} \cdot 4.184 = \text{Joules}$$

$$352.1 = M_N \cdot L + M_N \cdot C(-5 - (-181))$$

$$352.1 = M_N(47.7)(4.184) + M_N(0.25)(4.184)(176)$$

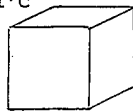
$$M_N = 0.917 \text{ gm nitrogen/gm rubber}$$

APPENDIX V

Nitrogen Consumption For Gas Phase Cooling Of Rubber

Gas Phase Cooling (Nitrogen Consumption)

Too = -181°C



To = 25°C

Basis: 1" cube

a) Time required for Tc = -100°C

$$T_c = T_{oo} + (\theta/\theta_1)_{\text{cube}}(T_o - T_{oo})$$

$$-100 = -181 + (\theta/\theta_1)_{\text{cube}}(25 + 181)$$

$$(\theta/\theta_1)_{\text{cube}} = 0.393$$

$$P(x) = P(x_1) + P(x_2) = P(x_3)$$

$$P(x) = ((\theta/\theta_1)_{\text{cube}})^{1/3}$$

$$= (0.393)^{1/3}$$

$$P(x) = 0.732$$

$$(\theta/\theta_1)_{\text{plate}} = 0.732 = \theta_o/\theta_1 * \theta/\theta_o \quad \text{where } \theta/\theta_o = 1 \text{ @ centre}$$

$$\text{Therefore, } \theta_o/\theta_1 = 0.732$$

From Figure 4.3

$$\text{@ } \theta_o/\theta_1 = 0.732 \text{ and } k/(hL) = 0.15/(20(0.0127)) = 0.591$$

$$Fo = 0.47 = \frac{\alpha t}{L^2} = \frac{6.2 \times 10^{-8} t}{(0.0127)^2}$$

$$t = 1222.7 \text{ sec}$$

b) heat-loss to Tc = -100°C, and t = 1222.7 sec

-heat-loss ratio for infinite plate

L = 0.0127 m , using properties of rubber;

$$hL/k = 20(0.0127)/0.15 = 1.69$$

$$FoBi^2 = \frac{h^2 \alpha t}{k^2} = \frac{20^2 (6.2 \times 10^{-8}) (1222.7)}{0.15^2}$$

$$= 1.35$$

From Figure 4.5

$$Q/Q_0 = 0.36$$

Since dimension in all directions are equal (cubed)
therefore, $Q/Q_0 = (Q/Q_0)_1 = (Q/Q_0)_2 = (Q/Q_0)_3$

$$(Q/Q_0)_{\text{tot}} = 0.36 + 0.36(1-0.36) + 0.36(1-0.36)(1-0.36) \\ = 0.713$$

$$Q_0 = \rho CV(T_0 - T_{\infty}) \\ = 1200(2010)(1.64 \times 10^{-5})(25 + 181) \\ = 8148.7 \text{ Joules}$$

The actual heat-loss is,

$$Q = 8148.7(0.713) \\ = 5810.0 \text{ Joules}$$

c) Nitrogen Consumption

$$Q_{\text{rubber}} = Q_{\text{nitrogen}} \quad (1)$$

where, Q_{rubber} is heat-loss for a 1" cube

$$Q_{\text{rubber}}/\text{gm of rubber} = 5810/19.7 = 294.9 \text{ J/gm}$$

From (1)

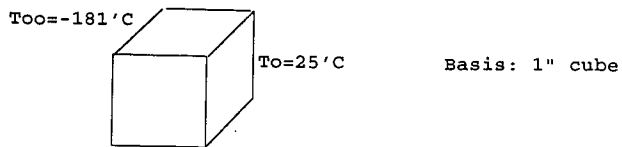
$$294.9 = M_N L + M_N C(-5 - (-181))$$

$$294.9 = M_N(47.7)(4.184) + M_N(0.25)(4.184)(176)$$

$$M_N = 0.769 \text{ gm nitrogen/gm rubber}$$

APPENDIX VI

Nitrogen Consumption For Spraying Of Rubber

Nitrogen Consumption By Spraying

a) Time required for Tc = -100°C

$$T_c = T_{oo} + (\theta/\theta_i)_{\text{cube}}(T_o - T_{oo})$$

$$-100 = -181 + (\theta/\theta_i)_{\text{cube}}(25 + 181)$$

$$(\theta/\theta_i)_{\text{cube}} = 0.393$$

$$P(x) = P(x_1) = P(x_2) = P(x_3)$$

$$P(x) = ((\theta/\theta_i)_{\text{cube}})^{(1/3)}$$

$$= (0.393)^{(1/3)}$$

$$P(x) = 0.732$$

$$(\theta/\theta_i)_{\text{plate}} = 0.732 = \theta_o/\theta_i * \theta/\theta_o \quad \text{where } \theta/\theta_o = 1 \text{ @ centre}$$

$$\text{Therefore, } \theta_o/\theta_i = 0.732$$

From Figure 4.3

$$\text{@ } \theta_o/\theta_i = 0.732 \text{ and } k/(hL) = 0.15/(400(0.0127)) = 0.03$$

$$Fo = 0.22 = \alpha t/L^2 = 6.2 \times 10^{-8} t / (0.0127)^2$$

$$\text{-----> } t = 572 \text{ sec}$$

b) heat-loss to Tc = -100°C, t = 572 sec

-heat-loss ratio for infinite plate

L = 0.0127 m , using properties of rubber

$$hL/k = (400 \times 0.0127) / 0.15 = 33.87$$

$$FoBi^2 = \frac{h^2 \alpha t}{k^2} = \frac{400^2 (6.2 \times 10^{-8}) (572)}{0.15^2}$$

$$= 252.2$$

From Figure 4.5

$$Q/Q_0 = 0.52$$

$$(Q/Q_0)_{\text{tot}} = 0.52 + 0.52(1-0.52) + 0.52(1-0.52)(1-0.52) \\ = 0.889$$

$$Q_0 = \rho CV(T_0 - T_{\infty}) \\ = 1200(2010)(1.64 \times 10^{-5})(25 - (-181)) \\ = 8148.7 \text{ Joules}$$

The actual heat-loss is,

$$Q = 8148.7(0.889) \\ = 7244.2 \text{ Joules}$$

c) Nitrogen consumption

$$Q_{\text{rubber}} = Q_{\text{nitrogen}} \quad (1)$$

where, Q_{rubber} is heat-loss for a 1" cube

$$Q_{\text{rubber}}/\text{gm of rubber} = 7244.2/19.7 = 367.9 \text{ J/gm}$$

From (1),

$$367.7 = M_N L + M_N C(-5 - (-181))$$

$$367.7 = M_N(47.7)(4.184) + M_N(0.25)(4.184)(176)$$

$$M_N = 0.958 \text{ gm of nitrogen/gm of rubber}$$

APPENDIX VII

Experiment One Results:

One Inch Cube Of Tire Rubber
Dipped Into Liquid Nitrogen.

FIGURE VII.1: ONE INCH CUBE OF RUBBER DIPPED INTO LIQUID NITROGEN (TEST 1).

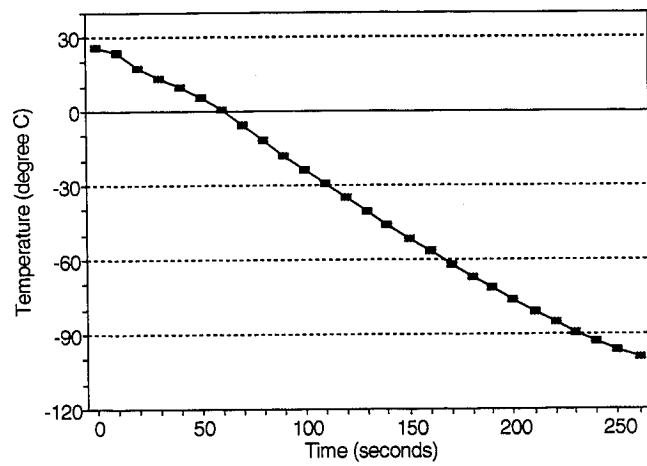


FIGURE VII.2: ONE INCH CUBE OF RUBBER DIPPED INTO LIQUID NITROGEN (TEST 2).

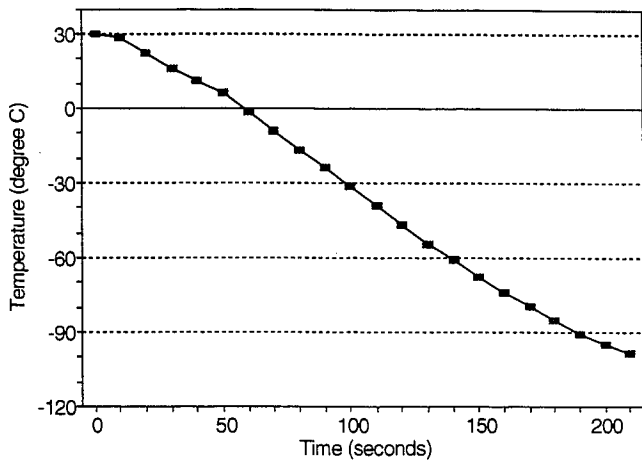


FIGURE VII.3: ONE INCH CUBE OF RUBBER DIPPED INTO LIQUID NITROGEN (TEST 3).

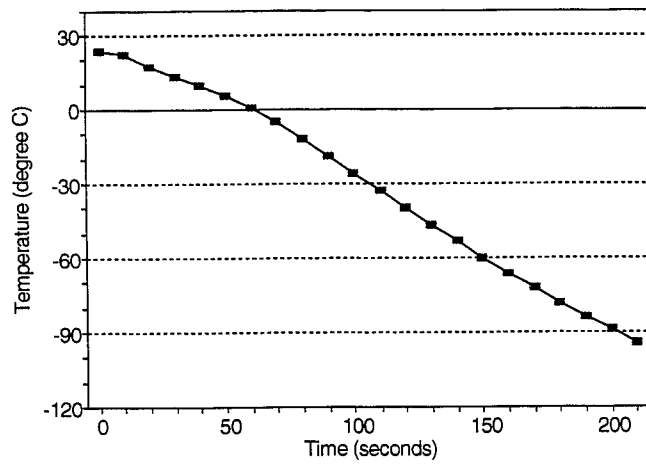


FIGURE VII.4: ONE INCH CUBE OF RUBBER DIPPED INTO LIQUID NITROGEN (TEST 4).

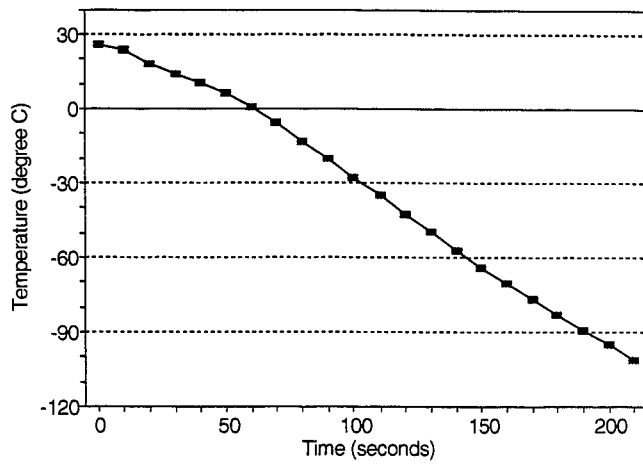


FIGURE VII.5: ONE INCH CUBE OF RUBBER DIPPED INTO LIQUID NITROGEN (TEST 5).

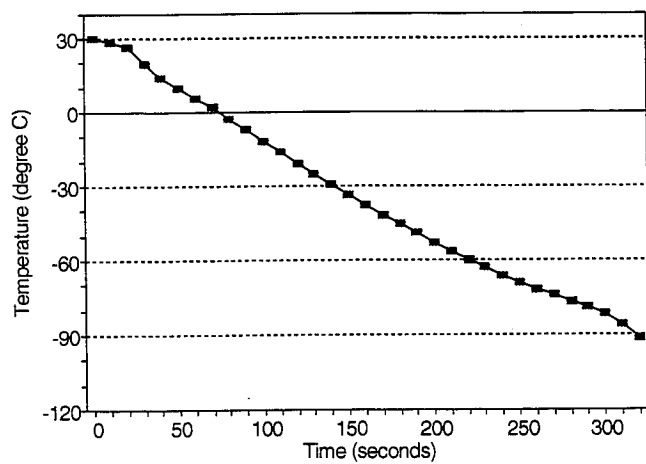


FIGURE VII.6: ONE INCH CUBE OF RUBBER DIPPED INTO LIQUID NITROGEN (TEST 6)

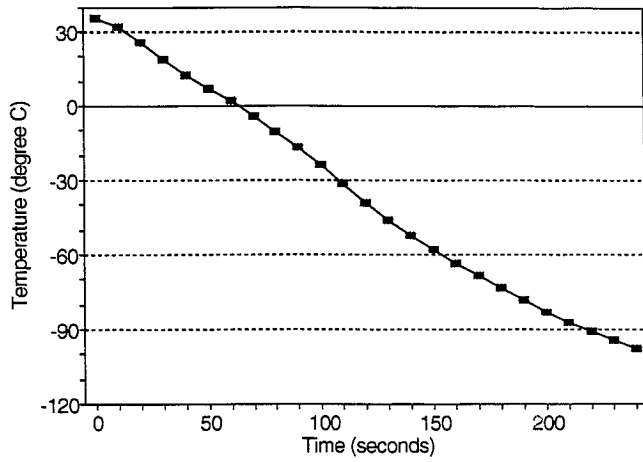


FIGURE VII.7: ONE INCH CUBE OF RUBBER DIPPED INTO LIQUID NITROGEN (TEST 7).

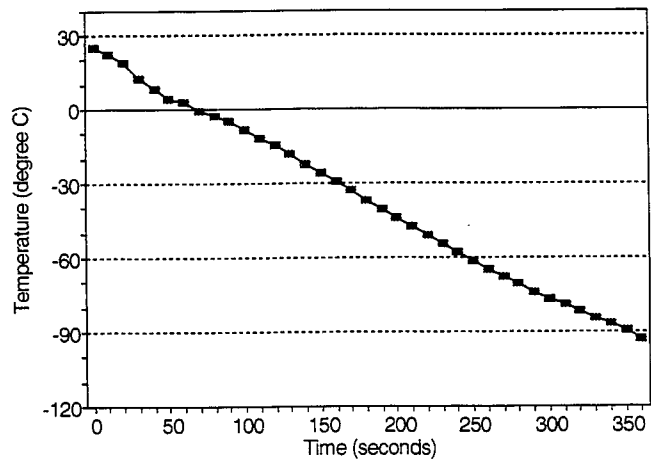


FIGURE VII.8: ONE INCH CUBE OF RUBBER DIPPED INTO LIQUID NITROGEN (TEST 8)

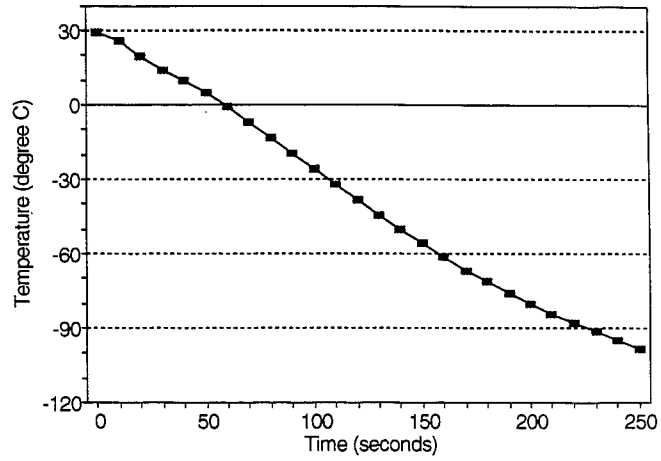


FIGURE VII.9: ONE INCH CUBE OF RUBBER DIPPED INTO LIQUID NITROGEN (TEST 9).

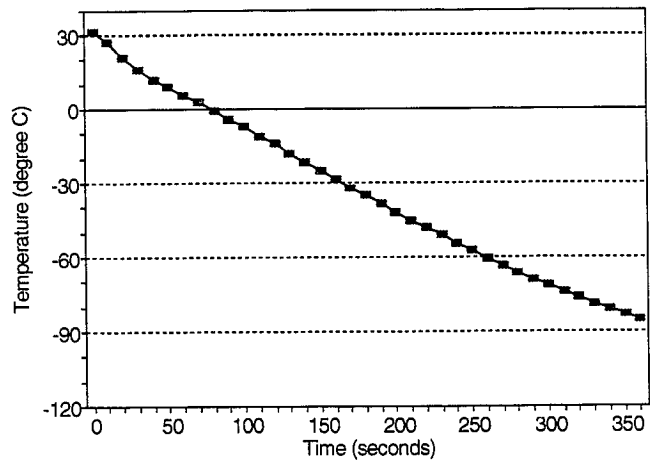
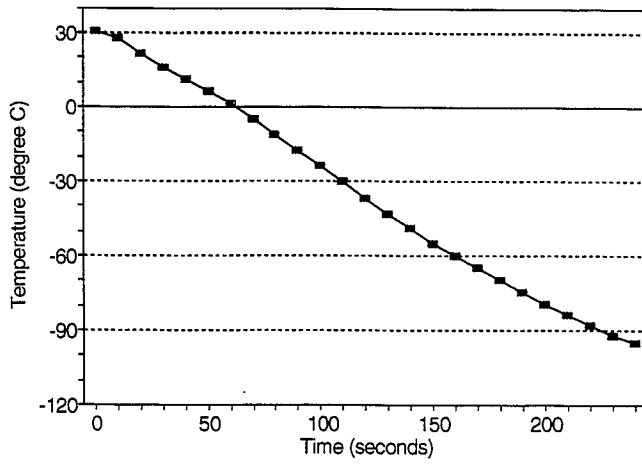


FIGURE VII.10: ONE INCH CUBE OF RUBBER DIPPED INTO LIQUID NITROGEN (TEST 10).



APPENDIX VIII

Experiment Two Results:

One Inch Cube Of Tire Rubber Cooled By
Liquid Nitrogen Vapour.

FIGURE VIII.1: ONE INCH CUBE OF TIRE RUBBER COOLED WITH LIQUID NITROGEN VAPOUR (TEST 1).

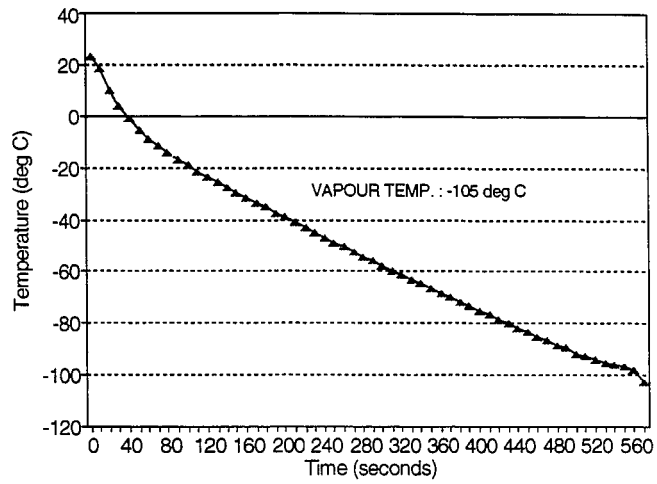


FIGURE VIII.2: ONE INCH CUBE OF TIRE RUBBER COOLED WITH LIQUID NITROGEN VAPOUR (TEST 2).

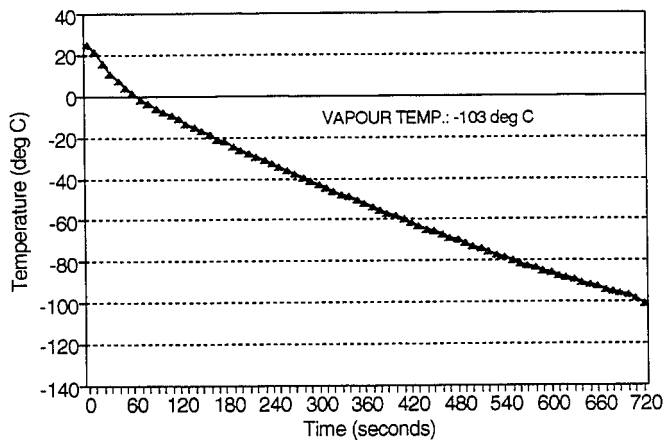


FIGURE VIII.3: ONE INCH CUBE OF TIRE RUBBER COOLED WITH LIQUID NITROGEN VAPOUR (TEST 3).

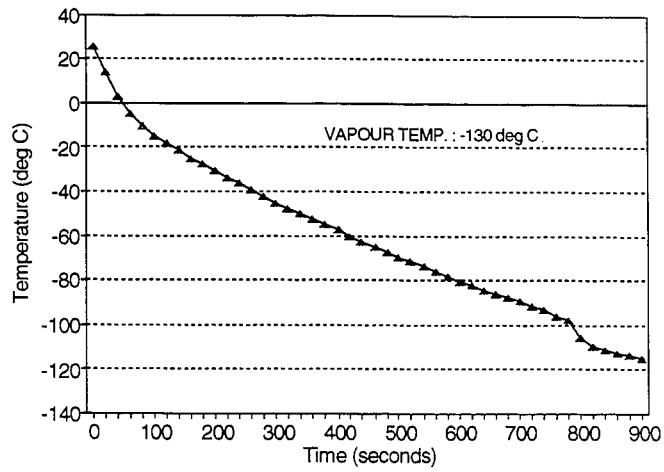


FIGURE VIII.4: ONE INCH CUBE OF TIRE RUBBER COOLED WITH LIQUID NITROGEN VAPOUR (TEST 4).

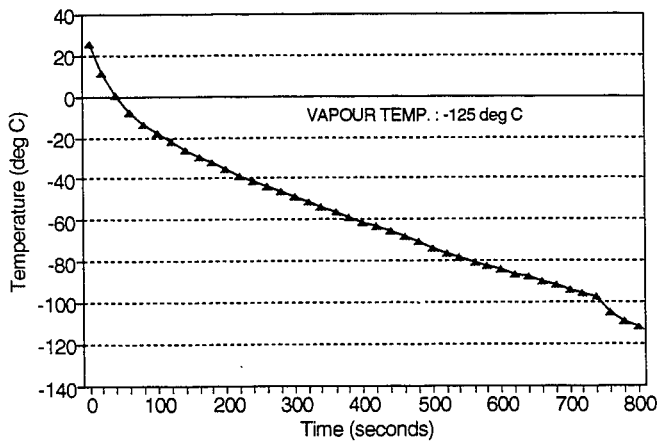


FIGURE VIII.5: ONE INCH CUBE OF TIRE RUBBER COOLED WITH LIQUID NITROGEN VAPOUR (TEST 5).

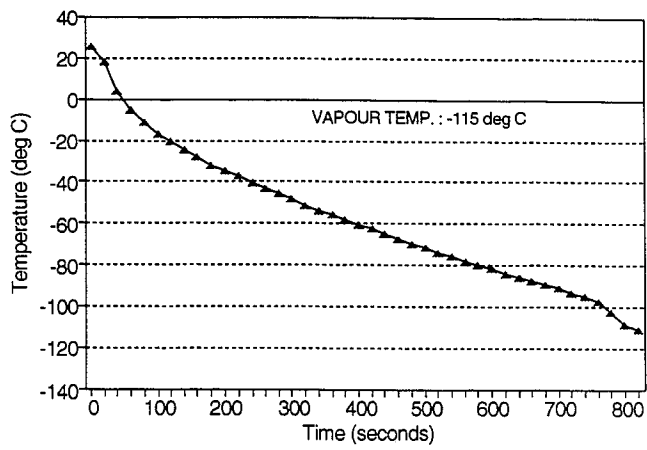


FIGURE VIII.6: ONE INCH CUBE OF TIRE RUBBER COOLED WITH LIQUID NITROGEN VAPOUR (TEST 6).

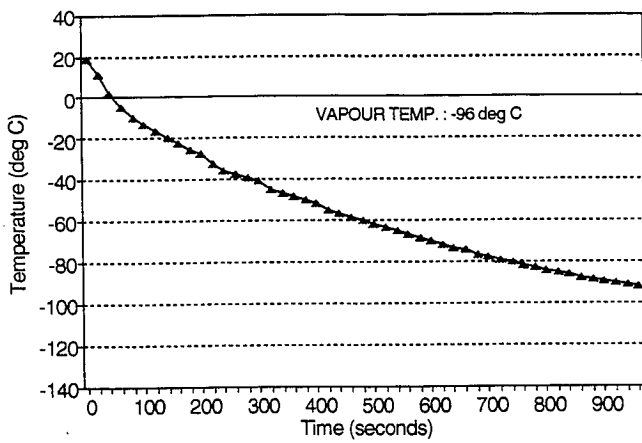


FIGURE VIII.7: ONE INCH CUBE OF TIRE RUBBER COOLED WITH LIQUID NITROGEN VAPOUR (TEST 7).

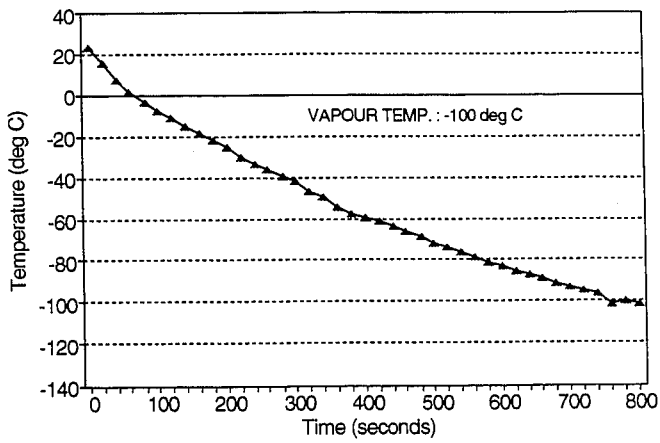


FIGURE VIII.8: ONE INCH CUBE OF TIRE RUBBER COOLED WITH LIQUID NITROGEN VAPOUR (TEST 8).

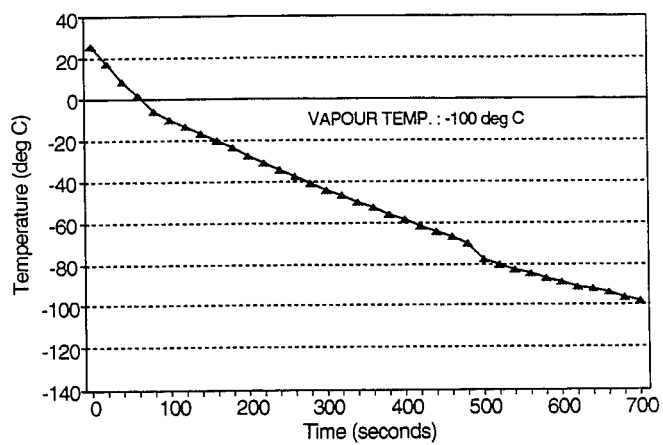


FIGURE VIII.9: ONE INCH CUBE OF TIRE RUBBER COOLED WITH LIQUID NITROGEN VAPOUR (TEST 9).

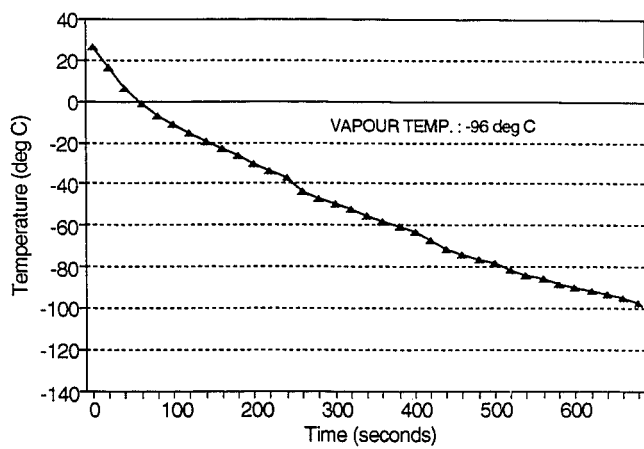
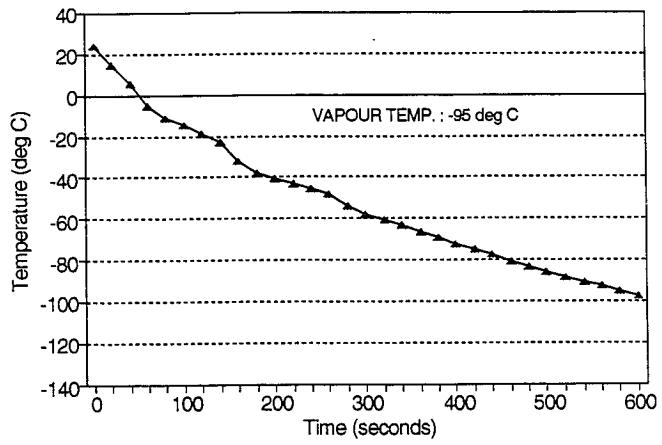


FIGURE VIII.10: ONE INCH CUBE OF TIRE RUBBER COOLED WITH LIQUID NITROGEN VAPOUR (TEST 10).



APPENDIX IX

Experiment Three Results:

Different Sizes Of Tire Rubber Specimens Cooled
Simultaneously By Liquid Nitrogen Vapour.

FIGURE IX.1: 1/4", 1/2", 3/4", 1 1/4" CUBES SIMULTANEOUSLY COOLED IN COLDER NITROGEN VAPOURS. (TEST 1)

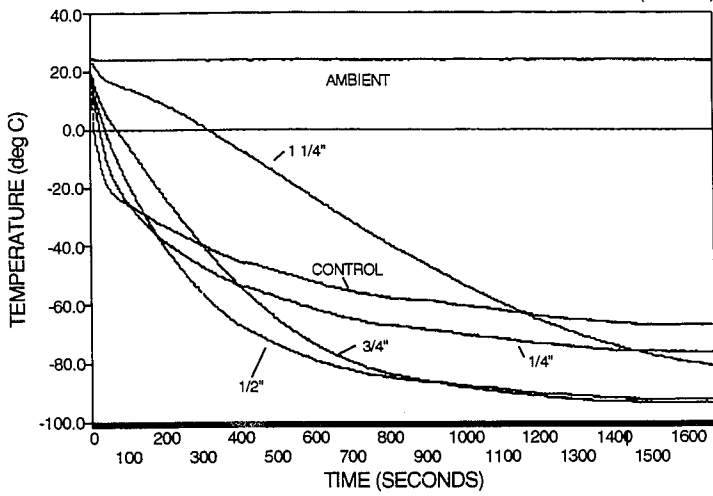


FIGURE IX.2: 1/4", 1/2", 3/4", 1 1/4" CUBES SIMULTANEOUSLY
COOLED IN COLDER NITROGEN VAPOURS. (TEST 2)

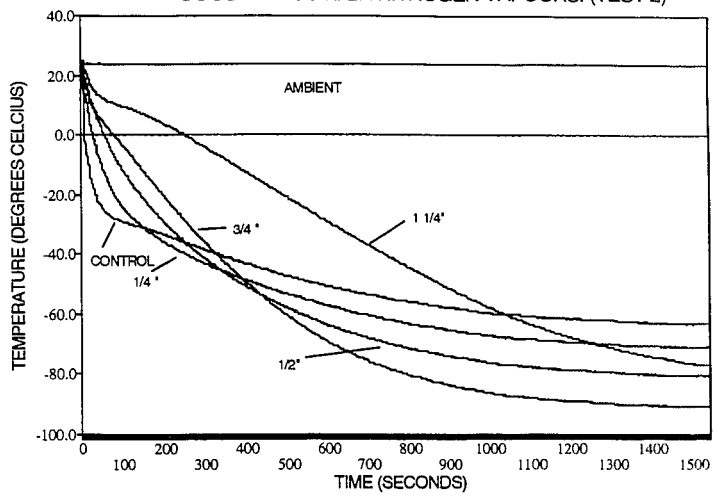


FIGURE IX.3: 1/4", 1/2", 3/4", 1 1/4" CUBES SIMULTANEOUSLY COOLED IN LIQUID NITROGEN VAPOUR. (TEST 3)

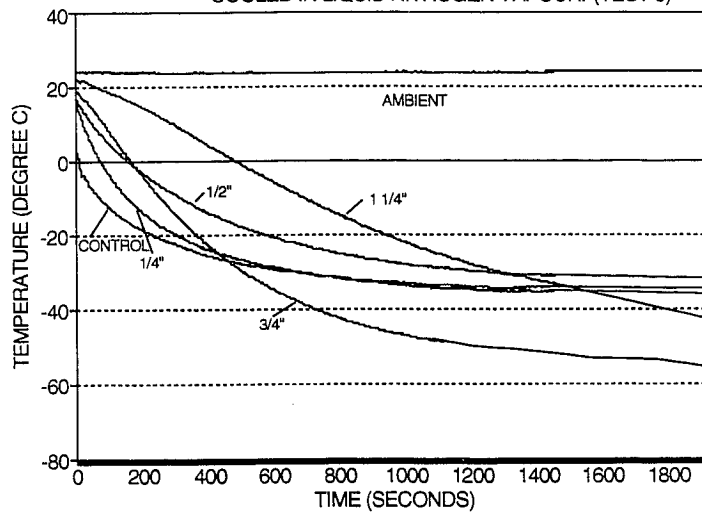


FIGURE IX.4: 1/4", 1/2" & 1" CUBES SIMULTANEOUSLY
COOLED IN WARMER NITROGEN VAPOURS. (TEST 4)

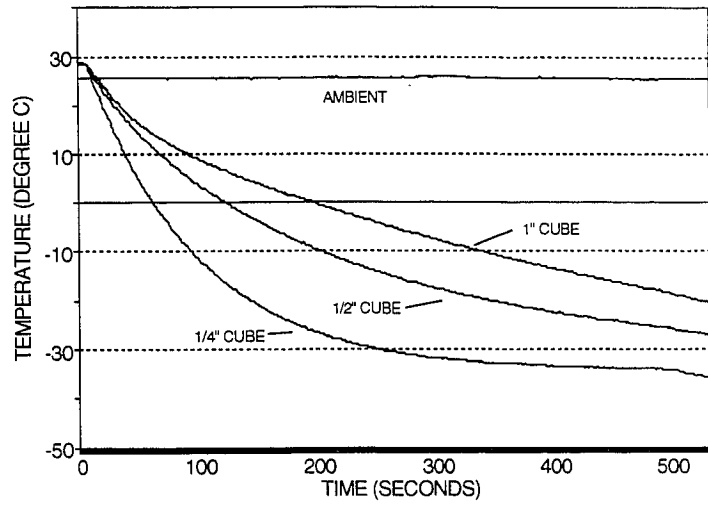
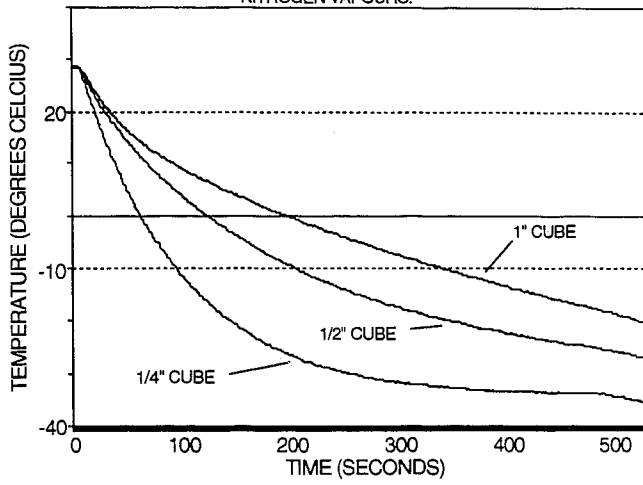


FIGURE IX.5: 1/4", 1/2", 1" CUBES COOLED SIMULTANEOUSLY IN WARMER NITROGEN VAPOURS.



APPENDIX X

Experiment Four Results:

**One Inch Cube Of Virgin Tire Rubber
Dipped In Liquid Nitrogen.**

FIGURE X.1: ONE INCH CUBE OF VIRGIN TIRE RUBBER DIPPED INTO LIQUID NITROGEN (TEST 1).

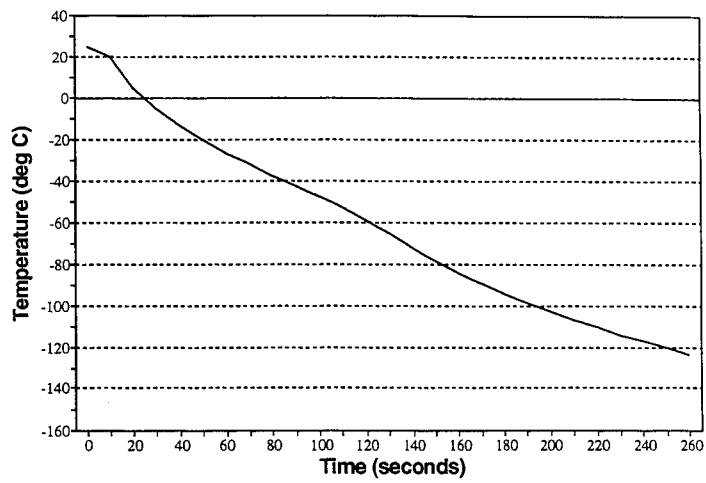


FIGURE X.2: ONE INCH CUBE OF VIRGIN TIRE RUBBER DIPPED INTO LIQUID NITROGEN (TEST 2).

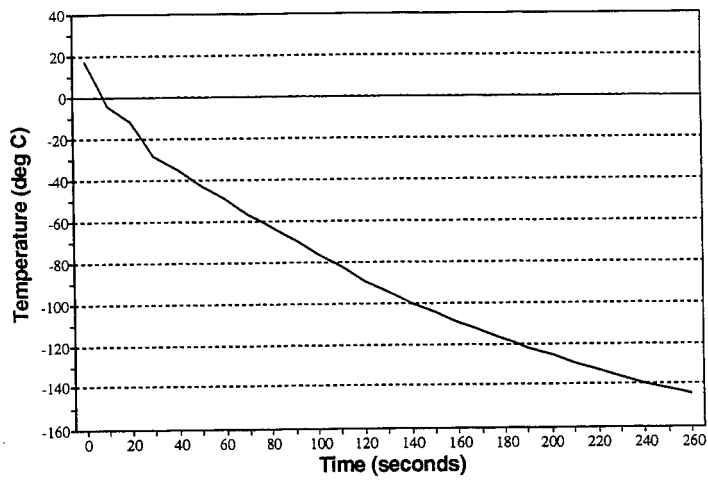


FIGURE X.3: ONE INCH CUBE OF VIRGIN TIRE RUBBER DIPPED INTO LIQUID NITROGEN (TEST 3).

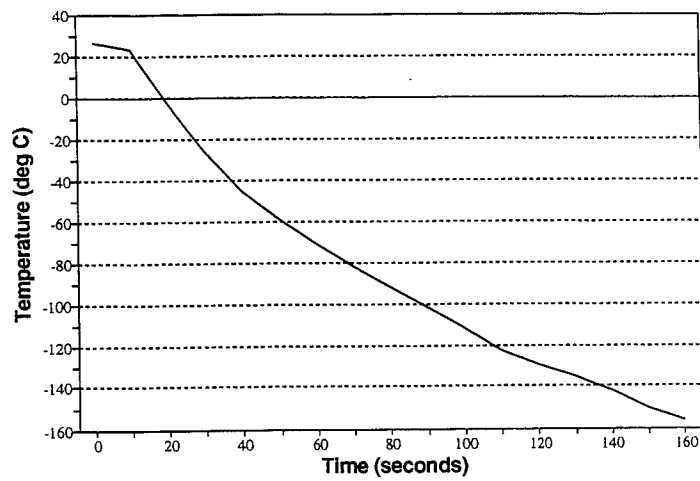


FIGURE X.4: ONE INCH CUBE OF VIRGIN TIRE RUBBER DIPPED INTO LIQUID NITROGEN (TEST 4).

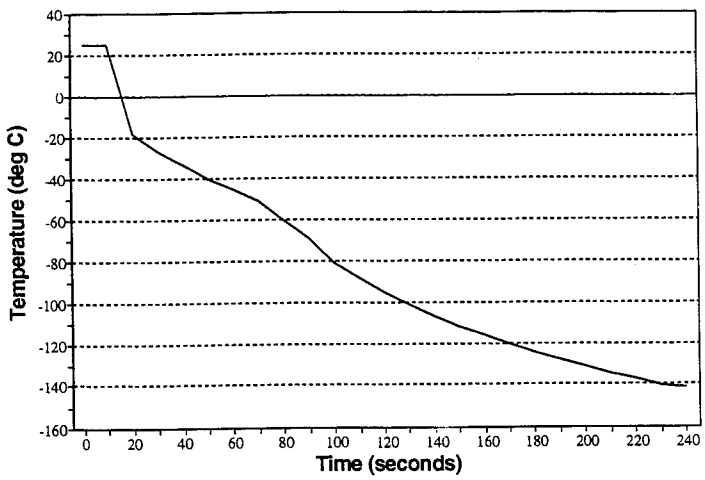


FIGURE X.5: ONE INCH CUBE OF VIRGIN TIRE RUBBER DIPPED INTO LIQUID NITROGEN (TEST 5).

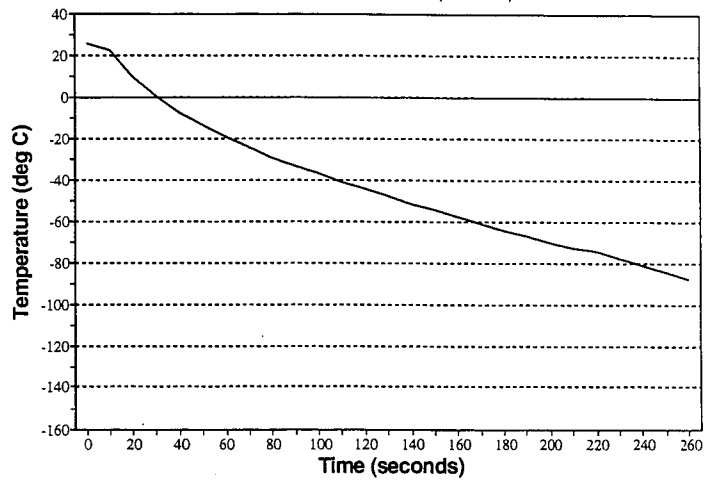


FIGURE X.6: ONE INCH CUBE OF VIRGIN TIRE RUBBER DIPPED INTO LIQUID NITROGEN (TEST 6).

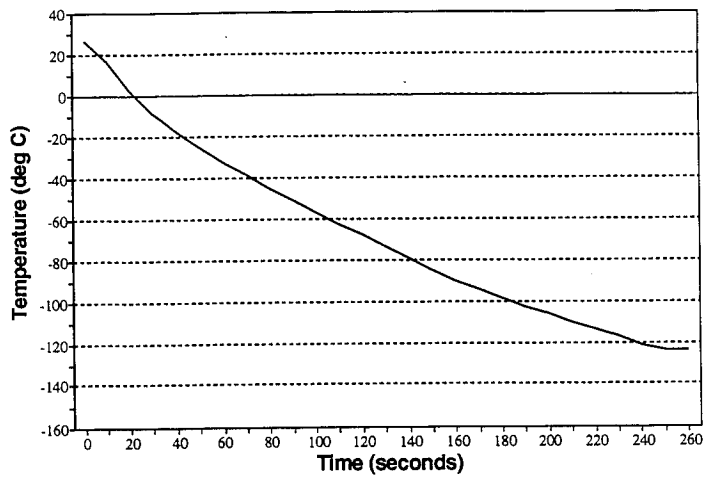


FIGURE X.7: ONE INCH CUBE OF VIRGIN TIRE RUBBER DIPPED INTO LIQUID NITROGEN (TEST 7).

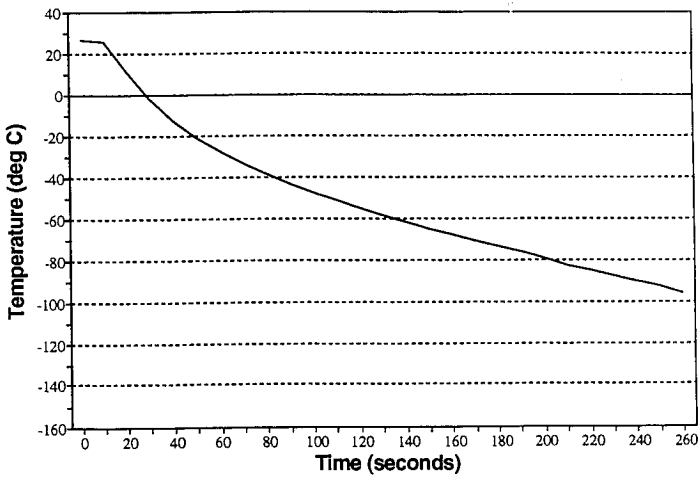


FIGURE X.8: ONE INCH CUBE OF VIRGIN TIRE RUBBER DIPPED INTO LIQUID NITROGEN (TEST 8).

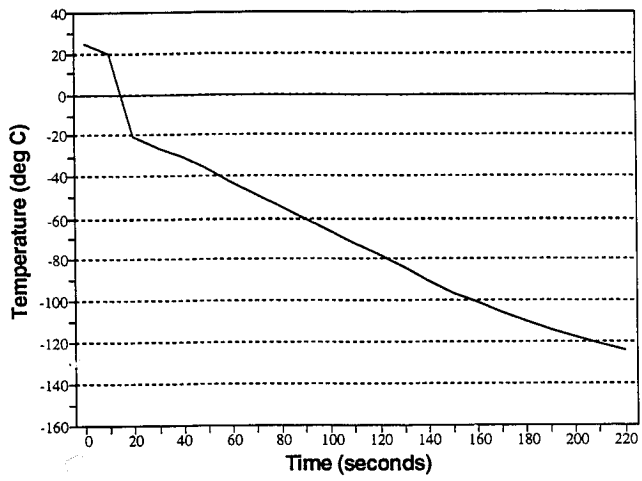


FIGURE X.9: ONE INCH CUBE OF VIRGIN TIRE RUBBER DIPPED INTO LIQUID NITROGEN (TEST 9).

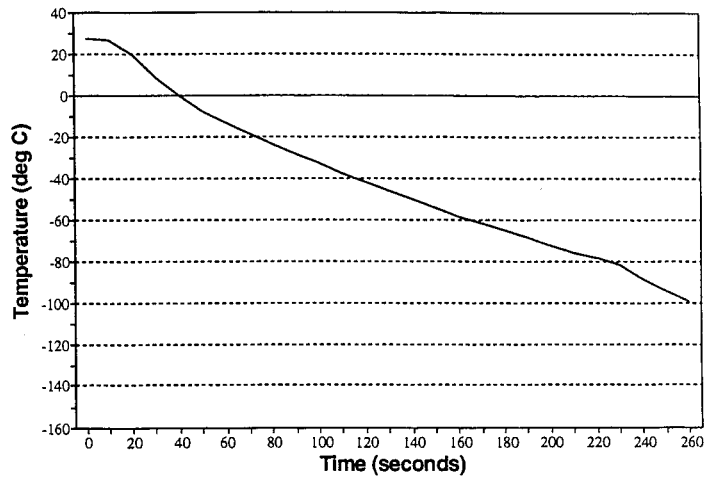
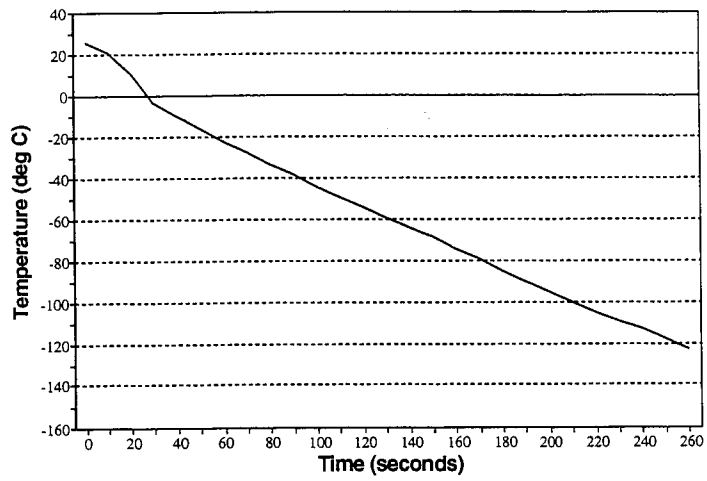


FIGURE X.10: ONE INCH CUBE OF VIRGIN TIRE RUBBER DIPPED INTO LIQUID NITROGEN (TEST 10).



APPENDIX XI

Experiment Five Results:

**One Inch Cube Of Tire Rubber
Resubmerged In Liquid Nitrogen.**

FIGURE XI.1: ONE INCH CUBE OF RUBBER RECOOLED IN LIQUID NITROGEN (TEST 1).

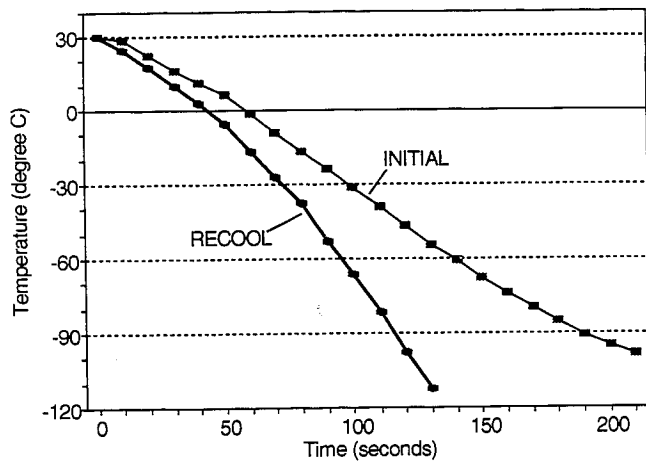


FIGURE XI.2: ONE INCH CUBE OF RUBBER RECOOLED IN LIQUID NITROGEN (TEST 2).

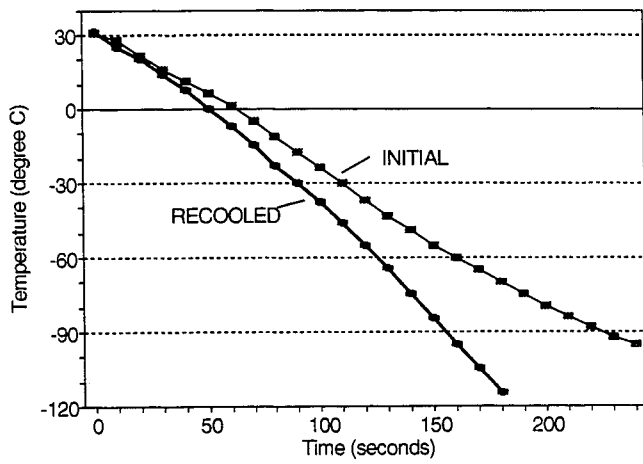


FIGURE XI.3: ONE INCH CUBE OF RUBBER RECOOLED IN LIQUID NITROGEN (TEST 3).

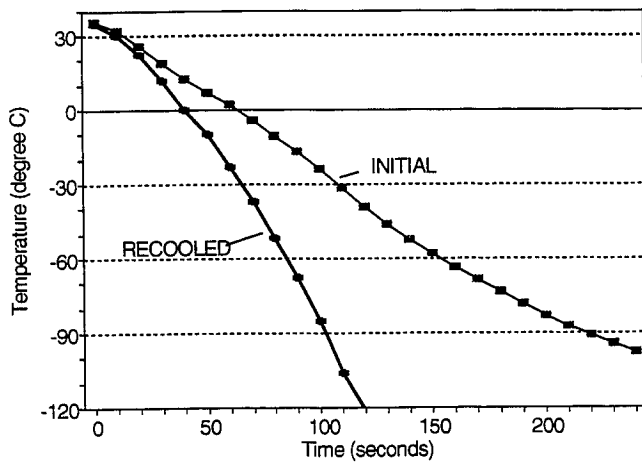


FIGURE XI.4: ONE INCH CUBE OF RUBBER RECOOLED IN LIQUID NITROGEN (TEST 4).

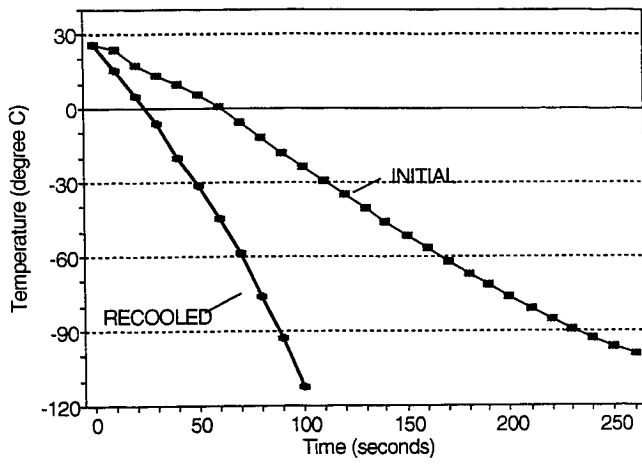
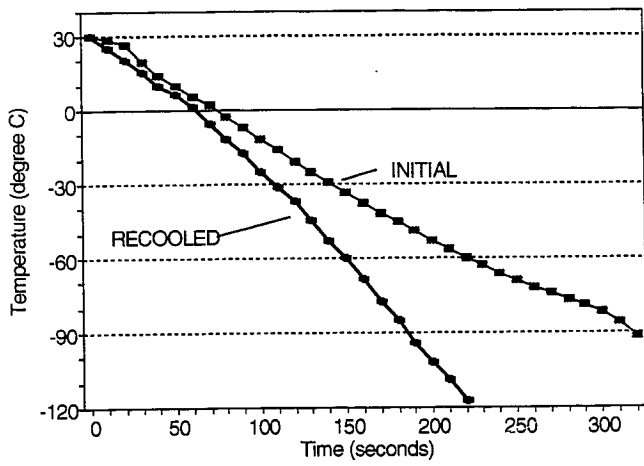


FIGURE XI.5: ONE INCH CUBE OF RUBBER RECOOLED IN LIQUID NITROGEN (TEST 5).



APPENDIX XII

Photomicroscopes Of Ambiently & Cryogenically
Ground Tire Rubber Of Different Material Sizes.

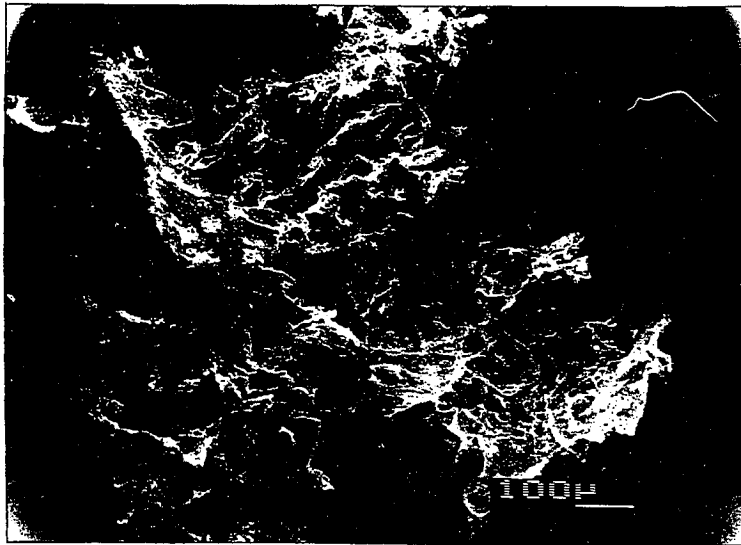


Figure XII.1: Photomicrograph Of Ambiently Ground
Tire Rubber (10 Mesh).

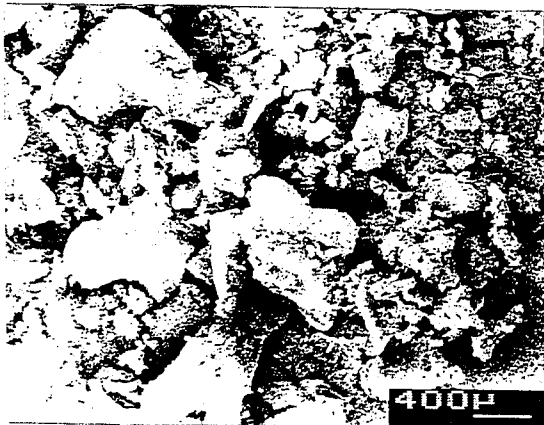


Figure XII.2: Photomicrograph Of Ambiently Ground Tire Rubber (20 Mesh).

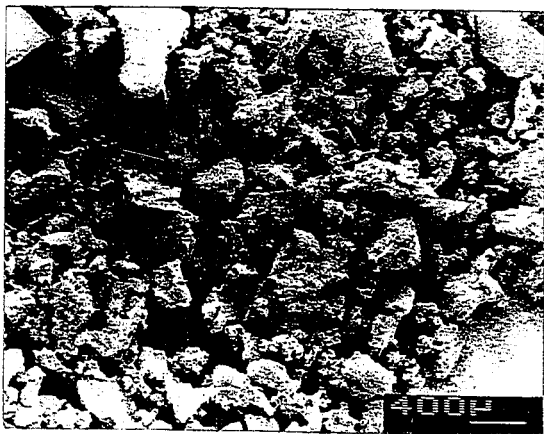
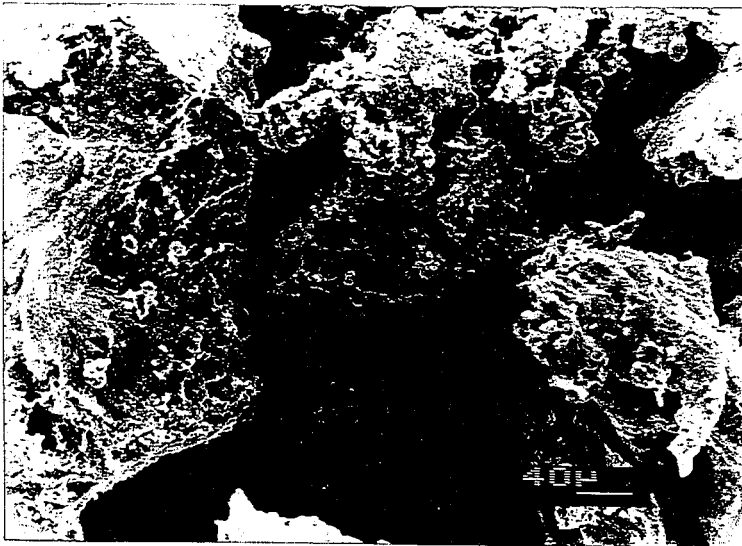


Figure XII.3: Photomicrograph Of Ambiently Ground Tire Rubber (30 Mesh).

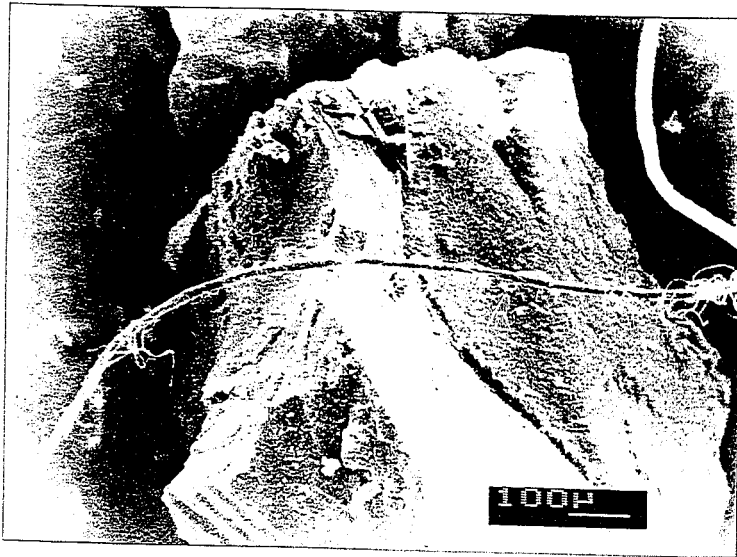


Figure XII.4: Photomicrograph Of Cryogenically
Ground Tire Rubber (10-20 Mesh).



Figure XII.5: Photomicrograph Of Cryogenically Ground Tire Rubber (20-30 Mesh).

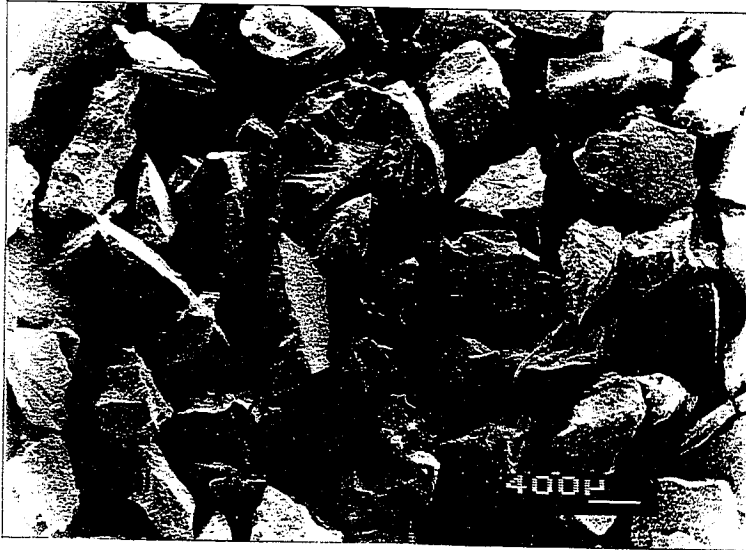


Figure XII.6: Photomicrograph Of Cryogenically
Ground Tire Rubber (30-40 Mesh).

VITA AUCTORIS

Name: Antonio S. Mancina

Place Of Birth: Windsor, Ontario, Canada

Year Of Birth: 1968

Education: W.D. Lowe Secondary School
Windsor, Ontario, Canada
Grade XIII Diploma
1982-1987

University Of Windsor
Windsor, Ontario, Canada
Major: Environmental Engineering B.A.Sc.
1987-1991

University Of Windsor
Windsor, Ontario, Canada
Major: Environmental Engineering M.A.Sc.
1991-1993